

**Prediction of hydraulic conductivity  
and conductive fracture frequency by  
multivariate analysis of data from  
the Klipperås study site**

Jan-Erik Andersson<sup>1</sup>, Lennart Lindqvist<sup>2</sup>

<sup>1</sup> Swedish Geological Co, Uppsala

<sup>2</sup> EMX-system AB, Luleå

February 1988

PREDICTION OF HYDRAULIC CONDUCTIVITY AND CONDUCTIVE  
FRACTURE FREQUENCY BY MULTIVARIATE ANALYSIS OF DATA  
FROM THE KLIPPERÅS STUDY SITE

Jan-Erik Andersson<sup>1</sup>, Lennart Lindqvist<sup>2</sup>

1 Swedish Geological Co, Uppsala  
2 EMX-system AB, Luleå

February 1988

This report concerns a study which was conducted for SKB. The conclusions and viewpoints presented in the report are those of the author(s) and do not necessarily coincide with those of the client.

Information on SKB technical reports from 1977-1978 (TR 121), 1979 (TR 79-28), 1980 (TR 80-26), 1981 (TR 81-17), 1982 (TR 82-28), 1983 (TR 83-77), 1984 (TR 85-01), 1985 (TR 85-20), 1986 (TR 86-31), 1987 (TR 87-33) and 1988 (TR 88-32) is available through SKB.

SVERIGES GEOLOGISKA AB  
Division Ingenjörsgologi  
Uppdragsgivare: SKB  
Uppdrag nr: 87-157

REPORT  
ID-no: IRAP 88214  
Date: 1988-02-24  
Revised: 1989-05-10

PREDICTION OF HYDRAULIC CONDUCTIVITY  
AND CONDUCTIVE FRACTURE FREQUENCY  
BY MULTIVARIATE ANALYSIS OF DATA  
FROM THE KLIPPERÅS STUDY SITE

Jan-Erik Andersson  
Lennart Lindqvist \*

Swedish Geological Co, Uppsala  
February 1988

\* Now with EMX-system AB, Luleå

Keywords: Hydraulic conductivity, conductive fracture frequency, Multivariate data analysis, Klipperås, nuclear waste, Sweden, statistics, geostatistical methods, hydrogeology, crystalline rock

## ABSTRACT

The present study is a pilot study on the possibility to predict the hydraulic conductivity and conductive fracture frequency in boreholes in crystalline rock using multivariate data analysis. The data set used was very extensive and included data from core mapping, fracture fillings, geophysical logs, tubewave measurements and hydraulic tests from five deep boreholes at the Klipperås study site. In the study, multivariate data analysis proved to be a powerful technique to systematically analyze an extensive data material and to study different correlation structures within the data set. With the models derived, about 80-90 % of the variation of hydraulic conductivity of an input data set (consisting of 233 conductivity values in 1 m-sections) could be explained by utilizing 35-45 % of the total information contained in the data set. The hydraulic conductivity of about 4500 one meter sections was predicted. The predicted transmissivity was generally in good agreement with measured transmissivity values in 20 m-sections. The predicted values in 1 m-sections provided a more detailed picture of the hydraulic conductivity distribution along the boreholes. The predicted conductivities were found to be very unevenly distributed. The highest values generally occur in borehole intervals with altered and deformed rock with increased fracture density.

The predicted conductive fracture frequency (CFF) was also unevenly distributed. Fissure fillings, in particular iron minerals, are regarded as useful information in predicting the CFF. The predicted average CFF of the rock mass varied between 0.17 and 0.25 (conductive) fractures per meter. This corresponds to an average fracture spacing of about 4-6 m. The frequency of subhorizontal fractures in granite generally correlates best to the hydraulic conductivity. The study also showed that both the geological and hydrogeological properties of different rock types may vary considerably within a site.

CONTENTS	Page
ABSTRACT	
1. INTRODUCTION	1
2. GEOLOGICAL OVERVIEW OF THE KLIPPERÅS STUDY SITE	3
2.1 Rock types and fracture zones	3
2.2 Borehole descriptions	6
2.3 Fissure filling minerals	7
3. MULTIVARIATE DATA ANALYSIS	9
3.1 Principal Component Analysis	10
3.2 PLS modelling	14
3.3 Data analytical strategy	17
4. AVAILABLE DATA AND PREPARATION OF DATA FILES	19
4.1 General	19
4.2 Description of variables used	23
4.3 Creating 1-meter sections	24
4.4 Tubewave measurements	28
4.5 Reference levels used	29
5. MULTIVARIATE ANALYSIS OF DATA FROM KLIPPERÅS	31
5.1 Hydraulic conductivity models	31
5.1.1 Initial PCA-analysis	31
5.1.2 PLS-modelling	32
5.2 Conductive fracture frequency models	36
6. PREDICTION OF HYDRAULIC CONDUCTIVITY	40
6.1 Properties of the models established	40
6.1.1 General	40
6.1.2 Model for KKLO1 and KKLO2	41
6.1.3 Model for KKLO9	45
6.1.4 Model for KKL12 and KKL14	49
6.1.5 Summary of models	52

6.2	Distribution of predicted hydraulic conductivity	53
6.2.1	General	53
6.2.2	Borehole KKL01	54
6.2.3	Borehole KKL02	59
6.2.4	Borehole KKL06	63
6.2.5	Borehole KKL09	65
6.2.6	Borehole KKL12	71
6.2.7	Borehole KKL14	75
7.	PREDICTION OF CONDUCTIVE FRACTURE FREQUENCY	82
7.1	Properties of the models established	82
7.1.1	General	82
7.1.2	Model for KKL01 and KKL02	82
7.1.3	Model for KKL09	85
7.1.4	Model for KKL12 and KKL14	87
7.1.5	Summary of CFF-models	90
7.2	Distribution of predicted conductive fracture frequency	91
8.	DISCUSSION OF RESULTS	95
8.1	Hydraulic conductivity	95
8.2	Conductive fracture frequency	105
9.	SUMMARY AND CONCLUSIONS	108
9.1	Summary of results	108
9.2	Conclusions	110
10.	REFERENCES	113
11.	APPENDICIES	118
	Appendix A	Distribution of predicted hydraulic conductivity and conductive fracture frequency in boreholes KKL01, KKL02, KKL06, KKL09, KKL12 and KKL14.
	Appendix B	Borehole descriptions (KKL01, KKL02, KKL06, KKL09, KKL12 and KKL14).

## 1. INTRODUCTION

The present work comprises a pilot study of the use of multivariate data analysis as a means to predict the hydraulic conductivity and conductive fracture frequency in detailed borehole sections. The work has been carried out by the Swedish Geological Company (SGAB) at the request of the Swedish Nuclear Fuel and Waste Management (SKB).

Data from the Klipperås study site were selected for the multivariate data analysis. From this site a comprehensive data material is available including core mapping, analysis of fissure fillings, geophysical logging, hydraulic testing and borehole radar measurements.

Before this study commenced, manual correlations of core data, geophysical logs and hydraulic test results from boreholes KKL01 and KKL02 were performed. The preliminary study indicated a good correlation between subhorizontal fracture clusters in granite and hydraulic conductivity and also between simultaneous anomalies of low sonic velocity and low (single-point) resistivity and hydraulic conductivity. Finally, the study showed that greenstones in boreholes KKL01 and KKL02 generally had a hydraulic conductivity below the measurement limit.

The main objectives of this study were to check the results of the preliminary investigations, to test the potential use of multivariate data analysis and to establish computerized techniques to be used in data analysis. The capability of such models to predict certain hydraulic parameters in the borehole by combining several data sets was also to be investigated. The deep boreholes KKL01, KKL02, KKL06, KKL09, KKL12 and KKL14 were selected for the pilot study.

Rather few studies concerning prediction of the hydraulic conductivity, other than from hydraulic tests, exist in the literature. Davison et al (1982) described investigations of

acoustic waveforms from geophysical logs to estimate the permeability of fractures in crystalline rock at the WNRE site in Canada. A few reports dealing with the correlation of hydraulic conductivity and tubewave parameters are also presented in the literature, e.g. Beydoun et al, Stenberg and Olsson (1985) and Stenberg (1987a).

Magnusson and Duran (1984) made a comparative study of different geological, hydrological and geophysical borehole investigations. One of the results of the study was that the flow of water is primarily channelled in a few discrete fractures in the rock, while most of the coated fractures mapped have very low hydraulic conductivity or below the measurement limit. A similar study was carried out by Poikonen (1983).

The determination of permeability of crystalline rocks by standard geophysical logs has been investigated by Katsube and Hume (1987). An empirical relationship between the transmissivity obtained from hydraulic tests and the ratio of formation factors derived from the focused-electrode log and the gamma-gamma (density) log was used to identify borehole intervals of potentially high hydraulic conductivity in granitic rock.

Mc Ewen et al (1985) compared potential flow zones predicted from neutron and gamma-gamma logging with those measured by temperature/conductivity logging and their relation to the fracturing and hydraulic conductivity of the rock.

Within the last few years attempts have been made to estimate the conductive portion of the total number of fractures mapped in a borehole or an underground opening in the rock. This may either be carried out indirectly by statistical methods (Carlsson et al 1984, Andersson et al 1988b) or directly by using actual fracture properties (Winberg and Carlsson, 1987). The statistical methods are generally based on the assumptions of statistical independence of fractures and statistically homogeneous rock.



## 2. GEOLOGICAL OVERVIEW OF THE KLIPPERÅS STUDY SITE

### 2.1 Rock types and fracture zones

The geological and tectonic description of the Klipperås area is presented by Olkiewicz and Stejskał (1986). The overall distribution of rock types in the boreholes within the Klipperås study site according to the core mapping (Egerth, 1986) is summarized in Table 2.1.

Table 2.1 Rock type distribution at the Klipperås study site.

Rock type	Percentage
Granite	85
Greenstone	7
Porphyry dykes	5.5
Mafic dykes, dolerite	1.4
basalt	0.1
Aplite	1
Total	100

The most dominating rock types is granite. This is normally grey-red, coarse to medium grained. A few thin dykes of aplite and pegmatites may occur within the granite.

Several porphyry dykes of acidic to intermediate composition occur within the area. According to the geological model the strike and dip of the porphyrys is WNW-ESE and 75-90° S, respectively. Different types of porphyry dykes occur with different petrophysical properties.

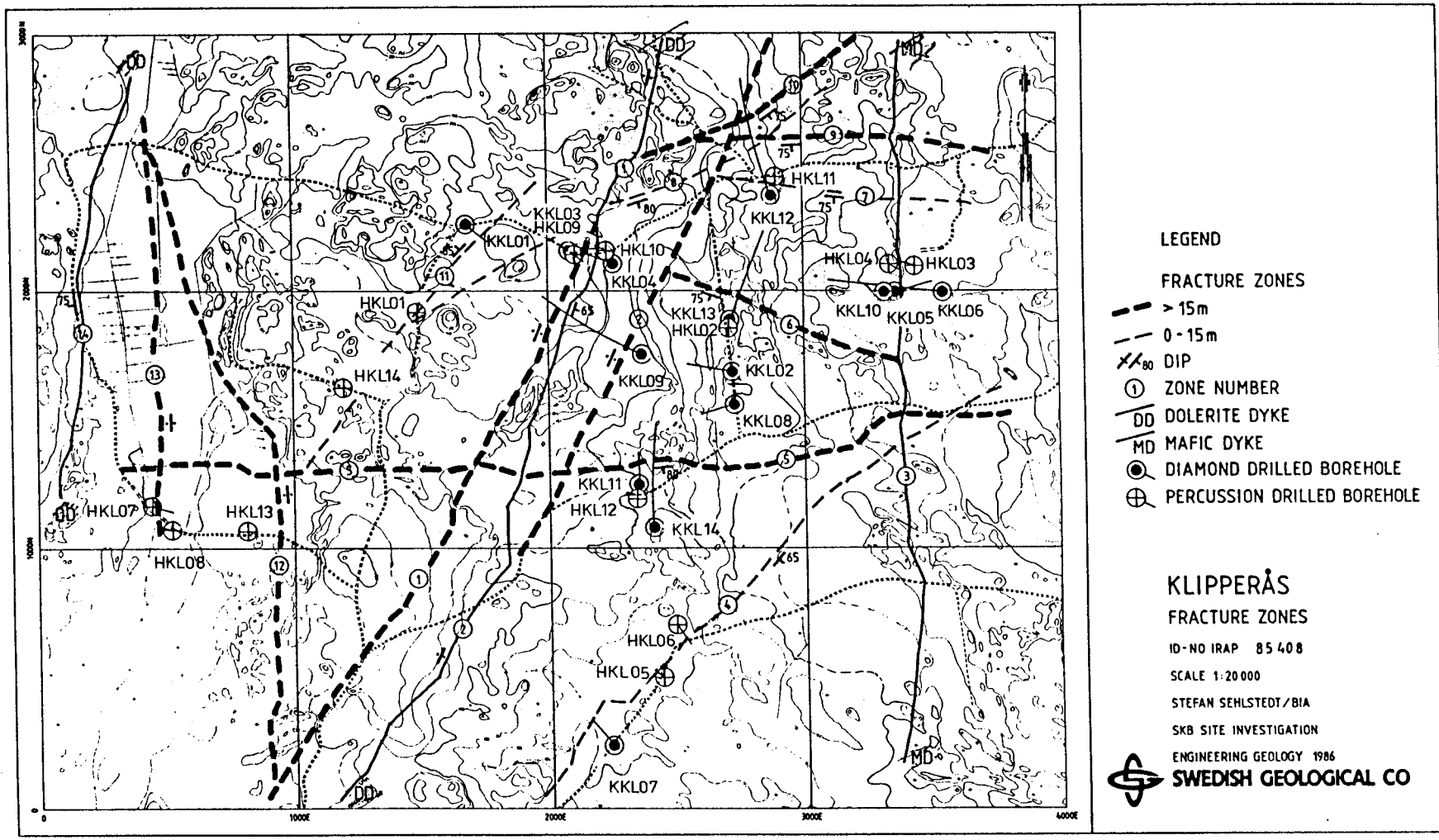
Greenstones are most frequently observed at the margins of the porphyrys with strike and dip directions parallel to the porphyry dykes.

The dolerite dykes strike in NNE-SSW and dip steeply to the east ( $65-90^{\circ}$ ) while other mafic dykes strike in N-S direction and dip steeply to the west ( $80-90^{\circ}$ ).

Deformed rock intervals consisting of tectonized rock, breccias and mylonites occur rather frequently in the boreholes. Alteration occurs within the deformed intervals or in discrete zones in the undeformed granite. According to Sehlstedt and Stenberg (1986) several types of alteration have been observed; chloritization, red colouring of the rock mass and along fractures, hematite stained fracture surfaces and fractures coated with e.g. hydrate iron-oxides.

The location of the fracture zones and mafic dykes penetrated by the boreholes used in this study together with the borehole locations and their direction is shown in Fig 2.1.1. Geometric data of the fracture zones penetrated by the boreholes investigated in this study are presented in Table 2.2.

Fig 2.1.1 Borehole locations and location of fracture zones and mafic dykes within the Klipperås study site.



- LEGEND**
- FRACTURE ZONES**
  - > 15m
  - - - 0 - 15m
  - X/80 DIP
  - ① ZONE NUMBER
  - DD DOLERITE DYKE
  - MD MAFIC DYKE
  - DIAMOND DRILLED BOREHOLE
  - ⊕ PERCUSSION DRILLED BOREHOLE


**KLIPPERÅS**  
**FRACTURE ZONES**  
 ID-NO IRAP 85 40 8  
 SCALE 1:20 000  
 STEFAN SEHLSTEDT/BIA  
 SKB SITE INVESTIGATION  
 ENGINEERING GEOLOGY 1986  
 **SWEDISH GEOLOGICAL CO**

Table 2.2 Geometric data of selected fracture zones at Klipperås.

Zone no	Borehole	Zone interval	Strike/dip	True width
1	KKL09	615-665 m	N30E/90°	29 m
2	KKL09	120-160 m	N30E/90°	22 m
2	KKL12	595-630 m	N15E/85°E	13 m
4	KKL14	368-410 m	N85E/80°	27 m
6	KKL12	70- 88 m	N75W/75°S	12.5 m
7	KKL12	288-306 m	N65E/80°S	13.5 m
8	KKL12	312-347 m	N85W/90°	28 m
9	KKL12	362-384 m	N60E/75°S	17.5 m
10	KKL01	280-310 m	N45E/85°NW	10.5 m
H1	KKL02	792-804 m	Sub-Horizontal	12 m

## 2.2 Borehole descriptions

Summaries regarding geometrical data, rock types, fracture frequency and fracture zones for each borehole studied in this report are presented in the Tables B.1 - B.12 and Figures B.1 - B.6 in Appendix B. All information is derived from Olkiewicz and Stejskał (1986), in which report more detailed borehole descriptions can be found.

A detailed discussion of specific borehole intervals is included in Section 6.2 in connection to the predicted hydraulic conductivity distribution in the boreholes.

### 2.3 Fissure filling minerals

The fissure fillings within the Klipperås study site have been investigated by Tullborg (1986). A short summary of the most important findings in this report are presented below. Indications of oxidation within fractures and fracture zones suggest an intense circulation of the groundwater within the Klipperås area. Several fracture zones have been reactivated. It is also suspected that relatively late movements have occurred and caused crushing of the rock.

Fracture zones in conjunction with mafic dykes exhibit lower hydraulic conductivity due to fracture sealing by chlorite, clay minerals and calcite. Fracture minerals identified within the Klipperås area are chlorite, epidote, hematite, Fe-oxyhydroxide, calcite, muscovite, quartz, adularia, pyrite and smectite within mafic dykes. The most dominating Fe-mineral at Klipperås is Fe-oxyhydroxide (rust).

The surface water has affected the uppermost part of the bedrock which has resulted in calcite dissolution and precipitation of Fe-oxyhydroxide. Calcite dissolution is more intense close to the fracture zones and less intense within the blocks. Within fracture zones Fe-oxyhydroxides can be found at great depths. A study of the deformation and fissure filling history in the granite at Klipperås showed that during the last traced event, probably still active, formation of low-temperature minerals as calcite, clay minerals and Fe-oxyhydroxide occurred (Tullborg, 1986).

In conjunction with the above study a preliminary assessment of possible relations between fissure minerals and the hydraulic conductivity in the Klipperås area was carried out by Tullborg (1987). In this study it was concluded that Fe-oxyhydroxide (rust) in most cases is related to conductive zones. From boreholes where Fe and hematite are mapped separately it could be deduced that sections containing rust almost always had a measurable hydraulic conductivity whereas hematite not

necessarily corresponds to conductive sections. Pyrite is uncommon in conductive sections (may possibly occur at greater depths).

Regarding calcite the pattern is more changing. In the upper parts of the boreholes the calcite is dissolved in conductive sections to be precipitated in deeper conductive sections. This gives a negative correlation between hydraulic conductivity and frequency of calcite coated fractures in the upper parts of the bedrock (from the surface down to 200 - 300 m) while at greater depths a positive correlation exists.

Chlorite seems to be the dominating mineral in non-conductive sections. An increased frequency of chlorite fractures has been observed in vertical fractures, e.g. K1 1. Epidote shows an increased frequency in steep fractures. Calcite is more common in horizontal fractures.

The fissure mineralizations in the greenstones + mafic rock and in the porphyrys differ from the mineralizations in granite. The basic rocks are entirely dominated by calcite and chlorite-healed fissures. Presumably also some clay minerals occur, effectively healing the basic rocks. The volcanic rocks have an increased frequency of pyrite-healed fissures. Epidote and hematite appear to be more uncommon than in the granite.

### 3. MULTIVARIATE DATA ANALYSIS

The starting point in all multivariate data analysis is a data matrix measured for  $N$  objects and  $K$  variables. In this study the objects correspond to 1 m-borehole sections and the variables constitute various parameters measured on cores, from geophysical logs and from hydraulic tests in the borehole sections. The objective of collecting these data is to evaluate a certain problem or to create a model of the features in a certain system.

Usually the system is complicated and several different features interact. In addition there may be a random component added to some variables as well as measurement errors which also vary in character between different variables and objects depending on the feature of the object.

In a data matrix there may also be objects that systematically or randomly differ from the main trends in the system. These are called outliers. Special care must be attended to the outliers, otherwise they will influence on the data evaluation too much. In most problems analysed, there exists a relation between the variables that are measured. This effect should of course be used to build the models of the data.

From theory and from our knowledge and experience we recognize a certain correlation of several variables as a certain feature. If some objects in the data matrix reveal this correlation we can be convinced that the object have this special feature. To just examine one variable at the time, it will be difficult or impossible to indicate the special feature of the object, see e.g. Wold et al (1983, 1987) and Wold (1985).

To evaluate the information in a data matrix it is important to understand and to have the knowledge of the system that is to be evaluated, the knowledge of the software to be used as well as a data analytical strategy to apply on the data analysis.

Multivariate modelling has been used extensively in several research fields, e.g. for mineral prospecting (Lindqvist and Lundholm, 1985), geochemical and geophysical exploration (Esbensen et al, 1987 and Lindqvist et al, 1987) and in predicting permeability and porosity from petrophysical logs (Esbensen and Martens, 1987).

The SIMCA software has been used in this study to evaluate and to model the features existing in the data matrix. Since the variables are for certain correlated, the multivariate approach to data analysis will give more information than using single variable evaluation of the data matrix.

For the data modelling there are two algorithms available in the SIMCA software. One for Principal Component Analysis (PCA) and one for Partial Least Squares regression analysis (PLS). These two algorithms are used for different objectives.

### 3.1 Principal Component Analysis

In general, the goals for the multivariate data analysis using the PCA method are the simplification of a data table, creating models, noise reduction, outlier detection, variable and object selection and correlation evaluation, classification and prediction.

Figure 3.1.1 shows an example where some objects indicated with black dots have been measured for three different variables. Depending on different features of the objects, they will of course be located in different places along these variables and in the three dimensional space.



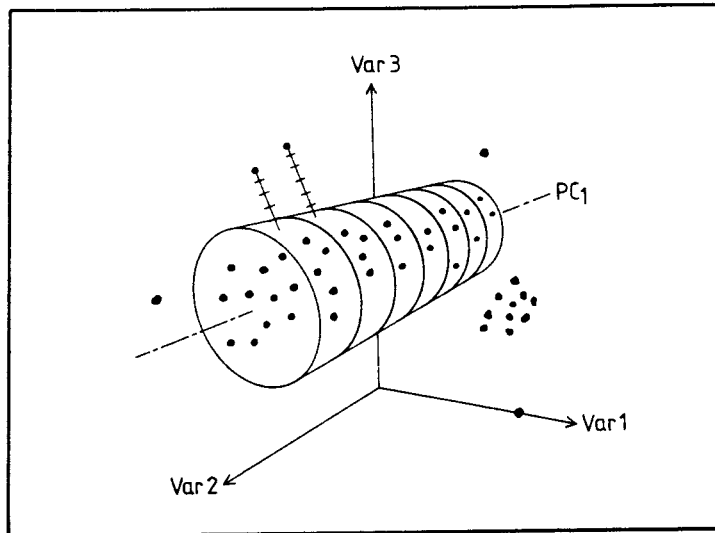


Fig 3.1.1 Calculating the first principal component (PC1) from three variables. Outliers are outside the confidence volume.

The idea of the PCA analysis is to find a direction in the data space that will indicate typical features. These features are indicated by a high variation in one direction or another. It is then a geometrical problem to find these directions in the data space. In most cases this direction will not coincide with any single variable. In Fig 3.1.1, the first principal component is indicated with PC1.

The second variable show a high correlation with the first component, the main direction along the elongated volume surrounding the objects. Since the second variable is closely correlated with the first component, it is interpreted as an important variable for the data structure expressed by the first component.

The location of each object along this feature, the first principal component, is expressed as a numerical value, usually ranging between  $\pm 3$  since it is expressed as a

standard deviation of the objects along the axis. This value is called the object score.

The next step in a PCA analysis is to find the second most important direction in the data space. This direction will be perpendicular to the first PC and it will indicate the second most important feature. These two first PC's can be seen as two vectors spanning up a feature plane as in Fig 3.1.2. On this plane all the objects can be projected.

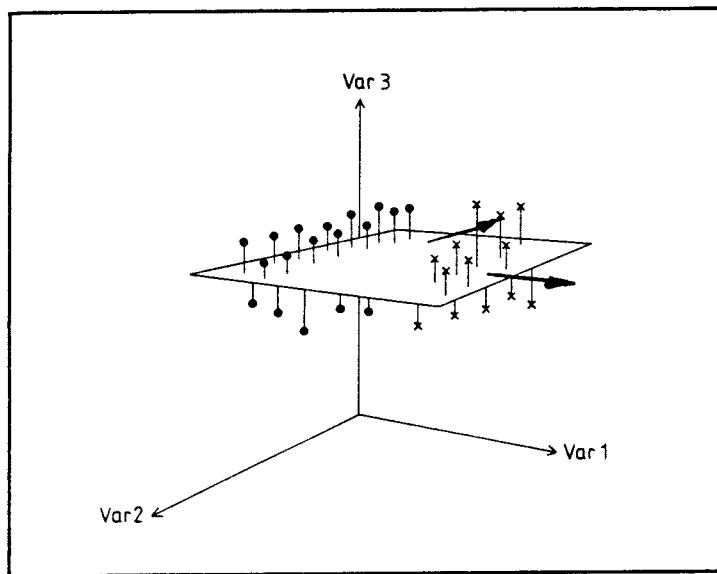


Fig 3.1.2 A feature plane defined by the first two principal components. The object residuals to the plane are also indicated.

The residual of each object to the plane surface can be explained as the object deviation from the two most important features. This residual could be interpreted in this example as a random noise component since it has a small and random variation. The residual variance, the noise, can then be excluded by using a two component model for the objects.

Using more variables than three will not be any problem for the SIMCA software. In fact, the program available at SGAB can handle up to 200 variables and 6000 samples with no problem. The program can also calculate as many principal components as the number of variables.

Having accepted that data will just be transformed to a new coordinate system in a geometrical manner, outlined by the data itself, the understanding of the transformation from the original variables to the principal components will not be difficult. By projecting the original variables along the components or the component planes, the data features are easily understood and expressed by the original variables.

In the data analysis, the first component will show the most obvious information in the data matrix. Components that come up later indicate successively less important features in the data matrix but they may be important for the solution of the problem or the data analytical strategy. It is the person having the knowledge of the problem that must decide the importance of the components.

If the components that are extracted shall indicate a main feature in the data, they must not be influenced by a few outlying samples. In this case, if outliers exist as in Figure 3.1.1, these must be excluded while running the PCA analysis. Otherwise the components can go in directions that are strongly influenced by single objects and they will not represent a dominating feature in the data matrix but rather the feature of an outlying object.

By running the data through the PC-analysis for several times, single variable outliers as well as multivariable outliers can be extracted from the data modelling. Having extracted all outliers, the resulting models will be robust and will not change significantly if some samples are excluded or included. This is a strong feature of the multivariate modelling approach.

To a model defined by one or several principal components also a confidence volume is calculated. In one dimension the confidence volume is a cylinder like neighbourhood as in Fig 3.1.1, in two dimension the confidence volume is a box and so on. The confidence volume is expressed in standard deviations giving approximately 95 percent of the objects inside of 2 standard deviations.

### 3.2 PLS modelling

In many data analytical problems some objects have been measured or analysed for two different kinds of variables. The important objective may be to evaluate or model the relation between these two groups of variables.

Examples of such problems are e.g. measurements of a patients health and drugs used, chemical analysis of food and taste of the food, geophysical loggings of the bedrock and corresponding hydraulic conductivity, geophysical logging of the bedrock and the relation to borehole radar intensity.

The difference between the two blocks are how the measurements are made or that they represent different features covering the same problem. In the PLS analysis the variables are divided into an X-block with the independent variables and the Y-block with the corresponding dependent variables.

The PLS method can be used in two different ways. Firstly, similar to the PCA method to evaluate the relation between different variables and objects. The advantage of using the PLS method instead of the PCA method is that the data structure for the Y-block is emphasized and the relation between the two blocks is obtained.

The second objective of the PLS method is to create a model between the two groups of variables, using a training set containing measurements on both the X and Y variables. After a

model is calculated between the two blocks, the Y-variables can be estimated based on new X variables. This kind of data analytical procedure is preferred when measurements of the Y variables are expensive or difficult.

If a model between X and Y can be obtained with a high degree of correspondence, the model can estimate the Y values from the X measurements with a high degree of accuracy as well. The PLS program also indicates if the object is within the training set model based on the X variables. If the object is far outside of the model the estimated value of y is not reliable.

The modelling procedure can be explained as in Fig 3.1.3. The basic procedure is to calculate one principal component in each block at the same time. Then the object location along the axis in the X and Y-blocks are used to connect the two models with a least square regression technique. The principal components are adjusted iteratively to achieve components in each block that are adjusted by the the principal component scores from the other block through the regression technique.

The model is build up gradually, one factor at the time, each factor representing a new feature and as much as possible of the remaining variation in the data using the PLS method the outlier detection and deletion is as important as for the PCA method.

In PLS modelling as well as for ordinary PCA classification, a distance of each object to the model is calculated that can be compared with the size of the confidence volume. Hence, outliers with a large distance to the model can be pinpointed and should be evaluated carefully. This feature of the SIMCA classification is an advantage, since new objects coming from other investigations can be compared with the model. If the objects are inside the confidence volume the objects are similar to the objects that have been used to create the model and the resulting interpretation of the new objects are comparable.

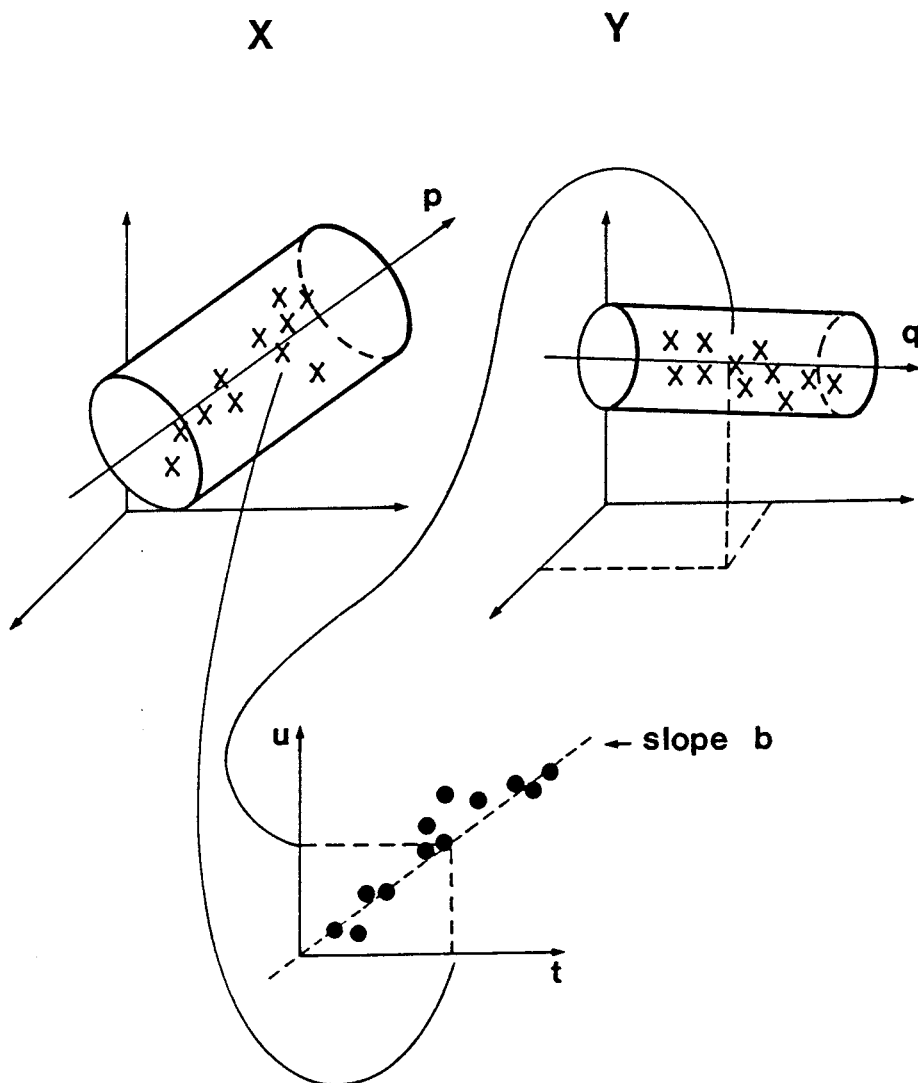


Fig 3.1.3 The PLS method applied on three X and three Y variables. The regression technique applied on the principal component scores are used to connect the two variable spaces.

### 3.3 Data analytical strategy

In the data analysis it is important to define a data analytical strategy. The most important issue is to define what shall be achieved by the data analytical procedure. The selection of objects, variables and type of treatment must be defined depending on the type of problem. The data analytical strategy must then be specially designed for every situation.

Our objectives are to create a model from different variables measured in the borehole, obtained from cores or from geophysical logs, to predict the hydraulic conductivity (HC) for one meter sections along the entire boreholes. Using the predicted one-meter hydraulic conductivity, called HP, the conductive fracture frequency should also be estimated. For the prediction of the HP-variable, a set of estimated HC-values was used as one Y block variable and the other variables were used in the X- block. The data analytical strategy of the first objective was decided to be:

- present and evaluate the correlation structure between objects and variables by using the PLS method,
- delete outlying objects by evaluating the principal component score plots for the objects,
- delete variables that are not relevant for the problem,
- interpretation of the principal components to understand the features they represent,
- obtain acceptable models for each borehole,
- predict hydraulic conductivity for one meter sections along the entire boreholes.

The second objective was to use the predicted hydraulic conductivity (HP) as a new variable and then try to model the conductive fracture frequency. This objective is difficult to achieve since there does not exist any variable that, with a high degree of confidence, can indicate this feature. As a first approximation, the best indicator of the conductive fracture frequency available was assumed to be the frequency of

fractures with the mineral Fe. This variable together with the predicted hydraulic conductivity (HP) was used in the Y block and the remaining variables in the X-block.

The data analytical strategy of the second objective was decided to be:

- evaluate the correlation structure,
- delete outlying objects,
- select variables that are relevant for the problem,
- interpretation of the component models,
- obtain a model between the X- and Y- block,
- estimate the conductive fracture frequency.



#### 4. AVAILABLE DATA AND PREPARATION OF DATA FILES

##### 4.1 General

To solve the objectives of the project the selection of variables could be guided on a theoretical basis. Since SIMCA is not sensitive to too many variables and the fact that the program can indicate the importance of each variable to a specific model, all variables that are available from the boreholes were initially used in the analysis.

Unfortunately, the data are recorded with different methods that give different support, some from different types of borehole logging, some from the core itself and some from the borehole fluid. Therefore different methods must be used to transform data to an equal support and a comparable unit.

In this case one meter sections was suggested for the transformation of each variable. This section length was not scientifically selected but rather defined from experience of the depth accuracy of the variables. To use a shorter section length than one meter might cause problems for several variables since the accuracy of the depth measurements varies for different methods. A short discrepancy between two methods may cause that the variables will not correlate as they should. Using a longer section length would smooth the variables too much, also causing a change in the correlation structure.

In preparing the data files large efforts were made to minimize potential errors in the depth recording of the variables by correcting the data for any cable stretching and using a common reference level for all measurements.

Variables of interest are from the following investigations:

- borehole logging
- fracture frequency mapping from the core
- fracture mineral mapping from the core
- rocktype coding
- borehole deviation measurements
- isotope analysis of fissure filling calcite
- physical properties determined from core analysis
- tubewave parameters
- hydraulic conductivity.

Most data are collected and used in this study as they are recorded but for the fracture frequency the coding is separated into six classes depending on the angle between the fracture and the core axis. The original coding is also separated into three classes, single fractures, fracture clusters and fractures in crush zones. The fracture frequency coding results in totally 16 variables. The variables and the code names used in this report as well as in the SIMCA plots are listed in Table 4.1.

Table 4.1 Variables used in the multivariate data analysis  
from Klipperås.

Borehole		KKL01	02	06	09	12	14
<u>Borehole logs</u>							
1	GA = Gamma	x	x	x	x	x	x
2	GE = Geohm (single-point res)	x	x	x	x	x	x
3	LR = Lateral resistivity	x	x	x	x	x	x
4	NR = Normal resistivity	x	x	x	x	x	x
5	SO = Sonic	x	x	x	x	x	x
6	SP = Self potential	x	x	x	x	x	x
7	SU = Susceptibility	x	x	x	x	x	x
8	QT = Fluid temperature	x	x	x	x	x	x
9	QG = Vertical temp. gradient	x	x	x	x	x	x
10	QR = Fluid resistivity	x	x	x	x	x	x
11	QS = Fluid salinity	x	x	x	x	x	x
<u>Fracture frequency</u>							
12	F0 = Fracture clusters (0-15°)	x	x	x	x	x	x
13	S0 = Single fractures (0-15°)	x	x	x	x	x	x
14	F1 = Fracture clusters (16-30°)	x	x	x	x	x	x
15	S1 = Single fractures (16-30°)	x	x	x	x	x	x
16	F3 = Fracture (31-45°)	x	x	x	x	x	x
17	S3 = Single fractures (31-45°)	x	x	x	x	x	x
18	F4 = Fracture cluster (46-60°)	x	x	x	x	x	x
19	S4 = Single fractures (46-60°)	x	x	x	x	x	x
20	F6 = Fracture clusters (61-75°)	x	x	x	x	x	x
21	S6 = Single fractures (61-75°)	x	x	x	x	x	x
22	F7 = Fracture clusters (76-90°)	x	x	x	x	x	x
23	S7 = Single fractures (76-90°)	x	x	x	x	x	x
24	F9 = Fracture cluster (0-90°)	x	x	x	x	x	x
25	S9 = Single fractures (0-90°)	x	x	x	x	x	x
26	C9 = Crush zones (0-90°)	x	x	x	x	x	x
27	FS = Total fracture freq(0-90°)	x	x	x	x	x	x
<u>Fissure filling minerals</u>							
28	Ca = Calcite	x	x	x	x	x	x
29	Fe = Fe-oxide	x	x	x	x	x	x
30	Hm = Hematite	m	m	m	m	m	m
31	Py = Pyrite	x	x	x	x	x	x
32	Ep = Epidote	x	x	x	x	x	x
33	Cl = Chlorite	x	x	x	x	x	x

Table 4.1 (continued)

Rock types

34	gr = granite	(PSE)	x	x	x	x	x	x
35	ge = greenstone	(MMB)	x	x	x	x	x	x
36	pp = plagioclase porphyry	(HSG)	x	x	x	x	x	x
37	qp = quartz porphyry	(HSF)	x	x	x	x	x	x
38	qd = quartz dyke	(HSE)	x	x	x	x	x	x
39	ap = aplite	(HSC)	x	x	x	x	x	x
40	pe = pegmatite	(HSB)	x	x	x	x	x	x
41	do = dolerite	(HBB)	x	x	x	x	x	x
42	av = acid volcanics	(VS)	x	x	x	x	x	x
43	ZZ = Vertical depth		x	x	x	x	x	x

Isotopes

44	IC = Isotope R-13-C		x	x	x	m	m	x
45	IO = Isotope R-18-O		x	x	x	m	m	x

Core parameters

46	De = Density		m	x	m	x	m	m
47	Po = Porosity		m	x	m	x	m	m
48	Su = Susceptibility		m	x	m	x	m	m
49	Qv = Q-value		m	x	m	x	m	m
50	Re = Remanense		m	x	m	x	m	m
51	Rs = Resistivity		m	x	m	x	m	m
52	Ip = Ip		m	x	m	x	m	m

Tube wave

53	TP = Tubewave (T+P)		m	x	m	m	m	m
54	TE = Tubewave, estim. P-wave		m	x	m	m	m	m
55	TR = Tubewave, ratio (T+P)/TE		m	x	m	m	m	m

Hydraulic conductivity

56	HC = Hydraulic conductivity		x	x	x	x	x	x
57	HP = Predicted hydr. cond.		x	x	x	x	x	x

x = The variable is present in the entire borehole or in parts of the hole.

m = The variable is missing.

---

#### 4.2 Description of variables used

All borehole log methods presented by Sehlstedt and Stenberg (1986) are used in this study (variables 1-11). They can be divided into logs sensitive to the lithology (GA, GE, SU), fracture occurrence (GE, NR, LR, SO, SP) and hydraulically sensitive logs (QG, QT, QS, QR).

The total frequency of coated fractures was firstly divided into single fractures, fractures in fracture clusters and fractures in crush zones (variables 12-27) according to the core mapping (Egerth, 1986). A fracture cluster is here defined as core intervals intersected by 10 (coated) fractures or more per meter of the core. Crush zones are treated as core intervals having 50 fractures per meter in the analysis. Fracture frequencies in fracture clusters and crush zones overlapping the actual 1 m section limits are calculated in proportion to their occurrence in the sections.

Secondly, the different fracture frequencies are divided in angle intervals ( $15^{\circ}$ ). By this calculation the frequencies of both parallel and crossing fractures are summed together. The division in angle intervals was made to study the correlation between different angle intervals and other variables, e.g. hydraulic conductivity. Also the total fracture frequency in each angle interval for each class (S9, F9, C9) and the total fracture frequency (FS) have been calculated.

The (total) frequencies of fractures coated with specific minerals according to the core mapping are also used (variables 28-33). The iron minerals Fe-oxyhydroxide (Fe) and hematite (Hm) are mapped separately in the boreholes KKL06, 09, 12 and 14. However, since different codes for hematite were used in the core mapping, this mineral has been omitted in the present study. In the boreholes KKL01 and KKL02, Fe-oxyhydroxide and hematite are not separated but mapped together as "Fe". In the other boreholes studied (KKL06, 09, 12 and 14) the code "Fe" represents Fe-oxyhydroxide only.

The rock type variables (34-42) are derived from the original core mapping file. The designations within brackets in Table 4.1 are the ones used in the presentation of the core mapping by Egerth (1986). It should be noted that both types of porphyrys occurring in the boreholes are denoted as acid volcanics in the core mapping file.

The depth variable (variable 43) represents the vertical depth calculated according to the borehole deviation logs.

Stable isotope analysis of  $\delta^{18}\text{O}$  and  $\delta^{13}\text{C}$  on calcite samples from open fractures are also included (variables 44-45). These variables were only used in the initial modelling.

Parameters determined from analysis of borehole cores from boreholes KKL02 and 09 (variables 46-52) presented by Stenberg (1986) were also used in the initial modelling only. The tubewave parameters are described in section 4.4.

Finally, hydraulic conductivity values measured in 20 m (25 m in KKL01) and 5 m sections presented by Gentzschein (1986) were used to estimate the hydraulic conductivity of selected 1 m sections as described in section 5.1.2 (variable 56). The lower measurement limit for these tests corresponds to a transmissivity of  $T = 2 \times 10^{-10} \text{ m}^2/\text{s}$ .

### 4.3 Creating 1-meter sections

To be able to statistically correlate and integrate different kinds of variables in the borehole the initial variables must be transformed to an equal section length. In our case the section length was selected to be one meter. Since the data are measured with several methods each having a different support in the surrounding rock, different kinds of methods are used for the representation of the variables in one meter sections. Five different methods are used:

- Averaging the measured values if there are several measured values within the section. Usually this method is convenient when the method used has a small support giving a highly varying value within the one meter section. This method is used for e.g. the gamma-log which has one recording on each 10 centimeter.
  
- Linear interpolation between surrounding samples. This method is used for variables that have a high support and the separation between measurement location is higher than one meter. This type is used for e.g. the borehole fluid salinity variable which has a 5 meter separation as well as for the temperature which has a slightly higher separation than one meter due to the depth correction for the stretching of the logging cable.
  
- The third type is to set the section value to the value from a single point measurement within the section, even though the measurement represents a value from a single fracture, fissure or similar. This type is used for e.g. the isotope measurements and the parameters from the core analysis.
  
- The fourth type is to set a missing value code to the section if the above methods can not be used to assign a value to the section. This is the case for the isotope analyses which have discrete values from single points in a few sections in the borehole.
  
- Binary coding is used to indicate if a section is similar or not to a specific variable. E.g. each rocktype is set to one single variable and coded by using 1 if the section contains the rocktype and 0 for dissimilarity.

This way of transforming the original data to a similar section length is necessary but it will also introduce a smoothing effect and partially a fictive correlation. Since SIMCA is used as a tool to separate the information in each single value into two parts, existing correlation and the

random noise variation part, the smoothing effect is partially handled by the SIMCA method.

There are also other effects that must be considered i.e. the tension of the logging cable that increases with the depth and is different for different methods. The fact that different methods are related to the ground level while some are related to the top of the casing for the borehole must also be treated.

For some sections, e.g. for the rocktype coding, the interface between different rock types is often located within one section. In this case the dominating rock type will be assigned to the section. In some cases a very thin dyke, completely within one section, may disappear. This kind of smoothing may cause that other variables will not correlate as they should. These sections may come out as outliers in the SIMCA analysis.

The depth of the midpoint of the first section used is set to 1.5 meter for all boreholes and all variables. The geophysical logging variables are used as the variable controlling the modelled interval of each borehole. For the other variables a missing value code is used to fill up the entire borehole lengths.

Table 4.2 Borehole intervals used in the analysis and total length of the boreholes.

Borehole	Interval (m) (midpoints)	Total length (m)
KKL01	1.5 - 531.5	563.95
KKL02	1.5 - 921.5	958.60
KKL06	1.5 - 796.5	808.00
KKL09	1.5 - 792.5	801.03
KKL12	1.5 - 721.5	730.14
KKL14	1.5 - 694.5	705.22



Averaging within the section is used for the following variables:

0.1 meter measurements --- GA, GE, SO, SP, SU  
LR, NR (for KL6, 9, 12, 14)

Linear interpolation is used for

1.0 meter measurements --- QT, QG  
LR, NR (for KL1, 2)

5.0 meter measurements --- QR, QS

Setting value to the section from a measurement within the section. For the geophysical variables where the measurements are located at the limit between two sections, the value is assigned to both neighbouring sections. This method is used for the following variables:

S0 - S9, F0 - F9, C9, FS, Ca, Fe, Hm, Py, Ep, Cl, ZZ, IC, IO, De, Po, Su, Qv, Re, Rs, Ip.

Binary coding is used for the rocktypes

gr, ge, pp, qp, qd, ap, pe, do.

Linear interpolation is used for the T+P-value and the TE-value from the tubewave measurements. The ratio (T+P)/TE is equal to the TR value for one meter sections, see section 4.4.

#### 4.4 Tubewave measurements

The variable easily retrieved from the tubewave measurements by a graphical procedure using the EBBA image analysis system is the sum (T+P) of the tube wave amplitude, T, and the compressional wave amplitude, P. A method must then be designed that can give the ratio between the two waves (T/P). From this ratio and the tubewave frequency, Beydon et al (Stenberg and Olsson, 1985) claim that it is possible to calculate the permeability of the fractures. The tubewave measurements in KKL02 are presented by Stenberg (1984). The tubewave ratio can be calculated using two different methods:

- Deleting high values and calculate a moving average to represent the P-value of the background.
- Selecting discrete values along the borehole to represent the local background of the P-value.

Using the obtained P-value the linear interpolation procedure is used to get the one meter section background P-values. The T+P-value is also transformed to one meter sections by linear interpolation. Using these two values, the ratio can be calculated for each one meter section. The ratio can now be used as a potential indicator of the hydraulic conductivity. The two methods are described below.

##### Method 1

The P-value can be estimated as a moving average of the T+P value over e.g 10 to 15 meters after deleting the high T+P values. The moving average estimate of the P-wave is named TE. The ratio (T+P)/TE can then be used to study the correlation with the hydraulic conductivity. The analysis procedure used is:

- store the tubewave image of the velocity in m/s in the EBBA image analysis system.

- manually set the location as a trench line of the first T-wave along the borehole.
  
- retrieve the amplitude by plotting this trench giving the (T+P)-value. Depending on difficulties in locating the trench line some values may be negative, indicating that the maximal values of the wave have not been located exactly. These negative values must be deleted before further analysis.
  
- smoothing the (T+P)-value by an neighbouring averaging procedure to estimate the background value of the P-wave called TE.
  
- calculate the ratio (T+P)/TE.

#### Method 2

The same procedure is used as above to obtain the T+P-value. The P-values are selected manually along the hole to get a value that represent the local background. These values are used to calculate the one meter section background P-value by a linear interpolation procedure. The ratio is calculated using the procedure described above.

In this study the second method was used. It is fast and gives a rough indication of the possibility to obtain a tubewave variable possibly correlating to hydraulic conductivity. In the SIMCA analysis all three variables were used, the T+P-value named TP, the estimation of the background P-wave, named TE, and the ratio (T+P)/TE named TR.

#### 4.5 Reference levels used

For the depth recording different reference levels are used for different methods and also for different boreholes. In the SIMCA analysis it is important that all variables in each

borehole are measured from the same location in the borehole. Therefore the depth recording must be adjusted for some of the variables. Since the most tedious variable to adjust are the core logging variables, all other variables in each borehole are adjusted to the same reference level as for these variables.

To be able to correlate the results from this study to other studies and measurements, the reference levels used in the different boreholes and the constants added to the depths recorded are shown in Table 4.3. The information of the reference levels used is taken from Persson (1986).

Table 4.3 Reference levels used and corrections applied for the different boreholes.

Borehole	Variable 1-11	12-52	53-55	Casing top above ground (m)
KKLO 1	ground	ground	-	0.65
KKLO 2	ground	ground	ground	0.35
KKLO 6	ground	ground	-	0.40
KKLO 9	0.20	casing	-	0.20
KKLO12	0.40	casing	-	0.40
KKLO14	0.30	casing	-	0.30

## 5. MULTIVARIATE ANALYSIS OF DATA FROM KLIPPERÅS

### 5.1 Hydraulic conductivity models

#### 5.1.1 Initial PCA-analysis

Initially, the intention was to establish a comprehensive model which could be used to predict the hydraulic conductivity distribution along all boreholes selected. The basic objectives of the initial modelling were firstly, to obtain an overview of the entire data material and secondly, to test if the tubewave ratio (TR) possibly would be a useful variable in predicting hydraulic conductivity. The tubewave ratio has previously been used to estimate the hydraulic conductivity in selected borehole sections by e.g. Beydon et al (Stenberg and Olsson, 1985) and Stenberg (1987a). This was done by a manual procedure. In this study the tubewave data were processed by using the EBBA image analysis system to obtain a value of the tubewave ratio (TR) in 1 m-sections, see Section 4.4.

In the initial PCA-analysis all variables listed in Table 4.1, except hydraulic conductivity (since this variable only exists from 20 m-sections), were used. In the initial runs the significance of the correlation between the tubewave ratio (TR) and the hydraulic conductivity could not be unambiguously established. Additional runs were then made with the PLS-method in order to study the TR-variable separately and look for any strong (and consistent) correlation between this variable and estimated hydraulic conductivity values in 1 m sections (obtained from the hydraulic tests in 20 m-sections and the core mapping). It seems that although high tubewave ratios are correlated to high-conductive sections they sometimes also correlate to non-conductive sections. The correlation between the tubewave measurements and hydraulic conductivity was considered as ambiguous when investigating the entire range of measured hydraulic conductivities. Therefore, the tubewave variables (53-55) were omitted in the further modelling. However, the correlation between hydraulic conductivity and

tubewave measurements should be further investigated but it is beyond the scope of the present study.

In the initial modelling it was also concluded that some of the variables most likely would contribute little to the prediction of hydraulic conductivity and conductive fracture frequency. These variables (isotope- and core physical parameters) were also omitted in the further modelling (variables 44-52). No sufficiently strong correlation between hydraulic conductivity and some other variable measured could be established in the PCA-analysis. The further analysis was therefore performed by means of PLS-modelling.

#### 5.1.2 PLS-modelling

The results from the hydraulic tests in 20 m-sections were basically utilized in the modelling. Since all other variables represent 1 m-sections, a number of representative values of the hydraulic conductivity in 1 m-sections must thus be deduced from the 20 m- (and 5 m) sections, see below. Hence, the hydraulic conductivity (in 1 m-sections) was used as an additional variable in the modelling and its correlation to other variables could be studied in a more direct way. In the PLS-modelling selected values of the hydraulic conductivity (HC) in 1 m-sections were used in the Y-block and the other variables in the X-block, see Section 3.2.

The selection of representative conductivity values in 1 m-sections was mainly based on results from the hydraulic tests in 20 m sections and the geophysical logs. As will be seen in the following figures a strong correlation exists between the resistivity logs (GE, LR and NR) on the negative side and the sonic travel time (SO) together with the fracture group variables (F0-F9) on the positive side along the X-axis, see Section 6.1. This correlation is consistent in all models derived in this study. Previous studies in Klipperås (e.g. Sehlstedt and Stenberg, 1986) and investigations in other

areas, e.g. Finnsjön (Stenberg, 1987b) and the Stripa Mine (Fridh, 1988) have clearly shown that fractured borehole intervals with simultaneous low resistivity and high sonic travel time most frequently correspond to increased hydraulic conductivity. At Finnsjön these characteristics are well documented, in particular within Fracture Zone 2 (Andersson et al, 1988a). This feature, which seems to be applicable to all rock types studied, has been utilized in the selection of 1 m-sections with high hydraulic conductivity from the 20 m- (and 5m-) sections in this study.

Within the most conductive 20 m- (or 5 m) sections a number of representative 1 m-sections with significant simultaneous resistivity and sonic anomalies were selected also using the core log. The total transmissivity of the actual 20 m- (or 5 m) sections was then distributed to such 1 m-sections to obtain as representative values on the hydraulic conductivity as possible. In most cases the total transmissivity of the 20 m- (or 5 m) sections was distributed to very few 1 m-sections.

Apart from high-conductive sections, also 1 m- sections with intermediate and low hydraulic conductivity were estimated to obtain a representative model. Representative low-conductivity sections were selected from the 20 m-sections with zero-flow and using the core log. Normally, such 1 m- sections were assigned a hydraulic conductivity (and transmissivity) value of  $10^{-10}$  m/s which is slightly below the lower measurement limit of the hydraulic tests, see Section 4.2. In 1 m-sections containing no fractures at all, according to the core log, the K-values are set to  $10^{-12}$  m/s representing the conductivity measured on tight core samples.

It should be pointed out that the K-values assigned to the 1 m-sections are not regarded as fixed values by the PLS-prediction but only as "best estimates". By the PLS regression analysis both the section properties (log response, fractures etc.) as characterized by the variables in the X-block, and the assigned

K-values are taken into account. This may lead to that the predicted K-value in some sections sometimes may differ significantly from the assigned value if the properties of the actual section are not compatible with the latter value (according to the principal components).

The statistical deviation of each object (section) from the actual model (residual distance) is also calculated. By systematically incorporating sections with large residual distances to the model, the character of one (or several) principal components may ultimately be modified to include the specific properties of such sections.

Several preliminary PLS-model runs were made with input data (K-values) from boreholes KKL01, 02, 09 and 12. It was considered that the input data from these boreholes were the most reliable since manual correlations between the geophysical logs and the core logs (and the hydraulic conductivity) had previously been undertaken in these boreholes. The number of zero-flow 20 m-sections from the hydraulic tests were also significantly larger in these boreholes compared to KKL06 and 14. This means that a larger number of non-conductive 1 m-sections (below the measurement limit) could be used as input data to the models. A model, based on input data from the subvertical boreholes KKL01 and 02 only, was also established.

It was found that the sum of predicted hydraulic conductivities in 1 m-section, based on the latter model, generally showed improved agreement with the measured transmissivity distribution in 20 m-sections and also had shorter residual distances to the model compared to the predicted values from the previous model. These facts are likely to depend on the different directions of the above mentioned four boreholes in relation to the dip and strike of the major structures within the area, see Chapter 2. Radar measurements at the Klipperås site also indicate different properties of boreholes drilled in different directions (Carlsten et al, 1987). The borehole directions affect a.o. the frequency of fractures with



different angles relative to the borehole axis. Therefore, it was decided to establish separate models for boreholes KKL01 and 02 in a first model group, KKL06 and 09 in a second group and KKL12 and 14 in a third group.

From the regional map in Fig 2.1.1 it can be seen that KKL06 and 09 are directed towards the west while KKL12 and KKL14 are directed towards the north. It was found that the predicted conductivity values in KKL06 and the residual distances showed poor agreement to the measured transmissivity in 20 m-sections and to the model for KKL06 and 09, respectively. However, very few sections from KKL06 were included in the model. Yet, this indicates that borehole KKL06 has different properties than KKL09 (which borehole showed rather good agreement to the same model), although the boreholes are drilled in the same direction.

In fact, KKL06 showed a slightly better conformance to the model established for KKL12 and 14. According to the radar measurements in KKL06, the most prominent radar reflecting structures are subparallel to this borehole or intersect the borehole axis at small angles (Carlsten et al, 1987). Data from KKL06 were then excluded and a new model, based on data from KKL09 only, was established. The hydraulic conductivity distribution in KKL06 was subsequently predicted according to the model for KKL12 and 14.

The different models were then successively improved by including deviating sections into the models until a reasonable agreement between the predicted and measured transmissivities in the 20 m-sections was achieved. In the preliminary models the predicted conductivity values in sections containing only single fractures were significantly overestimated. Thus, more such sections were then included in the models with assigned K-values below the measurement limit, c.f. Fig 5.1.2. The hydraulic conductivity distribution of the 1m-sections used as input values to the different models are presented in Fig 5.1.2. The input values were not selected in order to fit a

particular statistical distribution. The distributions of the input data are generally bimodal.

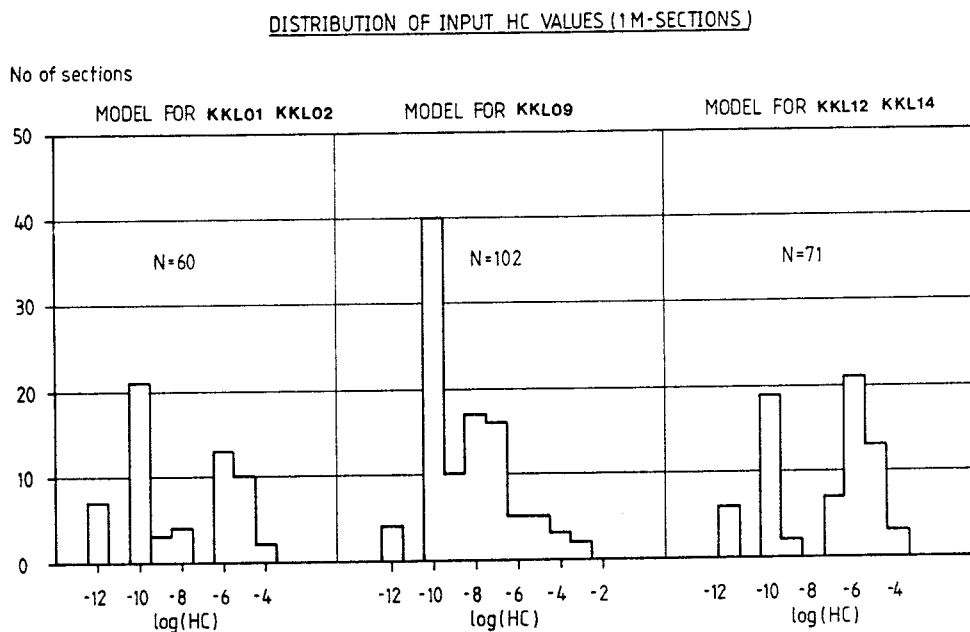


Fig 5.1.2 Distribution of input values of hydraulic conductivity of the different models at Klipperås.

## 5.2 Conductive fracture frequency models

Predicting the conductive fracture frequency (CFF) in a borehole is a difficult task since none of the variables used is specifically designed to measure or estimate this property. The definition of CFF is also somewhat subjective since the CFF depends on the definition of "conductive" in terms of hydraulic conductivity. The CFF can be regarded as a function of the hydraulic conductivity and depends on the (lower) measurement limit of the hydraulic tests.

Firstly, sections with predicted hydraulic conductivities below the lower measurement limit of the hydraulic tests ( $2 \times 10^{-10}$  m/s) are considered to contain zero conductive fractures in this study. Thus, such sections were excluded in the modelling. Secondly, sections within the interpreted local fracture zones were also excluded to obtain a measure of the rock mass only, see Table 2.2.

The conductive fracture frequency can be assumed to be correlated to the hydraulic conductivity. Therefore, the (predicted) hydraulic conductivity has been emphasized in the PLS-modelling. This is done by putting this variable in the Y-block. In the first model runs all fracture frequencies (variables 12-27 in Table 4.1) were also included in the Y-block together with the predicted hydraulic conductivity (HP). In the X-block the same variables were used as in the corresponding models for the hydraulic conductivity prediction (except the fracture frequencies). The predicted CFF with this configuration of variables appeared overestimated and too much governed by the total fracture frequency.

Clearly, to obtain a relevant estimation of CFF some kind of first approximation of this variable is needed. As the best possible estimate of CFF, a combination of predicted hydraulic conductivity (HP) and the frequency of fractures coated with ironoxide (Fe), according to the core logs, was then used. Thus, in the following model runs the variables HP and Fe were placed in the Y-block and the fracture frequencies in the X-block. To diminish the influence of the total fracture frequency the variables S9, F9, C9 and FS were excluded from the model.

Separate CFF-models, corresponding to the models used for prediction of the hydraulic conductivity, were established. The frequency of fractures coated with Fe in boreholes KKL06, 09, 12 and 14 is shown in Fig 5.2.1. In KKL12 and KKL14 also the frequency of calcite coated fractures is shown. Since iron oxide and hematite were not separately mapped in KKL01 and 02,

the total frequency of both minerals was used for these boreholes, see Section 4.2. The figure shows that the frequency of Fe-coated fractures, particularly in KKL14, is low and mainly concentrated to the uppermost part of the bedrock and in the fracture zones. In the CFF-model for KKL12 and 14 the fracture zones were not excluded due to the very few Fe-fractures in the rock mass. A characterization of the principal components of the different CFF-models and the variables used is shown in Section 6.2.

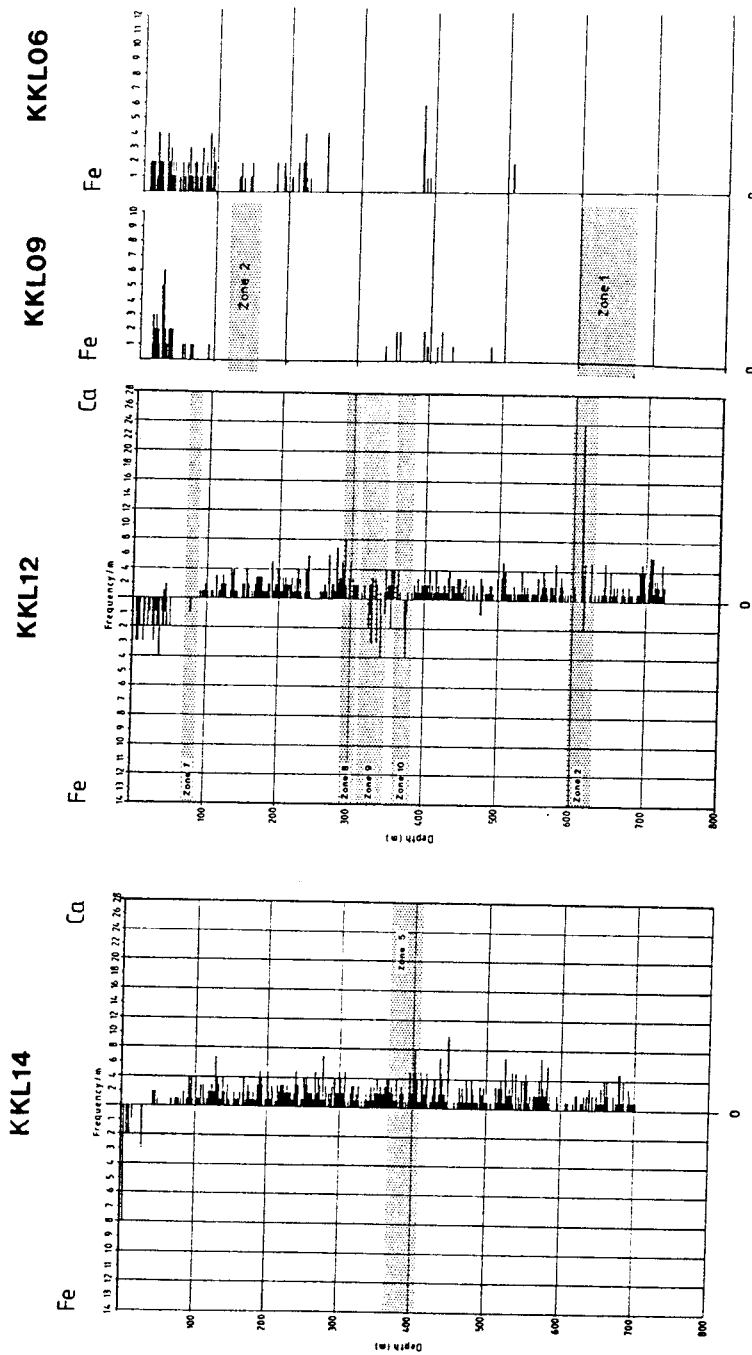


Fig 5.2.1 Frequencies of fractures coated with Fe in boreholes KKL06, KKL09, KKL12 and KKL14 (after Tullborg, 1986).

## 6. PREDICTION OF HYDRAULIC CONDUCTIVITY

### 6.1 Properties of the models established

#### 6.1.1 General

Plots of the variables, projected onto the hypothetical feature planes (Fig. 3.1.2) defined by the principal components used to predict the hydraulic conductivity in boreholes KKL01 and KKL02 are shown in the figures below. Normally, each principal component used is plotted on the Y-axis versus the first principal component on the X-axis in the plots, thus defining the different feature planes. On these planes, a positive and negative side is arbitrarily defined. The designations of the variables used are listed in Table 4.1. Before any calculation of the models all variables are scaled to unit variance. The scales of the axes (max and min-values) are shown below each diagram. The origin (marked by ++ ) of the plots has the coordinates (0,0). The variables represent high values where they are located in the plots and low values at the opposite side of the origin. The location (in the plots) of the sections used as input to the models, corresponding to the variable plots, can be studied in the object scores, see Section 3.1.

In the variable plots the correlation between two variables is expressed by the angle between the variables with respect to the origin. An angle of 90 degrees indicates totally independent variables whereas zero or 180 degrees indicate completely correlated variables, directly and inversely correlated, respectively. The distance from the origin to the location of the variables in the plots indicates the amount of expressed variance by the hypothetical feature plane. A long variable vector from the origin indicates high importance whereas a short vector indicates small importance of the actual variable.

As described above, the first principal component (PC1), which is plotted on the X-axis, represents the most dominating

properties of the model. The hydraulic conductivity variable (HC) is found in the upper right corner in the plots. This means that variables located towards the right in the diagrams (positive X-direction) correlate directly with the hydraulic conductivity for PC-1 whereas variables displayed towards the left (negative X-direction) correlate inversely to HC (the higher value on the variable the lower the hydraulic conductivity and vice versa).

The more extreme position of a variable on either side of the origin along the X-axis (for PC1), the stronger the correlation is to the hydraulic conductivity (either directly or inversely). The same is true with respect to the Y-axis for PC2. This means that the uppermost variables of PC2 show a direct correlation to the hydraulic conductivity in this component while the lowermost variables are inversely correlated to this parameter. Variables located near the origin are either uncorrelated or poorly correlated to the hydraulic conductivity and thus have little influence on the predicted conductivity values.

#### 6.1.2 Model for K1 1 and K1 2

For this model the following variables were used (Table 4.1):

X-block: 1-29, 31-35, 43

Y-block: 56.

Number of input HC-values: 60 (28 from K1 1 and 32 from K1 2)

Confidence volume distance = 0.798

In Table 6.1.1 the most dominating variables on the negative and positive sides of the model for KKL01 and KKL02 are listed. The variables on the negative side are ranked in decreasing importance (from left to right) whereas the variables on the positive side are ranked in increasing importance in the tables

Table 6.1.1 Explained variance of the X- and Y-block and important variables of the model for KKL01 and KKL02.

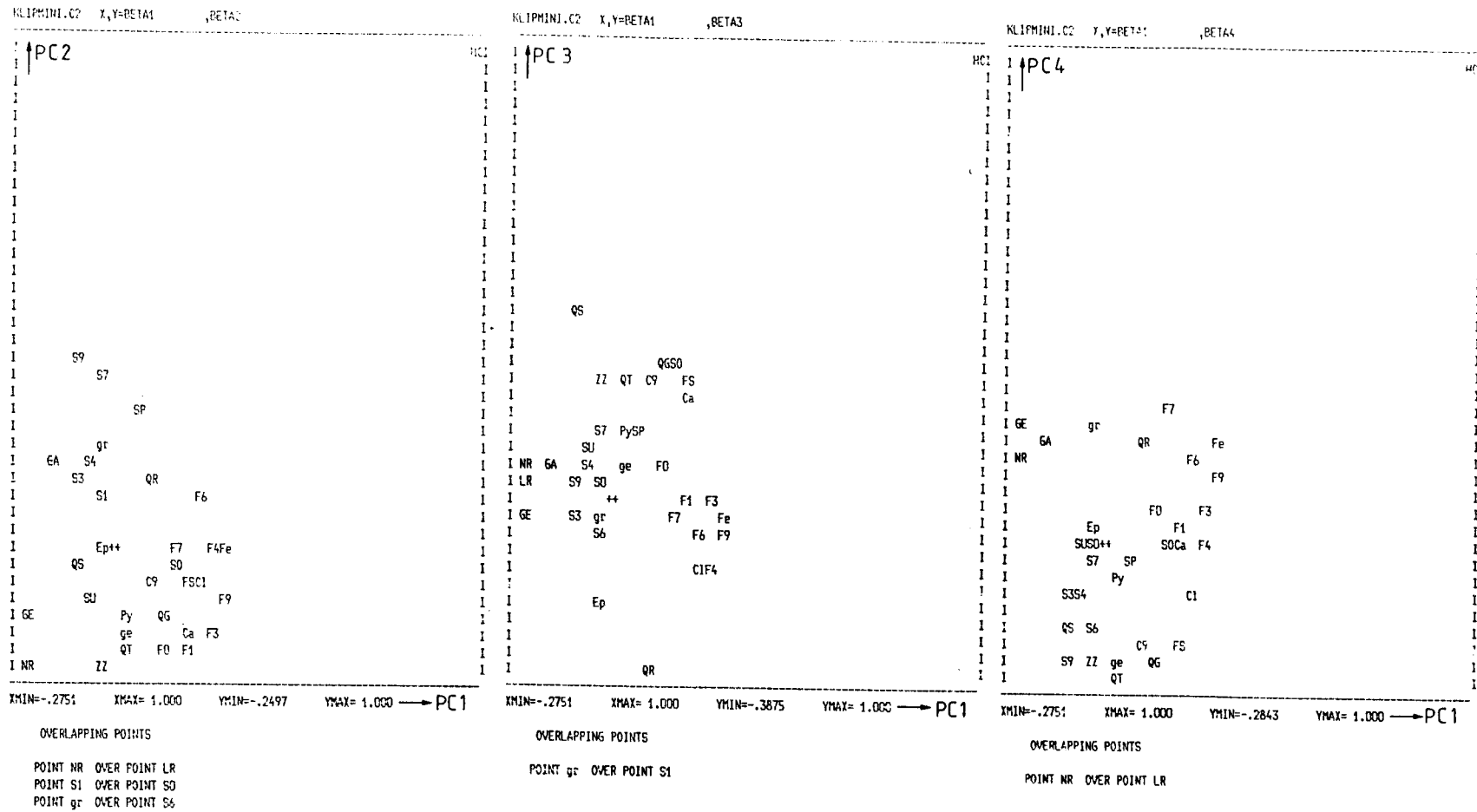
PC	X-block	Y-block	Important variables -/+
1	21.6	67.4	- NR, GE, LR, GA, S3, S9 + Ca, Cl, F6, F3, F4, Fe, F9, HC
2	29.6	78.8	- LR, NR, ZZ, F0, F1, ge + GA, gr, S6, SP, S7, S9, HC
3	35.9	82.1	- QR, Ep, Cl, F4, S6, S1 + ZZ, Ca, FS, C9, QG, S0, QS, HC
4	44.8	83.8	- QT, ZZ, C9, QG, FS, QS, ge + GA, F6, gr, Fe, GE, QR, F7, HC

below. For example, for PC1 normal resistivity (NR) and single-point resistivity (GE) are the most important (strongest) variables on the negative side of the feature plane whereas hydraulic conductivity (HC) is the most important variable on the positive side. This can be seen along the X-axes on the graphs in Fig. 6.1.1. In this figure the variable plots, defined by the four principal components of the model are presented.

For PC1, the fracture group variables F9, F4, F3 and F6 (Table 4.1) are the most pronounced on the positive side together with the fracture filling variables Fe, Cl and Ca and the hydraulic conductivity (HC). This means that these variables show a relatively strong and direct correlation with hydraulic conductivity. On the negative side the most dominating variables are the resistivity log parameters GE (geohm or single point), LA (lateral) and NR (normal resistivity) and GA (gamma) together with the single fractures S3 and S9. These variables thus show a relatively strong but inverse correlation



Fig 6.1.1 Variable plots of the principal components of the model for KKL01 and KKL02.



to HC. The other variables are relatively neutral in the first principal component with respect to HC.

For PC2, the most dominating features are the single fracture variables S9, S7 and S6 and the SP-log (self potential) in granite (gr), associated with the gamma log (GA) on the positive side. On the negative side again the resistivity variables, and the fracture group variables F0 and F1 in greenstone (ge) dominate. The depth variable (ZZ) indicates that the variables on the positive side of PC2 correspond to properties at relatively shallow depths while the variables on the negative side are associated with properties at greater depths.

The positive side of PC3 describes variables directly correlated to hydraulic conductivity, such as the fracture variables FS and C9, the borehole log variables QS, QG and S0 and the mineral Ca. The depth variable ZZ indicates that the properties are associated with relatively great depths. On the negative side of PC3 the variables Ep (epidote) and chlorite (Cl) and QR (resistivity of the borehole fluid) and the fracture variables F4, S6 and S1 are the most dominant. As before, these variables are inversely correlated to HC.

On the positive side of PC4 the fracture group variables F7 and F6 in granite (gr) at relatively shallow depths and GA dominate together with the variables QR and Fe. On the negative side fractured (FS) and crushed (C9) greenstones (ge) at greater depths (ZZ) with high salinity (QS), temperature (QT) and temperature gradient (QG) dominate.

A schematic geological interpretation of the different principal components is presented in Table 6.1.2.

Table 6.1.2 Schematic interpretation of the dominating features of the principal components used in the model for KKL01 and 02.

PC	Negative side	Positive side
1	tight rock	fractured rock (fracture groups)
2	tight deep green-stones	granite with single fractures
3	epidote and chlorite healed fractures	deep fractured rock
4	deep crushed green-stones	subhorizontal fractures in granite

### 6.1.3 Model for KKL09

For this model the following variables were used (Table 4.1):

X-block: 1-29, 31-35, 41-43

Y-block: 56.

Number of input HC-values: 102 (from K1 9)

Confidence volume distance = 0.8104

The geological conditions in this borehole are described in Appendix B. Two porphyry dykes occur in the borehole. This rock type is designed as 'av' in the variable plots. Also thin dykes of greenstone, dolerite and aplite occur. The five principal components used for prediction of hydraulic conductivity in KKL09 are shown in Figs 6.1.2a-b. The dominating variables for each principal component are shown in Table 6.1.3.

The positive side of PC1 mainly represents sections in granite with high frequency of fractures in fracture clusters, particularly F6 (61-750), coated with Fe and associated with

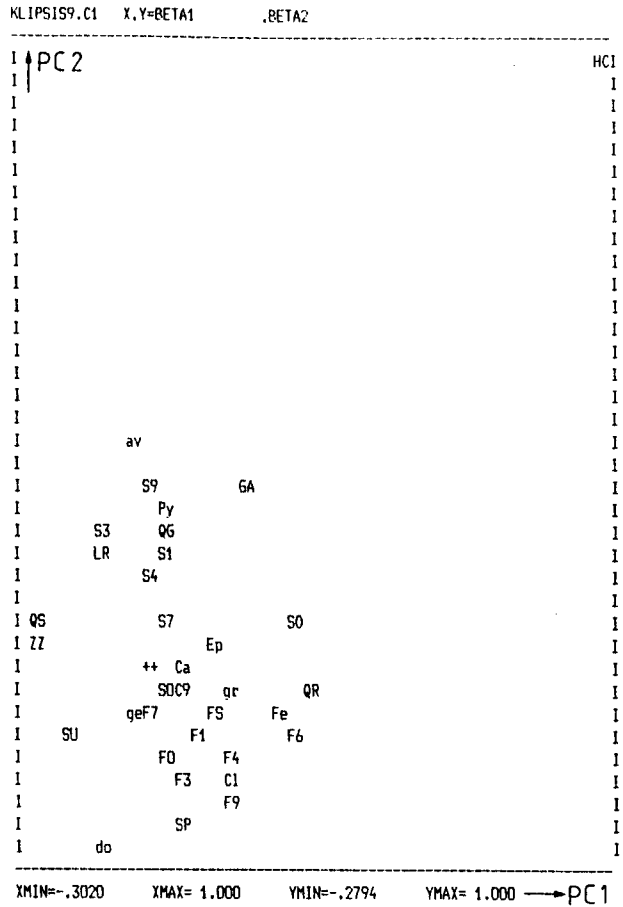
Table 6.1.3 Explained variance for the X- and Y-block and important variables of the model for KKL09.

<u>PC</u>	<u>X-block</u>	<u>Y-block</u>	<u>Important variables -/+</u>
1	13.6	62.1	- QS, QT, ZZ, SU, do, GE, LR, NR + gr, GA, Fe, F6, S0, QR, HC
2	24.0	71.3	- do, SP, F9, F3, C1, F4 + QG, GE, NR, Py, S9, GA, av, HC
3	33.2	76.0	- GE, NR, LR, GA, QG, S6, QR + ZZ, F0, F1, C1, F9, SP, HC
4	38.7	78.0	- Ca, LR, F9, F3, C1, ZZ, NR, F4 + S6, S3, QR, SU, do, HC
5	43.1	79.5	- S9, SU, do, S4, S1, S0, F4 + GE, NR, ge, F9, F3, F7, LR, HC

high values of sonic, natural gamma and fluid resistivity. On the negative side non-conductive sections in dolerite (with high susceptibility) at great depth with high fluid temperature and salinity dominate. The positive side of PC2 is dominated by conductive porphyrys (av) with single fractures with pyrite and high fluid temperature gradients. On the negative side of PC2 dolerites associated with fracture groups with chlorite and high values of self potential dominate.

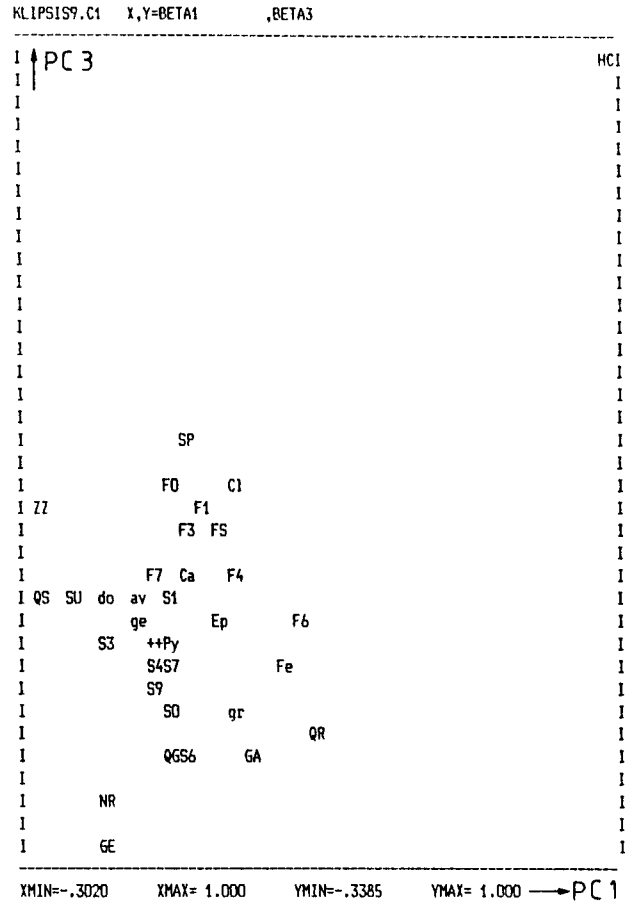
The positive side of PC3 constitutes relative deep conductive sections with fracture groups with chlorite-coated fractures and high self potential. On the negative side high resistivity sections with single fractures (S6) and high fluid temperature gradients and fluid resistivity.

Fig 6.1.2a Variable plots of the first, second and third principal component of the model for KKL09.



OVERLAPPING POINTS

POINT NR	OVER POINT GE
POINT S3	OVER POINT NR
POINT C9	OVER POINT S6



OVERLAPPING POINTS

R	OVER POINT LR
5	OVER POINT S0
1	OVER POINT C9
	OVER POINT F9

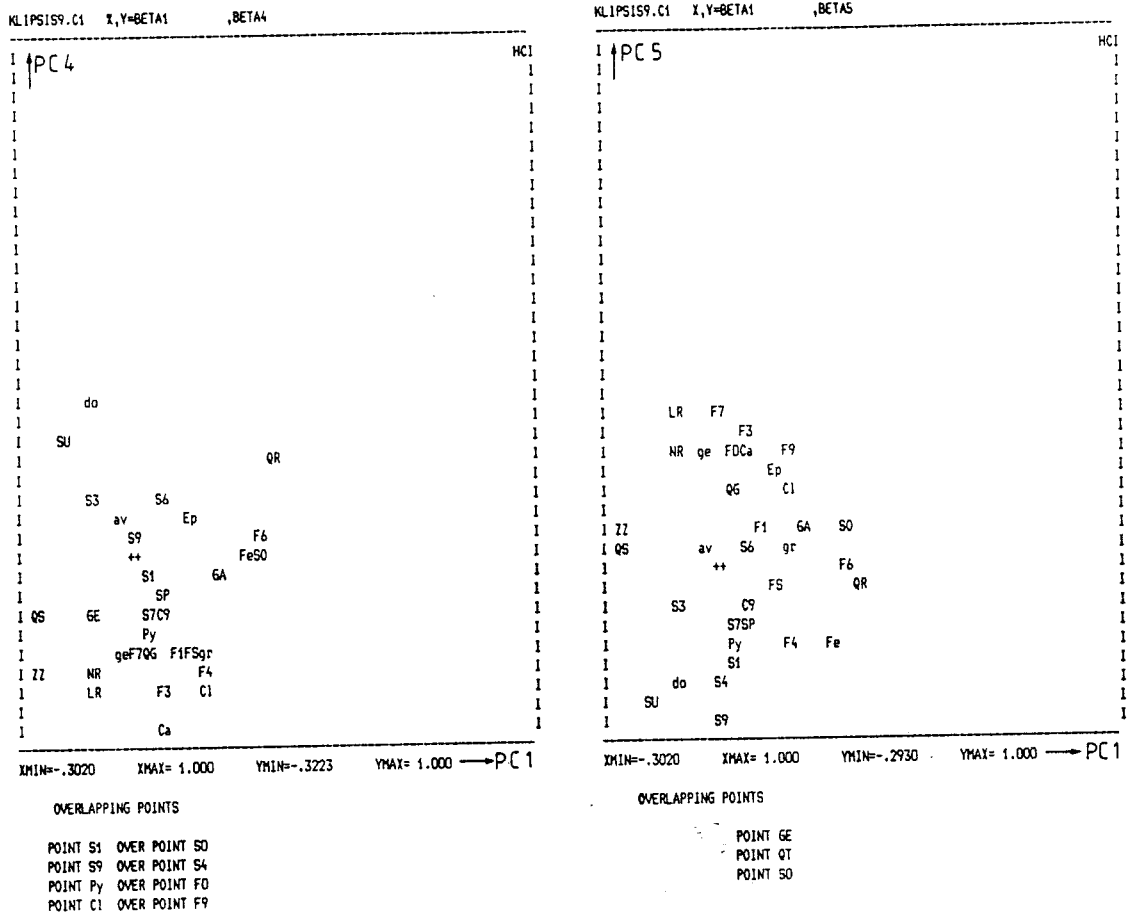


Fig 6.1.2b Variable plot of the forth and fifth principal component of the model for KKL09.

PC4 mainly describes conductive dolerites with single fractures, particularly S3 (31-45°) and S6 (61-75°), with high susceptibility and fluid resistivity. On the negative side deep low-conductive (greenstones) with fracture groups (F3, F4 and F9) with calcite and chlorite dominate.

PC5 describes conductive greenstones with fracture groups (with the minerals calcite, epidote and chlorite with high resistivity and fluid temperature gradients). On the negative side low-conductive dolerites with single fractures (coated with pyrite) and high susceptibility dominate.

A schematic interpretation of the dominating features of the different principal components is presented in Table 6.1.4.

Table 6.1.4 Schematic interpretation of the principal components used in the model for KKL09.

PC	Negative side	Positive side
1	deep dolerites	fractured granite
2	fractures dolerite with chlorite	porphyrys with single fractures with pyrite
3	tight rock with single fractures	(deep) fractured rock with chlorite
4	deep fractured rock with calcite and chlorite	dolerite with single fractures
5	dolerite with single fractures	fractured greenstones

#### 6.1.4 Model for KKL12 and KKL14

For this model the following variables were used (Table 4.1):

X-block: 1-29, 31-35, 42, 43

Y-block: 56

Number of input HC-values: 70 (53 in KKL12 and 18 in KKL14)

Confidence volume distance: 0.8603

The borehole descriptions are found in Appendix B. The five principal components (PC1-5) used for prediction of hydraulic conductivity in KKL12 and KKL14 (plotted versus PC1) are shown in Fig 6.1.3. The dominating variables of the principal components are shown in Table 6.1.5. As before, the positive side of PC1 constitutes conductive borehole sections (in granite) with fracture groups with the mineral Cl, (Fe and

Ep) and high sonic travel times. On the negative side of PC1 low conductive, high-resistivity greenstones at great depth with single fractures and high fluid temperature dominate. On the positive side of PC2 conductive sections with high frequency of single fractures and high fluid temperature gradients occur. The negative side of PC2 is dominated by deeply located sections with high fluid temperature and high frequency of fracture groups with the mineral Ca (Fe and Cl).

PC3 describes on the positive side sections with high frequency of calcite-filled fractures, particularly F6-fractures, with high fluid salinity. On the negative side high frequency of single fractures with the minerals Fe and Ep and high sonic times and fluid resistivity occur.

Table 6.1.5 Explained variance and important variables of the model for KKL12 and KKL14.

<u>PC</u>	<u>X-block</u>	<u>Y-block</u>	<u>Important variables -/+</u>
1	20.5	69.7	- GE, NR, LR, ge, QT, SU, S9, ZZ, S3 + F3, F1, S0, Cl, F9, HC
2	26.9	85.9	- QT, F4, ZZ, F9, Ca, F0 + S4, QG, S7, S3, S9, HC
3	30.3	88.9	- Fe, QR, Ep, S1, S7, S3, S0 + QS, F6, Ca, HC
4	35.2	89.9	- QS, C9, FS, S7, S9, S4, Ca + gr, Fe, NR, LR, Py, QR, QG, HC





On the positive side of PC4 conductive sections in granite with the minerals Fe and pyrite and high fluid temperature gradients and fluid resistivity dominate. On the negative side low-conductive sections with high total fracture frequency and fractures in crush zones occur with high fluid salinity.

A schematic interpretation of the dominating features of the different principal components is presented in Table 6.1.6.

#### 6.1.5 Summary of models

Using the established models to predict the hydraulic conductivity of the boreholes reveals that most data are within the statistical confidence volume of the models. The main feature of the models, consistently appearing in the first principal component, is the polarization between rocks with high frequency of clustered fractures on the positive side and homogenous rocks with few or no fractures on the negative side. The second most important feature, represented by the second principal component, is the polarization between high and low frequencies of single fractures. In both principal components the hydraulic conductivity is positively correlated to high fracture frequencies.

The explained variance in the X- and Y-block by the principal components is expressed as a percentage of the total variance. This percentage indicates how much of the information in the X-block that is utilized to predict the HC-variable in the Y-space. As an example for KKL01 and KKL02, 21.6 percent of the variation of the X-variables is utilized to predict 67.4 percent of the variation in hydraulic conductivity, just by using the first principal component.

Table 6.1.6 Schematic interpretation of the dominating features of the principal components used in the model for KKL12 and KKL14.

PC	Negative side	Positive side
1	deep greenstones with single fractures	fractured (granite) with chlorite
2	deep fractured rock with calcite	single fractures with high temp. gradients
3	single fractures with Fe and Ep	subhorizontal fractures with calcite
4	fractured rock with high salinity	granites with high temp. gradients and pyrite

## 6.2 Distribution of predicted hydraulic conductivity

### 6.2.1 General

The predicted hydraulic conductivities in 1 m-sections according to the actual PLS-models are presented in Figs A.1-A.6 in Appendix A. Firstly, all predicted values in 1 m-sections are plotted along each borehole. Besides the hydraulic conductivity also the conformance of the properties of the predicted sections to the actual model, expressed by the residual distance of the X-variables to the actual model, is presented. Predicted values falling outside the scales of the strips in the figures in Appendix A are truncated at the maximum or minimum values of the scales. The hydraulic conductivity range plotted is  $10^{-13}$  -  $10^{-3}$  m/s and the residual distance range plotted is 0-2. The transmissivity range plotted is  $10^{-11}$  -  $10^{-3}$  m<sup>2</sup>/s.

To compare the predicted conductivity values in 1 m-sections with the hydraulic conductivity obtained from hydraulic tests in 20 m (or 25 m) sections, predicted transmissivity values for

corresponding 20 m sections have been calculated by summing up the 1 m-transmissivity values within the 20 m-sections. Both the measured and predicted transmissivities of the 20 m sections are presented in Appendix A and also shown in cross-plots in figures below. To obtain a detailed picture of the predicted hydraulic conductivity distribution within the interpreted local fracture zones, these intervals are shown on an enlarged scale.

#### 6.2.2 Borehole KKL01

The overall predicted hydraulic conductivity distribution in 1 m-sections of the subvertical borehole KKL01 together with the residual distances to the model is shown in Fig A.1 in Appendix A.

The conformance of the predicted sections to the actual PLS-model is rather good in KKL01. For this model, one standard deviation of the confidence volume (RSD) corresponds to a residual distance of 0.798. Most sections in granite fall within this residual distance (Fig. A.1). However, for sections in greenstones and aplites and in particular porphyrys below 450 m the conformance to the model is much lower. This is likely to depend on the fact that too few sections in these rock types are included in the actual PLS-model. However, porphyrys and aplites only constitute about 10% of the total borehole length in KKL01, see Table A.1 in Appendix A. Most greenstones, porphyrys and aplites occur below c. 330 m in KKL01.

The predicted conductivity values for greenstones, porphyrys and aplites at depth are generally very low. This is consistent with the hydraulic test results which indicated a hydraulic conductivity below or near the lower measurement limit below 331 m (Gentzschein, 1986). However, predicted values in these rock types, associated with large calculated distances to the model, are considered as very uncertain.

The measured transmissivity distribution in 25 m-sections from the hydraulic tests is also shown in Fig A.1 together with the predicted transmissivity in corresponding sections. A cross-plot of predicted and measured transmissivity in the 25 m sections is shown in Fig 6.2.1. By this comparison, corrections due to the inaccuracies in the depth recordings for the hydraulic tests, depending on the stretching of the multi-hose used for the tests, have been made. A constant correction factor of +1.012 (1.2 %) has been applied for all borehole sections.

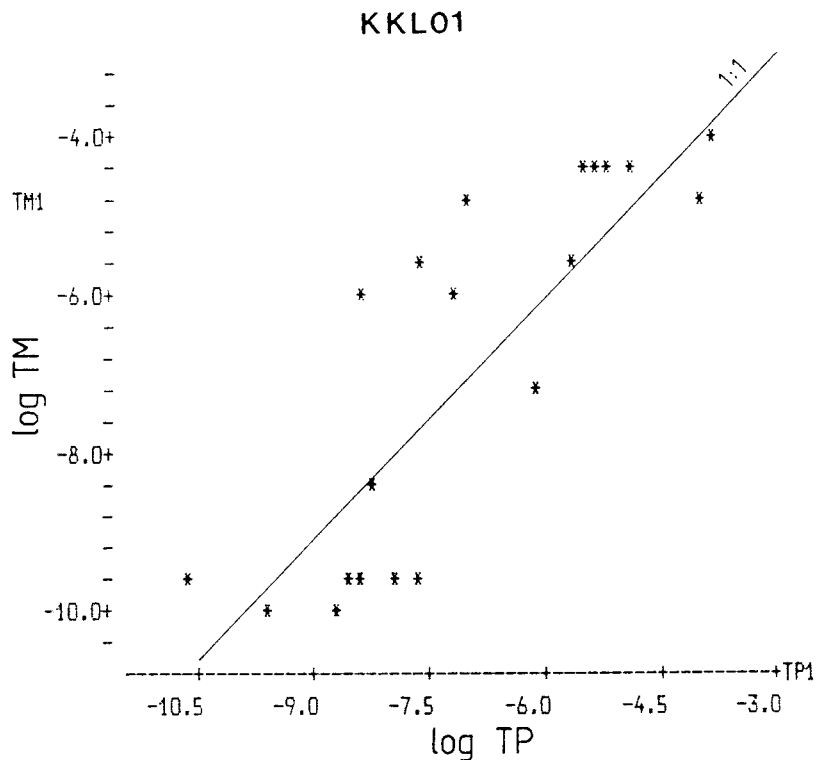


Fig 6.2.1 Crossplot of the logarithm of measured (TM) and predicted (TP) transmissivity values in 25 m sections in borehole KKL01.

From Fig A.1 it can be seen that the general pattern of predicted transmissivity is in fair agreement with the measured

one in the 25 m-sections. The predicted transmissivity is though somewhat underestimated in the upper half of the borehole and slightly overestimated in the lower half, compared to the measured ones. The predicted low-conductivity interval 88-122 m is consistent with the core log which indicates relatively tight rock with only a few (single) fractures in this interval and also with the geophysical logs which show very calm responses. Below 312 m, the predicted hydraulic conductivity is low which is consistent with the hydraulic test results. Greenstones and porphyrys are rather frequent in this interval. The crossplots of predicted and measured transmissivities show good agreement between results.

Large deviations between predicted and measured transmissivity values occur in the interval 156-231 m (corrected 157.87 - 233.77 m) in KKL01. In this interval, which consists of alternating granites and greenstones with a few aplite sections, the predicted transmissivity is significantly underestimated in comparison to the measured. Inspection of the core in this interval reveals no obvious signs of water-conducting fractures. The sonic- and resistivity logs show a few small anomalies. Both single fractures and fracture clusters occur within the interval. The reasons for the underestimation of the predicted transmissivity are not clear in this case. However, some of the predicted 1m-sections conform poorly to the actual model in this interval and are therefore uncertain.

In the interval 331-381 m (corrected 334.97 - 385.57 m), which mainly consists of granite, the predicted transmissivity is overestimated. The hydraulic tests indicate a hydraulic conductivity below the measurement limit in the entire interval. The sonic log is rather calm whereas the resistivity logs indicate a few intervals with decreasing resistivity. The overestimation of predicted transmissivity is probably due to a few sections with single fractures and fracture groups coated with ironoxide (in addition to other minerals). The presence of ironoxide in fractures is important when calculating predicted

values (according to the principal components of the models). In the remainder of the borehole the predicted transmissivities agree relatively good with the measured.

The highest hydraulic conductivity values predicted in KKL01 mainly correspond to the two major structural units defined by Sehlstedt and Stenberg, 1986: Unit A (64 - 88 m) and Zone 10 (280 - 310 m). According to the predicted values the lower part of Unit A is the most conductive. The highest conductivity is located in a thin, highly fractured greenstone and the contacts between the granite and greenstone. The predicted and measured (average) hydraulic conductivities of unit A and Zone 10 are shown in Table 6.2.1.

A detailed picture of the distribution of predicted hydraulic conductivity within Zone 10 and its adjacent parts is shown in Fig 6.2.2. The figure shows that the most conductive part of Zone 10 is concentrated to the middle and lower part in the interval 289-305 m. In this table the estimated hydraulic conductivity of Zone 10 from hydraulic tests (Gentzschein, 1986) is also shown. The hydraulic conductivity of unit A was not measured separately but the measured section 81-106 probably includes this unit. The measured K-value of this section is shown in Table 6.2.1 within brackets.

Table 6.2.1 Measured and predicted hydraulic conductivity of zone 10 and unit A in KKL01.

Rock unit	Borehole interval (m)	Effective width (m)	Hydraulic conductivity measured (m/s)	Hydraulic conductivity predicted (m/s)
Zone 10	280-310	10.5	9.3 E-7	7.2 E-6
Unit A	64-88	24	(5.8 E-6)	6.3 E-6

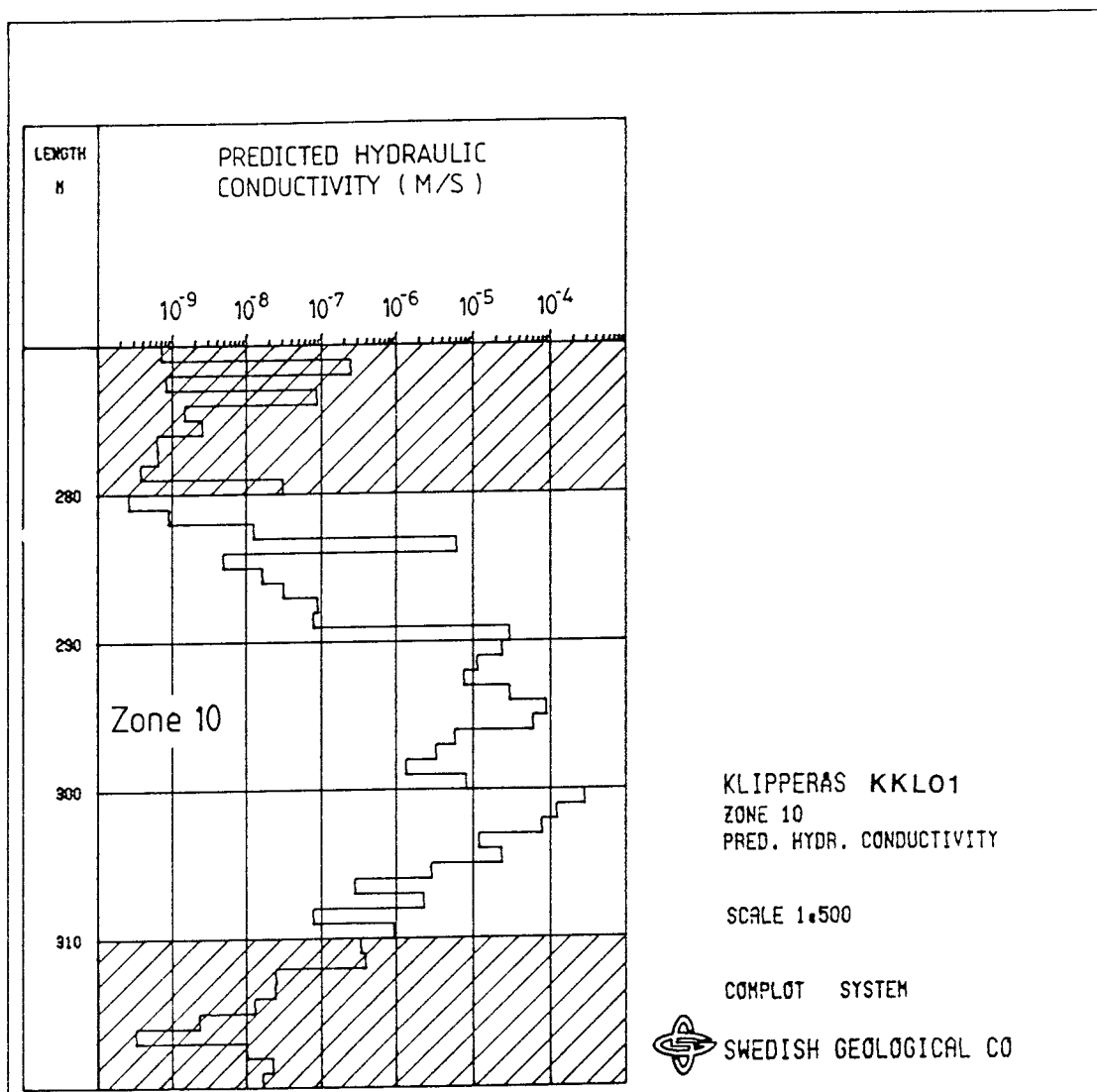


Fig 6.2.2 Distribution of predicted hydraulic conductivity within Zone 10 in KKL01.



### 6.2.3 Borehole KKL02

The overall predicted hydraulic conductivity distribution in 1 m-sections in KKL02 together with the residual distances to the model are shown in Fig A.2 in Appendix A. The conformance of the predicted sections to the actual PLS-model is relatively good in KKL02. For the actual model one standard deviation of the confidence volume corresponds to a residual distance of 0.798.

Most predicted conductivity values, both in granite and greenstone, fall within this residual distance. Exceptions are the low-conductive greenstone interval at 587-621 m (particularly the lower part), section 774-777 m (where the core is missing), the extremely conductive section at about 803 m (belongs to Zone H1) and the crushed zone at about 867 m. As also pointed out by Sehlstedt and Stenberg (1986) the latter zone has distinct sonic and resistivity anomalies and was interpreted as a subhorizontal shear-zone by Olkiewicz and Stejskal (1986). The lower part of the greenstone interval 587-621 m is highly magnetic, which is exceptional for greenstones in KKL02 (Sehlstedt and Stenberg, 1986). This fact may influence the residual distance to the model in this interval. Most of the sections with large residual distances from the model also correspond to the largest differences between predicted and measured transmissivities in KKL02.

The measured transmissivity distribution in 20 m sections in KKL02 is presented in Fig A.2 together with the predicted transmissivity of the corresponding 20 m-sections. By this comparison consideration was taken to the stretching of the hose used for the hydraulic tests, c.f. section 6.2.2. A crossplot of predicted and measured transmissivities in KKL02 is shown in Fig 6.2.3.

From Fig A.2 it can be seen that the general pattern of predicted transmissivities in 20 m-sections is in fair agreement with the measured one. The hydraulic conductivity is

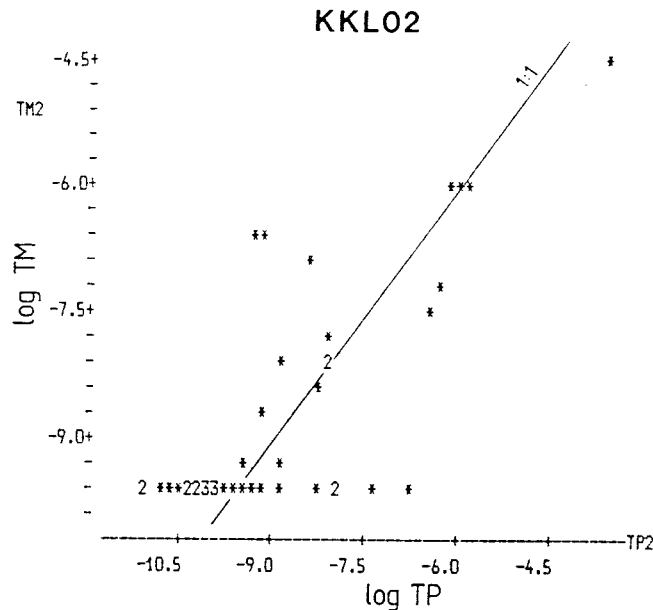


Fig 6.2.3 Crossplot of the logarithm of measured (TM) and predicted (TP) transmissivity in 20 m sections in KKLO2.

generally low in KKLO2. The largest deviations between predicted and measured transmissivities occur in the (uncorrected) sections 80-100 m, 340-380, 600-620, and 740-760 m. In the interval 80-100 m (corrected 80.96-101.20 m) the predicted transmissivity is significantly underestimated in comparison to the measured. This section only contains a few (single) fractures and the calm responses of both the sonic and resistivity logs indicate rather low-conductivity rock which is consistent with the predicted value. An inspection of the hydraulic test plots for this section indicates that the test results in this section may be unreliable due to a possible packer (or rock) leakage.

In the interval 340-380 m (corrected 344.08-384.56 m) the predicted transmissivity is overestimated. This is probably due to a few 1 m-sections containing single fractures with low resistivity but no sonic anomaly and a mapped thin crush zone, again with low resistivity but no significant sonic anomaly. According to the hydraulic tests the interval 340-380 m has a

transmissivity (hydraulic conductivity) below the measurement limit.

Also in the section 600-620 m (corrected 607.20-627.44 m) the measured transmissivity is below the measurement limit. However, the predicted transmissivity is  $T = 1.8 \times 10^{-7} \text{ m}^2/\text{s}$ . This value may be explained by two 1 m-sections in granite with rather high frequency of predominantly subhorizontal fractures (type F7) and single fractures (type S7) filled with chlorite, calcite and iron oxide (Fe). An inspection of the core in this interval indicates potential water-conducting fractures. This interval also has low resistivity and high sonic travel time and should thus, according to the features of the PLS-model, be conductive. This interval may be included in the next lower measured 20 m-section, 620-640 m (corrected 627.44-647.68 m) considering the uncertainties in the depth recording. The measured transmissivity of this section is  $T = 1.1 \times 10^{-8} \text{ m}^2/\text{s}$ .

In the section 740-760 m (corrected 748.88-769.12 m) the predicted transmissivity is significantly underestimated compared to the measured. The hydraulic tests reveal a transmissivity of  $T = 2.1 \times 10^{-7} \text{ m}^2/\text{s}$  in this section. The section contains relatively few (single) fractures in granite with rather calm resistivity and sonic curves down to 764.30 m. However, it should be noted that core data are missing in the interval 764.30-796.50 m. The geophysical logs indicate high fracturing and a number of greenstone sections (e.g. at about 768 m) in this interval. The prediction of hydraulic conductivity is thus here based on the geophysical logs only which makes the prediction more uncertain.

The highest predicted hydraulic conductivities in KKL02 are found in the upper parts of the bedrock, e.g. at about 60 m and at 121-123 m. The latter interval is highly fractured and partly crushed with clay alteration and ironoxide as fracture filling mineral (in addition to calcite and chlorite). Down to about 800 m only a few moderately conductive borehole intervals are found.

According to the geophysical logs the subhorizontal Zone H1 is located in the interval 792-804 m. A detailed picture of the predicted hydraulic conductivity distribution within Zone H1 and its adjacent parts is presented in Fig 6.2.4. According to this figure the most conductive part of Zone H1 is located between 800 and 804 m. The predicted and measured hydraulic conductivities of Zone H1 are shown in Table 6.2.2.

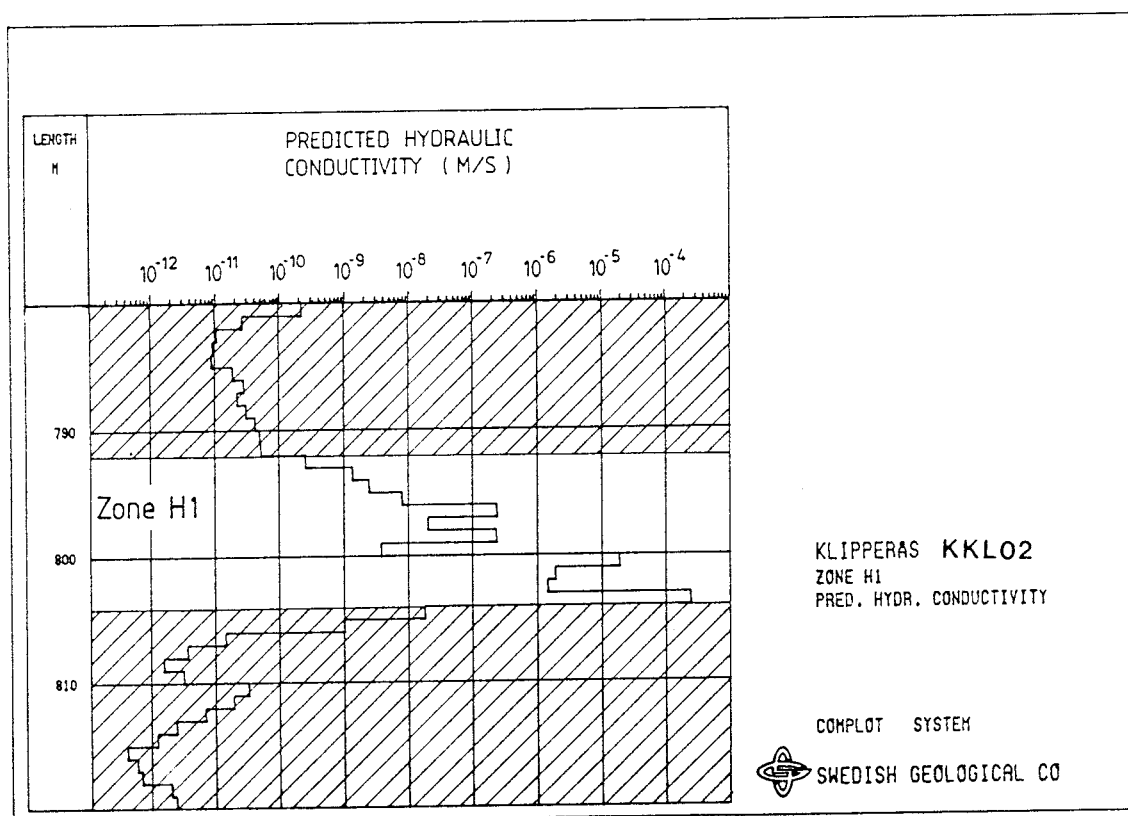


Fig 6.2.4 Distribution of predicted hydraulic conductivity within Zone H1 in KKL02.

Table 6.2.2 Measured and predicted hydraulic conductivities of zone H1 in borehole KKL02.

Fracture zone	Borehole interval (m)	Effective width (m)	Hydraulic conductivity measured (m/s)	Hydraulic conductivity predicted (m/s)
H1	792-804	12	2.0 E-6	3.5 E-5

#### 6.2.4 Borehole KKL06

As discussed in Section 5.1.2 the prediction of hydraulic conductivity in borehole KKL06 was based on the model for KKL12 and KKL14 since the borehole properties in KKL06 better conformed to this model compared to the model for KKL09. The overall predicted hydraulic conductivity distribution in 1 m-sections in KKL06 together with the residual distances of the sections to the model are presented in Fig A.3 in Appendix A. For the actual model one standard deviation of the confidence volume corresponds to a residual distance of 0.848.

As shown in Table B.5 in Appendix B granite is the dominating rock type in the borehole (c. 71 %) but also greenstone and porphyrys occur rather frequently (c. 15 % and 12 %, respectively). The greenstone and porphyry often alternate along the borehole (Sehlstedt and Stenberg, 1986). Several mafic dykes (basalt) are recorded in the borehole interval 338-371 m. High fracture frequency is closely correlated to greenstones and other mafic rocks.

As can be seen from Fig A.3 the predicted sections show rather poor conformance to the model in the borehole interval 219-300 m which is dominated by greenstone (unit A in Sehlstedt and Stenberg, 1986). Also the unit B between 338-372 m and unit C between 424-531 m conform poorly to the model. In these intervals granite, mafic rocks and porphyry alternate. Unit D

(552-569 m), which consists of granite, shows better conformance to the model. The deviations from the model in the units A-C are likely to depend on the fact that too few borehole sections in mafic rocks and porphyry are included in the actual model to accurately represent the properties of these rock types.

Large deviations also occur at 625 m (granite), in the greenstone interval 689-697 m and in the porphyry interval 728-744 m. The deviation in the latter interval is probably caused by a curious single-point resistance log indication. According to Sehlstedt and Stenberg (1986) this anomaly might be due to surface conduction in ironoxide in highly resistive rock. The most extreme deviation from the model occurs at about 469 m in a highly fractured porphyry with alternating thin greenstones. A step-like change in temperature occurs at 465 m according to Sehlstedt and Stenberg (1986). The transmissivity is accordingly high in this interval.

The measured and predicted transmissivity distributions in 20 m sections in KKL06 are shown in Fig A.3. A crossplot of measured and predicted transmissivities is shown in Fig 6.2.5. Corrections of the length values recorded for the borehole sections are made as described in section 6.2.2. As can be seen from these figures the agreement is generally poor between the measured and predicted transmissivities although the general pattern of the distributions is similar. The predicted transmissivities are in most cases underestimated in comparison to the measured ones.

The above facts show that borehole KKL06 has deviating properties compared to the other boreholes and a separate model for KKL06 would be required for an accurate prediction. One reason for the deviating properties of KKL06 may possibly be due to the alternating rock types in the borehole. It has clearly been shown that the model for KKL12 and KKL14 (and also other models derived) is not appropriate to model the hydraulic conditions in KKL06.

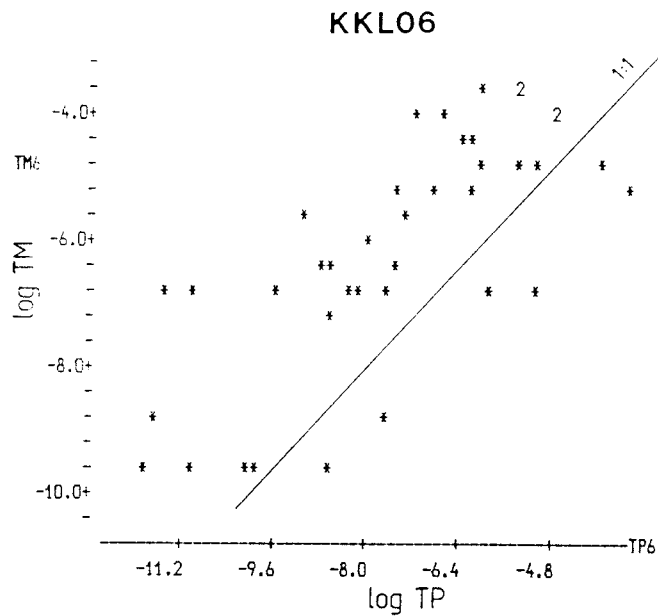


Fig 6.2.5 Crossplot of logarithm of measured (TM) and predicted (TP) transmissivity in 20 m sections in KKL06.

#### 6.2.5 Borehole KKL09

The overall predicted hydraulic conductivity distribution in 1 m sections in KKL09 together with the residual distances to the PLS-model are shown in Fig A.4 in Appendix A. As can be seen from this figure the predicted sections conform relatively good to the PLS-model for KKL09. For the actual model one standard deviation of the confidence volume (RSD) corresponds to a residual distance of 0.810.

Table B.7 in Appendix B shows that KKL09 consists of about 81 % granite and two porphyry dykes, greenstone, dolerite (and aplite). With a few exceptions the predicted sections in granite fall within (or close to) one RSD of the PLS-model. For greenstone sections the residual distances are generally larger. The predicted sections in the upper (quartz) porphyry

dyke at 269-300 m generally fall within one RSD while sections in the lower (plagioclase porphyry) dyke at about 731-780 m generally fall outside this range. This may be a reflection of the different mineralogical composition of the dykes. The predicted sections in dolerite and aplite normally fall within one standard deviation of the confidence volume of the model.

The measured and predicted transmissivity distributions for 20 m sections in KKL09 are presented in Fig A.4. Consideration is taken to the stretching of the multi-hose used for the hydraulic tests, c.f. section 6.2.2. A crossplot of predicted and measured transmissivities in KKL09 is shown in Fig 6.2.6. The figures show that the agreement between predicted and measured transmissivities is relatively good in KKL09.

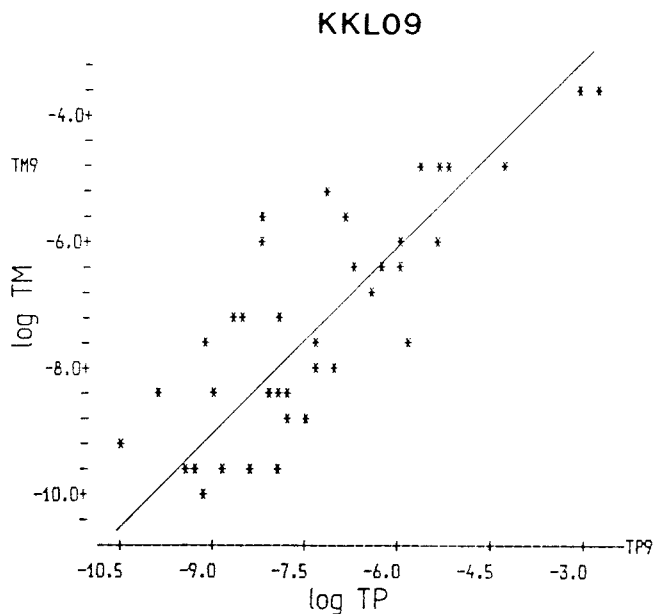


Fig 6.2.6 Crossplot of the logarithm of measured (TM) and predicted (TP) transmissivity in 20 m sections in KKL09.



The largest deviations occur in the (uncorrected) sections 150-170 m, 230-250 m, 410-430 m and 670-710 m. The predicted transmissivity in the section 150-170 m (corrected 151.80 - 172.04 m) in granite is overestimated compared to the measured. This is mainly due to the high predicted values in the low-resistive interval 152-160 m (which belongs to Zone 2) with small sonic anomalies. This interval contains both single fractures and fracture groups with a frequent abundance of hematite (together with chlorite) indicating potential water conducting fractures.

In the section 230-250 m (corrected 232.76 - 253.00 m) in granite the predicted transmissivity is significantly underestimated compared to the measured. The section mainly contains single fractures coated with calcite and chlorite. The resistivity- and sonic logs exhibit small anomalies at about 235 and 244 m. These two levels also correspond to the highest predicted conductivity values within the section. At about 244 m large calcite crystals (3 - 5 mm) and loss of drillwater was reported in the core log indicating conductive fractures.

In section 410-430 m (corrected 414.92 - 435.16 m), which mainly consists of granite with a thin aplite, the predicted transmissivity is again underestimated compared to the measured. The section contains rather few (single) fractures and exhibits very calm resistivity- and sonic responses, particularly below 420 m thus indicating rather low-conductive rock. A minor resistivity- and sonic anomaly between 414-415 m (near the upper packer) corresponds to the highest predicted conductivity. Possibly, leakage around the upper packer may have occurred during the hydraulic testing which then could explain the similar transmissivities measured in the section next above i.e. 390-410 m. The section 414-415 m contains a fracture parallel to the core axis, which may speak in favour of potential packer leakage.

In the entire interval 670-750 m (corrected 678.04-759.00 m) the predicted transmissivity is significantly underestimated,

particularly in the section 690-710 m. Granite dominates the entire interval but greenstone occurs in the upper part and plagioclase porphyry in the lower part. The section 690-710 m (corrected length 698.28-718.52 m) consists of granite with single fractures and a few fracture groups. Distinct resistivity- and sonic anomalies occur at a fractured zone at 698-700 m. Apart from this anomaly both logs are very calm.

Again the upper packer was located within or close to a fractured zone. This fact may possibly have increased the measured transmissivity of the section 690-710 m (and 670-690 m). The fractured zone at 698-700 m also contains fractures parallel to the core. This explanation is also supported by the hydraulic tests with a packer spacing of 5 m in KKL09. Inconsistent results from the 20 m and 5 m-tests were obtained in the sections 670-690 m and 690-710 m. The possibility of leakage around the packers was also indicated by Gentschein (1986).

The interval 710-750 m is dominated by plagioclase porphyry. Very few conductive 1 m-sections have been predicted in this interval. The resistivity and sonic logs only show two minor anomalies at about 731 m, close to a very thin dolerite dyke, and at about 740 m close to a fracture group in the porphyry. Although these anomalies are associated with a slight increase of predicted conductivities, the measured transmissivities in the sections 710-730 m and 730-750 m are more than one order of magnitude higher.

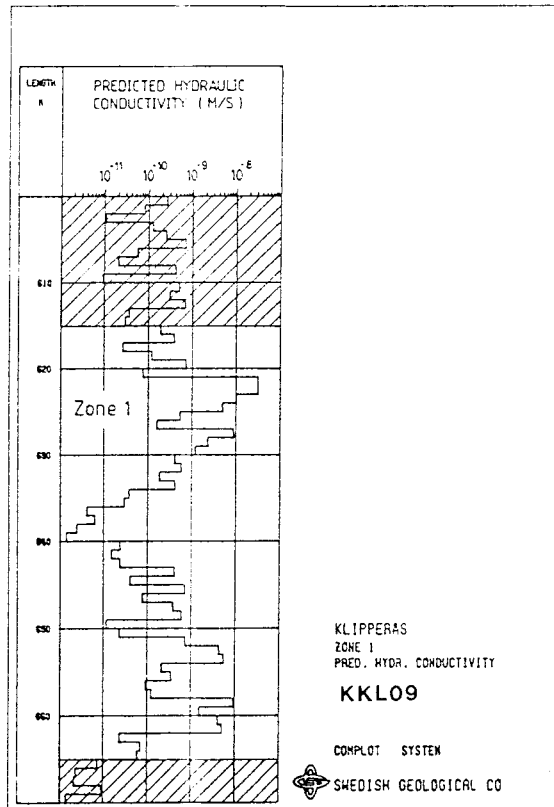
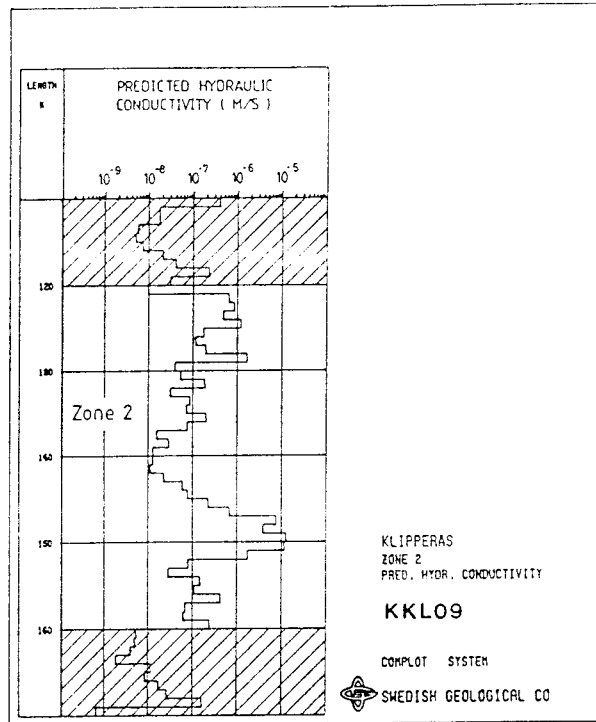
The highest predicted hydraulic conductivities in KKL09 are located within the upper c. 200 m of the borehole. Fracture Zone 2 is according to the geophysical logs located in the interval 120-160 m. The predicted hydraulic conductivity distribution in KKL09 within Zone 2 is presented in Fig 6.2.7. The figure indicates that the upper and lower parts of Zone 2 are the most conductive. The interval 146-156 m, where the resistivity and sonic anomalies are most prominent, is intensely altered with frequent hematite stained fracture

surfaces and clay altered fractures (Sehlstedt and Stenberg, 1986). The predicted and measured hydraulic conductivities of Zone 2 are shown in Table 6.2.3.

High predicted hydraulic conductivities also occur at about 188 m. This is due to a highly fractured low-resistive interval in granite with small sonic anomalies. The fracture surfaces are frequently coated with hematite in the interval. Also at about 395 m the predicted conductivity is high. This is again due to a highly fractured low-resistive interval in granite with small sonic anomalies and hematite stained fractures. The high conductivity of this interval is also confirmed by hydraulic testing in the section 390-395 m (corrected 394.68 - 399.74 m). The measured transmissivity of this section was  $5.7 \times 10^{-6} \text{ m}^2/\text{s}$  (Gentzschein, 1986). The predicted transmissivity in the same interval is  $T = 1.9 \times 10^{-6} \text{ m}^2/\text{s}$ .

Below about 400 m the predicted hydraulic conductivities in KKL09 are rather low. Fracture Zone 1 occurs in the interval 615-665 m. The predicted hydraulic conductivity distribution within Zone 1 is shown in Fig 6.2.7. The highest predicted conductivities occur in the fractured interval 622-627 m in granite, where the rock is strongly brecciated or mylonitized and altered (Sehlstedt and Stenberg, 1986). Hematite is also common as fracture filling mineral. The highest predicted conductivities of the lower part of Zone 1 occur in the crush zone in granite at about 653 m and in the fractured interval 658-662 m in granite. Hematite is also common in this interval. The predicted and measured hydraulic conductivities of Zone 1 are shown in Table 6.2.3.

The predicted hydraulic conductivities within unit A (356-374 m) and unit B (764-776 m), defined by Sehlstedt and Stenberg (1986), are rather low. This is also consistent with the hydraulic test results. Unit A is a very low-resistive interval and consists mainly of a dolerite dyke which is partly brecciated and crushed at the lower contact with clay altered



6.2.7 Distribution of predicted hydraulic conductivity within fracture zones 1 and 2 in borehole KKL09.

fractures. Unit B consists of a strongly mylonitized plagioclase porphyry with a high content of pyrite.

Table 6.2.3 Measured and predicted hydraulic conductivities of Zone 1 and Zone 2 in KKL09.

Fracture zone	Borehole interval (m)	Effective width (m)	Hydraulic conductivity (measured) (m/s)	Hydraulic conductivity (predicted) (m/s)
1	615-665	29	3.1 E-10	4.2 E-9
2	120-160	22	5.4 E-7	2.0 E-6

#### 6.2.6 Borehole KKL12

The overall predicted hydraulic conductivity distribution in 1 m-sections in KKL12 according to the actual PLS-model together with the residual distance of the predicted sections to the model are shown in Fig A.5 in Appendix A. For the actual model one standard deviation of the confidence volume (RSD) corresponds to a residual distance of 0.848. Table B.9 in Appendix B shows that KKL12 is dominated by granite. Minor dykes of quartz porphyry and aplite occur together with small inclusions of greenstone.

Fig A.5 shows that, with a few exceptions, most of the predicted values fall within or close to one RSD from the model. However, predicted values in greenstone and porphyry show somewhat higher deviations from the model. Large deviations in granite occur at the tectonic brecciated and mylonitized interval at about 299 m with a low natural gamma radiation. In general, low gamma radiation is associated with greenstones (Sehlstedt and Stenberg, 1986). High deviations from the model also occur in the intensely fractured,

mylonitized and brecciated granite sections at about 365 m (within Zone 9) and at about 614 m (within Zone 2).

The measured and predicted transmissivity distributions for 20 m sections in KKL12 are presented in Fig A.5. Corrections for the stretching of the multi-hose used for the hydraulic tests are made, see section 6.2.2. A crossplot of predicted and measured transmissivities in KKL12 is shown in Fig 6.2.8. The agreement between predicted and measured transmissivities is quite good in the upper half of the borehole (above c. 400 m). The largest deviations occur in the lower half, particularly in the intervals 400-460 m, 480-520 m and 540-560 m in which sections the predicted transmissivity is significantly lower than the measured. In the section 600-620 m the predicted transmissivity is overestimated.

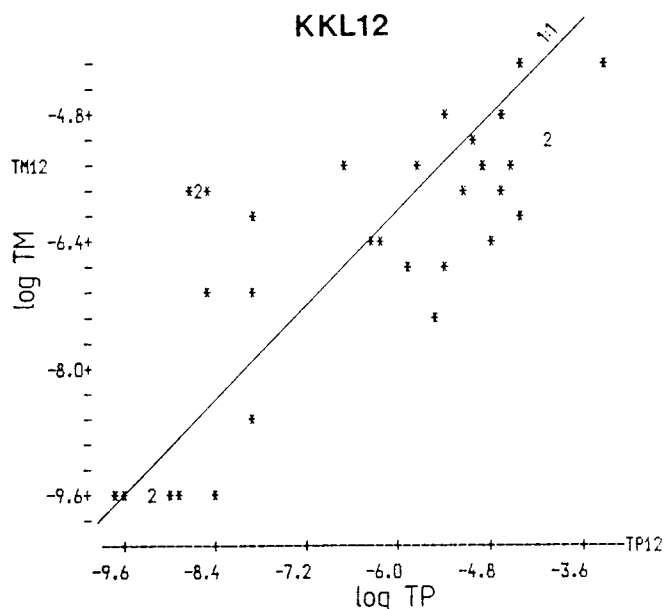


Fig 6.2.8 Crossplot of the logarithm of measured (TM) and predicted (TP) transmissivity in KKL12.

The interval 400-460 m (corrected 404.80 - 465.52 m) is dominated by granite with relatively few (single) fractures. Very few fractures coated with iron minerals occur in the interval except some hematite stained fractures. This interval, which is located between the fracture Zones 9 and 2, is characterized by a generally high resistivity close to the background level for unfractured rock (except minor indications at two mylonites at 427 m and about 447 m and in the greenstone at about 435 m). The sonic curve is also generally very calm in the interval except a few minor anomalies. According to Sehlstedt and Stenberg (1986) there is a small temperature anomaly at 435 m in the greenstone in connection to a minor sonic anomaly. Apart from this anomaly it is difficult to detect any other potential conductive sections within the entire interval based on the geophysical logs and core logs. Instead, both these logs indicate low-conductive rock. Neither a visual inspection of the core in this interval indicates any signs of potential conductive sections.

Thus, there exists a major inconsistency between predicted and measured transmissivities in the interval 400-460 m (uncorrected lengths). The possibility of leakage in the test equipment or either rock- or packer leakage, resulting in an overestimated measured transmissivity, could not be excluded. Although not directly evident from the core log the latter phenomena could possibly be due to fractures parallel with the borehole axis or removal of rock fragments during drilling close to some of the packer seats used. On the other hand, isolated conductive features, not detectable from the geophysical logs or core logs or by visual inspection of the cores, may occur (single conductors). If possibly, this borehole interval should be re-tested with alternative packer seats in order to resolve the inconsistency between predicted and measured conductivity values.

In the measured intervals 480-520 m (corrected 485.76 - 526.24 m) and 540 - 560 m (corrected 546.48 - 566.72 m) the predicted transmissivity is also significantly underestimated. Again,

these intervals are characterized by a relatively low fracture frequency and rather calm resistivity and sonic logs. Minor resistivity and sonic anomalies occur at 489 m, 499 m and 508 m. At 565 m a small resistivity anomaly occurs but no sonic anomaly. Although the predicted hydraulic conductivity is slightly increased at these depths the predicted transmissivity of these 20 m-sections is still about three orders of magnitude lower than the measured.

In the section 600-620 m (corrected 607.20 - 627.44 m), which is located within Zone 2, the predicted transmissivity is significantly higher than the measured. This is due to a single 1 m-section (614-615 m) with high predicted hydraulic conductivity ( $K = 2.7 \times 10^{-6}$  m/s). Since the distance for this section deviates more than three standard deviations from the PLS-model, the predicted value is regarded as very uncertain. Still, relatively strong resistivity and sonic anomalies in the interval 614-616 m indicate a potential high-conductivity section. A temperature anomaly also occurs at 616 m (Sehlstedt and Stenberg, 1986). In the fractured interval at about 626 m relatively strong resistivity and sonic anomalies occur too. During the hydraulic test in the section 600-620 m a relatively low injection pressure was achieved indicating a rather high hydraulic conductivity. Below 620 m both the predicted and measured transmissivities are very low which is consistent with the geophysical logs and the core log.

High predicted hydraulic conductivities occur down to about 400 m in KKL12 apart from the low-conductivity interval 220-290 m. Below 400 m, relatively high conductivities are predicted in the highly fractured and altered interval 471-475 m with hematite and the fractured interval of 597 m in the uppermost part of Zone 2. As discussed above a high hydraulic conductivity is also predicted at 614 m within Zone 2.

Borehole KKL12 is intersected by several local fracture zones. Table 6.2.4 shows the interpreted zone intervals in the borehole, the estimated effective width and the measured and



predicted hydraulic conductivities of the zones. Detailed pictures of the predicted hydraulic conductivity distribution within each zone are presented in Fig 6.2.9a-b. The uppermost Zone 6 seems to be highly conductive, particularly in its uppermost and lowermost parts. The Zones 7, 8 and 9 seem to be connected hydraulically according to the predicted conductivities. The lowermost Zone 2 appears to have two distinct peak values at 597 m and 614 m with very low-conductive rock in between and above and below the zone.

Table 6.2.4 Measured and predicted hydraulic conductivities of the Fracture Zones penetrated by borehole KKL12.

Fracture Zone	Borehole interval (m)	Effective width (m)	Hydraulic measured (m/s)	conductivity predicted (m/s)
6	70- 88	12.5	4.4E-7	9.0E-6
7	288-306	13.5	2.5E-7	3.7E-7
8	312-347	28	3.2E-7	4.6E-6
9	362-384	17.5	5.5E-7	1.1E-6
2	595-630	13	9.6E-9	2.4E-7

#### 6.2.7 Borehole KKL14

The overall predicted hydraulic conductivity distribution in 1 m-sections in KKL14 is shown in Fig A.6 in Appendix A. Also the residual distances of the predicted sections to the PLS-model together with the measured and predicted transmissivities in 20 m sections are shown in the figure. A crossplot of predicted and measured transmissivities are presented in Fig 6.2.10.

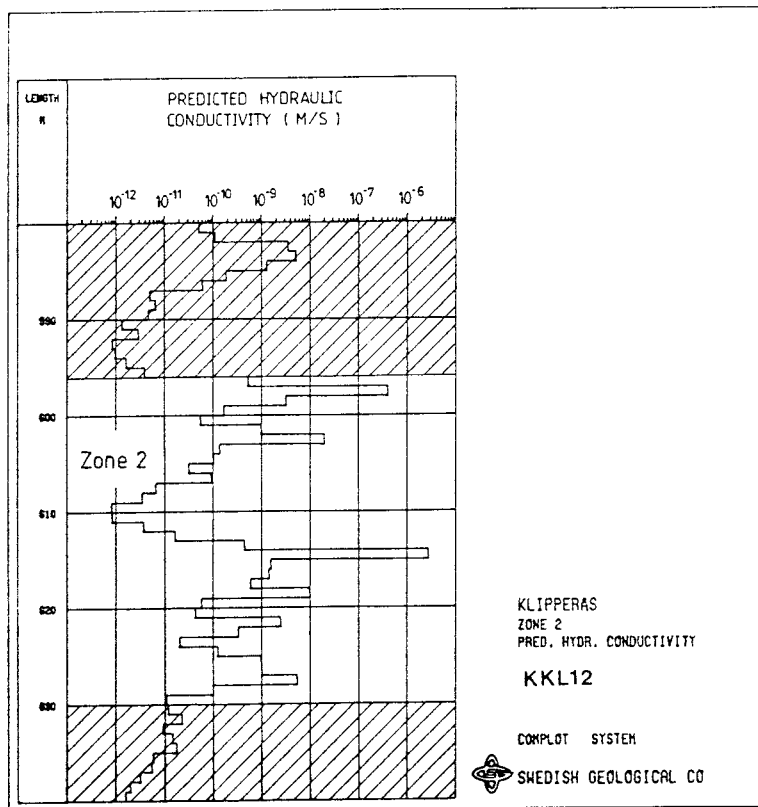
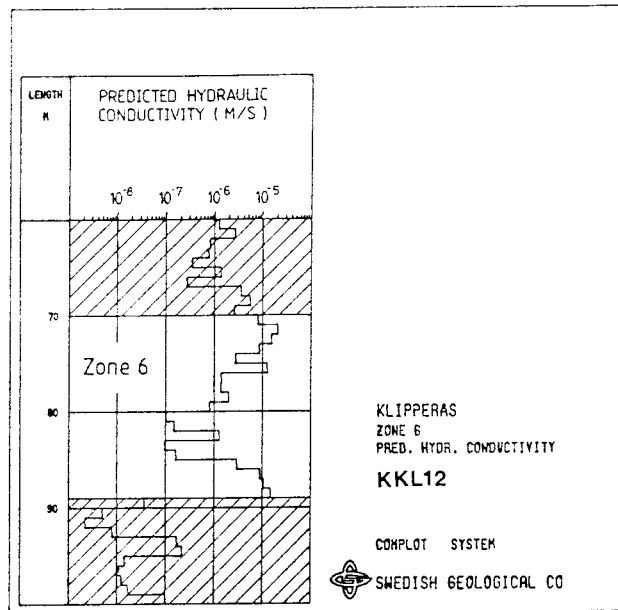


Fig 6.2.9a Distribution of predicted hydraulic conductivity within Fracture Zones 2 and 6 in borehole KKL12.

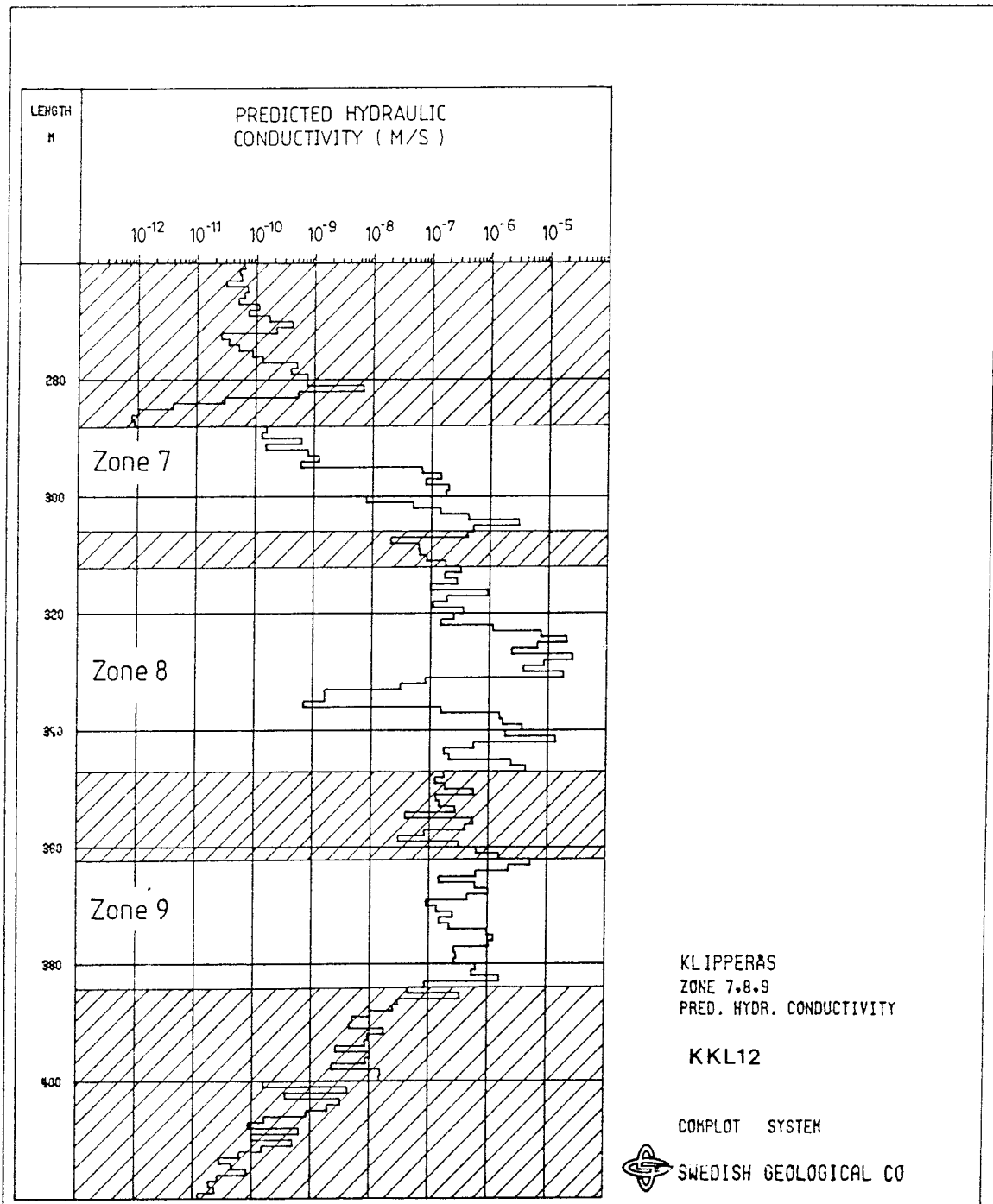


Fig 6.2.9b Distribution of predicted hydraulic conductivity within the Fracture Zones 7, 8 and 9 in KKL12.

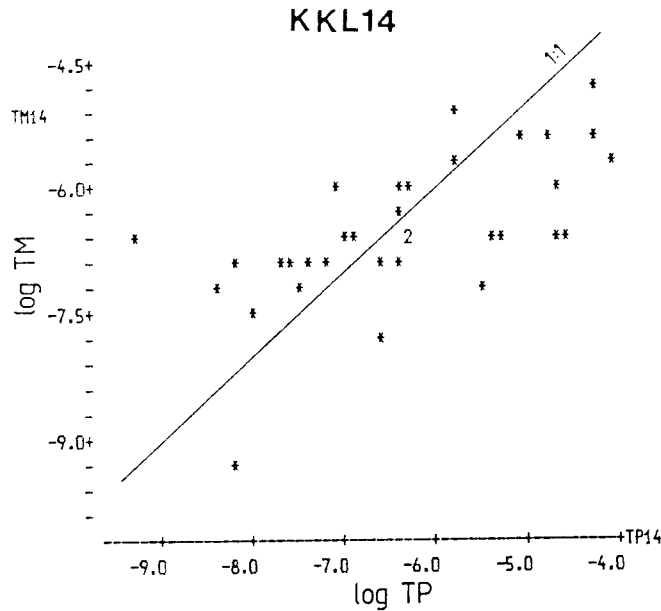


Fig 6.2.10 Crossplot of the logarithm of measured (TM) and predicted (TP) transmissivities in 20 m sections in KKL14.

According to Table B.11 in Appendix B, KKL14 consists to about 80% of granite intersected by minor dykes of porphyry (c. 10%) and dolerite (c. 6.5%). Greenstone and aplite constitute the remainder. One standard deviation of the confidence volume of the model corresponds to a residual distance of 0.860. In the granite and dolerite the conformance to the model is generally good except in the intervals 15-30 m, 379-384 m and at 401 m, 551 m and 648 m. Also in the upper porphyry (215-248 m) the agreement is relatively good but the deviations in the lower porphyry (271-305 m) are greater. In sections in greenstone the conformance to the model is somewhat lower.

The measured and predicted transmissivity distributions for 20 m sections in KKL14 are presented in Fig A.6. A crossplot of measured and predicted transmissivities is shown in Fig 6.2.10. By the comparison, corrections for the stretching of the multi-hose is made, see Section 6.2.2. The figure shows

that the general agreement between predicted and measured transmissivities in KKL14 is quite good. Exceptions are the sections 280-300 m, 380-400 m, 560-580 m and 640-660 m. In the last three sections the predicted transmissivities are overestimated compared to the measured. In section 280-300 m (corrected 283.36 - 303.60 m) the predicted transmissivity is significantly underestimated. This section entirely comprises (the lower) porphyry dyke. As discussed above the conformance to the model is slightly lower in this interval. According to Sehlstedt and Stenberg (1986) the lower porphyry has a very high resistivity and low-resistivity indications within the porphyry are mainly due to greenstones. These facts most likely explain the predicted low transmissivity in this section.

In the section 380-400 m (corrected 384.56 - 404.80 m) located within Zone 4 the predicted transmissivity is overestimated compared to the measured. In this section high conductivities are predicted in the fractured interval 399-404 m, where the granite is very altered and deformed with significant resistivity and sonic anomalies (Sehlstedt and Stenberg, 1986). The hydraulic tests also show that this interval is conductive. Since the properties of a few of the predicted sections within this interval deviate from the model they must be regarded as somewhat uncertain, which may explain the difference between the measured and predicted transmissivities in this section.

In the section 560-580 m (corrected 566.72 - 586.96 m) the predicted transmissivity is again overestimated. The granite is here intersected by a thin greenstone at 571-575 m, characterized by a spike like resistivity anomaly (Sehlstedt and Stenberg, 1986). In the middle of this interval (573-574 m) a high conductivity is predicted which governs the total transmissivity of the 20 m-section. Since this conductivity value significantly deviates from the model it is considered as very uncertain (overestimated) which may explain the difference between the measured and predicted transmissivities.

In the section 640-660 m (corrected 647.68 - 667.92 m) the predicted transmissivity is also overestimated. The granite is here intersected by a thin greenstone at 656 m, which is associated with increased fracturing and alteration and a 0.40 m thick crushed zone (Sehlstedt and Stenberg, 1986). Immediately below this greenstone, relative high conductivities are predicted which account for the differences between measured and predicted transmissivities.

As can be seen from Fig A.6 predicted high hydraulic conductivity values generally occur down to about 130 m and in the intervals 377-404 m, 438-448 m and at 573 m in KKL14. In the upper part of the borehole (6 - 130 m) the highest conductivity values predicted generally correspond to simultaneous low-resistivity and distinct sonic anomalies in fractured, altered granite. In the lower part of the porphyry (271-305 m) very low conductivities are predicted as discussed above.

Fracture Zone 4 is located in the interval 368-410 m. A detailed picture of the predicted hydraulic conductivity distribution within Zone 4 in borehole KKL14 is shown in Fig 6.2.11. The measured and predicted hydraulic conductivities of Zone 4 are presented in Table 6.2.5. According to the predicted values the most conductive parts of Zone 4 seem to coincide with the altered granite intervals at 377-382 m, 389-392 m and 399-404 m. The uppermost and lowermost parts of the greenstone at 406-420 m are also relatively conductive. Within the intensely fractured and altered interval at 430-450 m, defined as Unit A by Sehlstedt and Stenberg (1986), high conductivities are also predicted, particularly at 444 m and 447 m. A temperature anomaly and loss of drillwater was reported at 446 m.

Table 6.2.5 Measured and predicted hydraulic conductivities of Zone 4 in KKL14.

Fracture Zone	Borehole interval (m)	Effective width (m)	Hydraulic conductivity measured (m/s)	Hydraulic conductivity predicted (m/s)
4	368-410	27	3.9 E-7	2.9 E-6

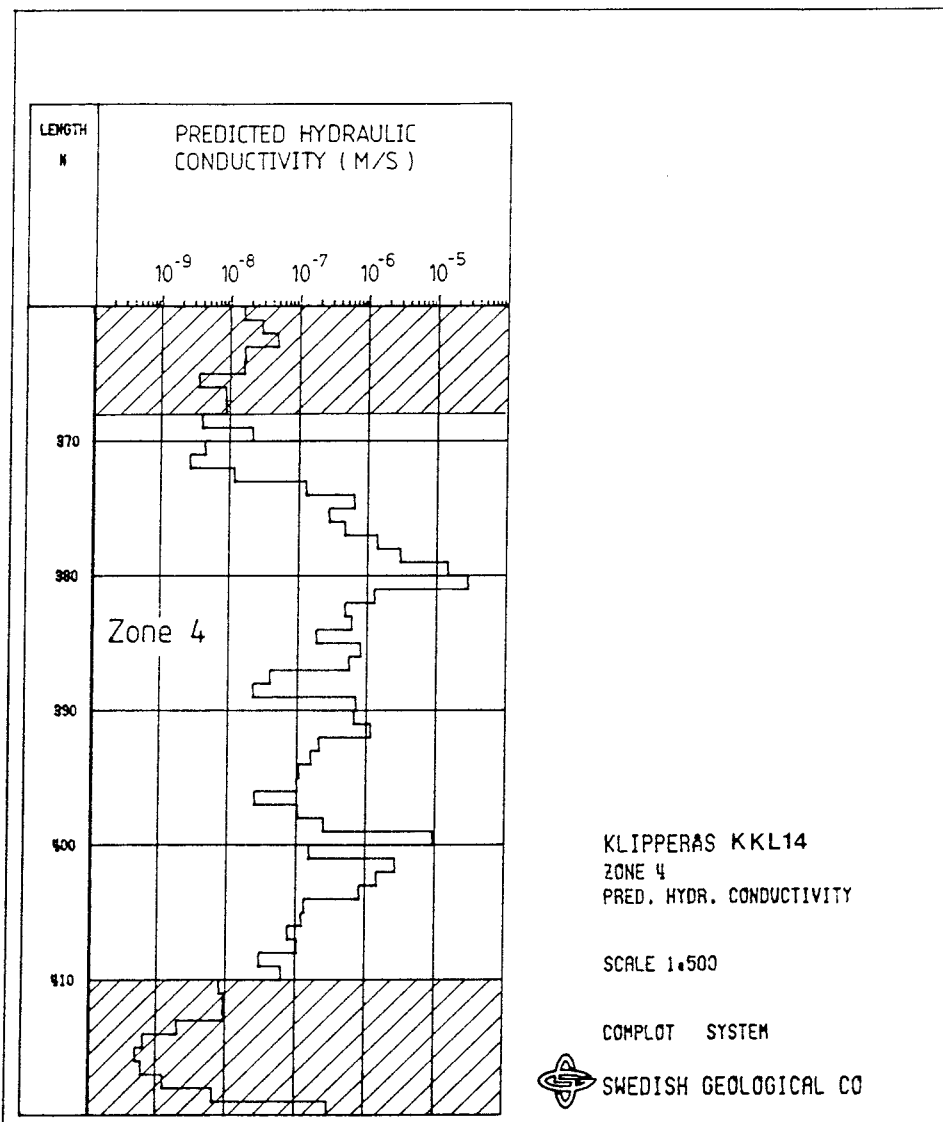


Fig 6.2.11 Distribution of predicted hydraulic conductivity within Fracture Zone 4 in KKL14.

## 7. PREDICTION OF CONDUCTIVE FRACTURE FREQUENCY

### 7.1 Properties of the models established

#### 7.1.1 General

Variable plots of the principal components used in the different models to predict the conductive fracture frequency (CFF) are shown in figures below. The most important variables in the different plots are also shown in tables. The designation of the variables used are shown in Table 4.1. The variable plots should be interpreted as described in section 6.1 for the hydraulic conductivity prediction. Basically the same variables were also used for the prediction of the conductive fracture frequency. The main differences in the layout of the two model sets are that the frequency of Fe-coated fractures was used in the Y-block together with the predicted hydraulic conductivity values ( $HP > 2 \times 10^{-10}$  m/s) in the latter modelling and that the total fracture frequency variables (24-27) were excluded. As a consequence, the Fe and HP-variables are more emphasized in the modelling. In summary, the following variable configuration was used for all CFF-models (Table 4.1):

X-block: variables 1-23, 28, 31-35, 41-43

Y-block: variables 29 and 57

#### 7.1.2 Model for KKL01 and KKL02

Variable plots of the four principal components used to predict the CFF in KKL01 and KKL02 are shown in Fig 7.1.1. The most important variables on the negative and positive sides are presented in Table 7.1. As before, the variables on the negative side are ranked in decreasing importance and in increasing importance on the positive side.





Table 7.1 Important variables of the CFF-model for KKL01 and KKL02.

PC	Variables -/+
1	- NR, ZZ, QT, QS, LR, GE + F6, Ca, QR, C1, F4, F3, Fe, HP
2	- HP, S7, GA, GE, gr, F7, QR + QT, ZZ, Ep, F3, F1, Fe
3	- QR, GE, S1, S3, S6, ge + Ca, NR, SU, ZZ, QT, Fe, HP
4	- HP, QG, Ca, QT, ZZ, S1, ge, av + gr, NR, S0, GA, LR, GE, Fe

The first principal component represents conductive Fe-coated fractures together with fracture groups with calcite and chlorite-coated fractures on the positive side. On the negative side of PC1 deeply located high-resistivity sections with high fluid temperature and salinity appear.

The positive side of PC2 describes low-conductive (greenstone) sections at depth with fracture groups containing epidote and Fe. On the negative side of PC2 conductive sections in granite with subhorizontal (single) fractures dominate.

The positive side of PC3 shows conductive sections at depth with high susceptibility and fluid temperature with fractures coated with Fe (and calcite). The negative side of PC3 describes low-conductive sections in greenstone with single fractures with high geohm and fluid resistivity.

Finally, PC4 shows low-conductive sections in granite with high geohm, lateral resistivity and gamma values and Fe-coated fractures on the positive side and conductive sections in

greenstone and acid volcanics (porphyrys) with calcite-coated fractures and high temperature gradients.

A schematic interpretation of the dominating features of the principal components is presented in Table 7.2.

Table 7.2 Schematic interpretation of the principal components of the CFF-model for KKL01 and KKL02.

PC	Negative side	Positive side
1	Deep, low-conductive rock	Conductive, fractured rock with Fe, Cl and Ca
2	Conductive granite with subhorizontal fractures	Deep low-conductive fractured rock with Fe and Ep
3	Low-conductive greenstone with single fractures	Deep, conductive rock with Fe and Ca
4	Deep, conductive greenstone and porphyry with Ca-coated single fractures.	Low-conductive granite with Fe.

### 7.1.3 Model for KKL09

The variable plot of the first and second principal components used to predict the CFF in KKL09 is shown in Fig 7.1.2 and the corresponding most important variables are listed in Table 7.3.

Table 7.3 Important variables of the CFF-model for KKL09.

PC	Variables -/+
1	- QS, ZZ, NR, Ge, av, SU + F6, gr, S0, SP, QR, Fe, HP
2	- gr, SP, QR + Py, F4, F6, Cl, av, Fe, HP

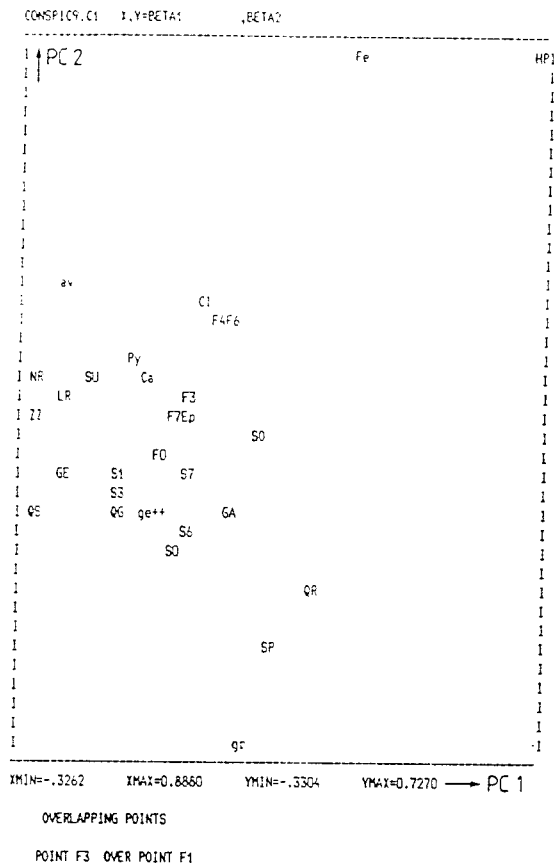


Fig 7.1.2 Variable plot of the first and second principal component of the CFF-model for KKL09

The negative side of PC1 describes deep, low-conductive sections in porphyry with high fluid salinity and susceptibility. The positive side of PC1 shows conductive sections in fractured granite with high sonic travel time, self potential and fluid resistivity and Fe-coated fractures. PC2 describes sections in granite with high self potential and fluid resistivity on the negative side and conductive, fractured sections in porphyry with the minerals Fe, C1 and Py on the positive side.

The interpretation of the dominating features of the principal components is summarized in Table 7.4.

Table 7.4 Schematic interpretation of the principal components of the CFF-model for KKL09.

PC	Negative side	Positive side
1	Low-conductive porphyry	Conductive granite with Fe
2	Low-conductive granite	Conductive porphyry with Fe, Cl and Py.

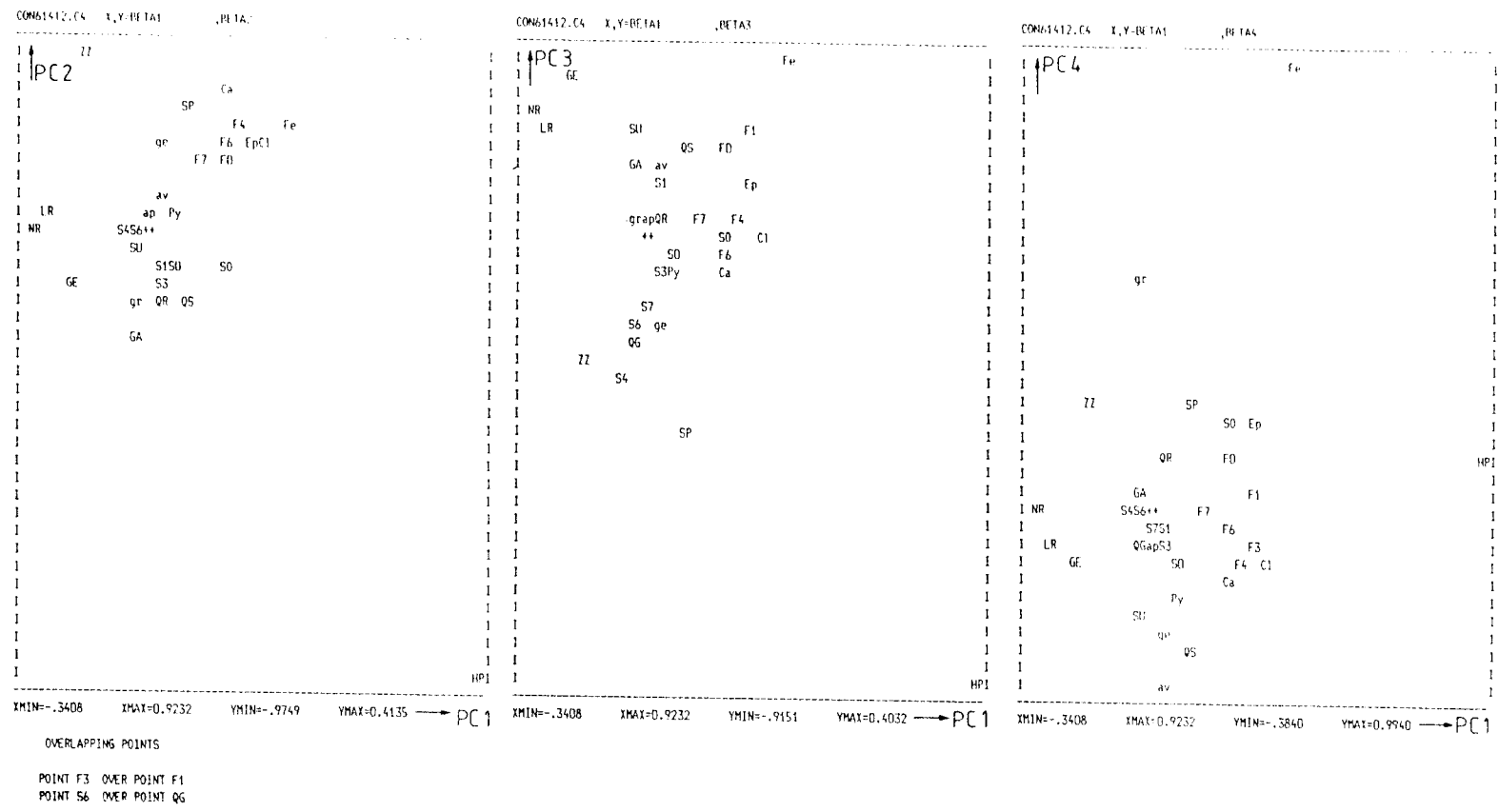
#### 7.1.4 Model for KKL12 and KKL14

The variable plots of the four principal components used to predict the CFF in KKL12 and KKL14 are shown in Fig 7.1.3 and the most important variables are listed in Table 7.5. As for the prediction of hydraulic conductivity the CFF-prediction in KKL06 are based on this model.

Table 7.5 Important variables of the CFF-model for KKL12 and KKL14 .

PC	Variables -/+
1	- NR, LR, GE, ZZ + SO, Ep, F4, F3, F1, Cl, Fe, HP
2	- HP, GA, gr, QS, QR, S3, GE + F3, Cl, Fe, F4, SP, Ca, ZZ
3	- HP, SP, S4, ZZ, QG, S6, ge, S7 + QS, FO, LR, SU, F1, Nr, Ge, Fe
4	- av, QS, ge, SU, Py + SO, Ep, SP, ZZ, gr, Fe

Fig 7.1.3 Variable plots of the principal components of the CFF-model for KLL12 and KLL14 .



The negative side of PC1 describes deep, low-conductive sections with high resistivity and the positive side conductive, fractured sections with the minerals Fe, Cl and Ep.

The negative side of PC2 shows conductive sections in granite with single fractures with high fluid salinity and fluid resistivity while the positive side describes deep low-conductive, fractured sections (mainly in greenstones) with Ca, Fe, Cl and Ep-coated fractures.

PC3 describes deep, conductive sections in greenstone with single fractures and high self potential and temperature gradient on the negative side. On the positive side of PC3 low-conductive sections in porphyry with steep fractures coated with Fe and high resistivity, susceptibility and fluid salinity.

Table 7.6 Schematic interpretation of the principal components of the CFF-model for KKL12 and KKL14 .

PC	Negative side	Positive side
1	Deep low-conductive rock.	Conductive, fractured rock with Fe, Cl and Ep.
2	Conductive granite with single fractures.	Deep, low-conductive (greenstone) with Ca, Fe, Cl and Ep.
3	Deep, conductive greenstone with single fractures.	Low-conductive porphyry with steep fractures coated with Fe.
4	Porphyry and greenstone with pyrite.	Deep granite with Fe and Ep.

In PC4 the hydraulic conductivity variable is relatively neutral. On the negative side sections in porphyry and greenstone with high susceptibility and fluid salinity and pyrite-coated fractures dominate. On the positive side

relatively deep sections in granite with high self-potential and sonic and Fe- and epidote-coated fractures dominate.

The interpretation of the dominating features of the principal components is summarized in Table 7.6.

#### 7.1.5 Summary of CFF-models

As for the hydraulic conductivity prediction the dominating feature of the CFF-models, appearing in the first component, is the polarization between low-conductive, sparsely fractured rock with high resistivity on one side and conductive, fractured rock frequently with Fe-coated fractures on the other side. The other components generally represent the properties of different rock types (low-conductive and conductive) and associated type of fracturing and fracture filling minerals. It is evident that both conductive and low-conductive Fe-fractures occur.

Concerning the explained variance in each block no reliable calculations could be obtained. The conformance of the properties of the sections to the actual CFF-models is not as good as for the models used to predict the hydraulic conductivity. Moreover, the models for KKL09 and for KKL12 and 14 appear somewhat unstable and the results vary rather much with the number of principal components included in the models. This is likely to be due to the properties of the Fe-variable used in the Y-block which influence the models rather strongly. As can be seen from Fig 5.2.1 the frequency of Fe-coated fractures in the boreholes is low, except in the uppermost parts of the boreholes and in the fracture zones. The results from the CFF-model for KKL01 and KKL02 are not directly comparable with the results from the other CFF-models since the first model is based on the total frequency of both Fe-oxyhydroxide and hematite-coated fractures, c.f. Section 5.2.



## 7.2 Distribution of predicted conductive fracture frequency

The predicted conductive fracture frequency (CFF) in 1 m sections is shown for each borehole together with the predicted hydraulic conductivity in the figures in Appendix A. By the calculation of the CFF the number of fractures in each section has been rounded off to an integer number. Although the CFF-models were mainly based on data from the rock mass (excluding fracture zones) the CFF is predicted along the entire boreholes. As described in Section 5.2 the fracture zones were though included in the CFF-model for KKL12 and KKL14 due to the low frequencies of Fe-coated fractures in these boreholes.

Histograms showing the distribution of the predicted number of conductive fractures in 1 m-sections with a (predicted) hydraulic conductivity greater than  $2 \times 10^{-10}$  m/s in each borehole are presented in Fig 7.2.1. Statistical data of these distributions for each borehole are shown in Table 7.7.

Table 7.7 Statistical data of the number of conductive fractures predicted in the boreholes.

Borehole	N	n	Mean	Median	Stdev
KKL01	234	606	2.590	1.000	3.165
KKL02	157	273	1.739	1.000	2.646
KKL06	406	156	0.384	0.000	0.826
KKL09	407	241	0.592	0.000	0.894
KKL012	405	(338)	(0.835)	0.000	(2.370)
KKL14	613	146	0.238	0.000	0.538

In Table 7.7, N denotes the number of sections used to construct the CFF-models in the different boreholes, i.e. sections with a predicted K-value greater than  $2 \times 10^{-10}$  m/s

(lower measurement limit). The n-values denote the total number of conductive fractures predicted in the boreholes. The mean ( $n/N$ ) and median values of conductive fractures per section thus correspond to conductive sections only. These numbers should not be confused with the true (average) CFF, which is averaged over the entire borehole lengths. As can be seen from Table 7.7 the predicted mean values are considerably higher in KKL01 and KKL02. This is likely to be due to the difference in the Fe-frequencies mapped in these boreholes.

The predicted number of conductive fractures in KKL12 is very much influenced by the uppermost (25 m) borehole interval, which account for about 50 % of the total number. The number of Fe-coated fractures is also high in this interval, c.f. Fig. 5.2.1. The sections modelled in the upper 25 m of the borehole show extremely large distances to the CFF-model indicating very poor conformance to the model. The reasons for this are not clear.

To calculate the predicted CFF the total number of conductive fractures should be averaged over the entire borehole lengths predicted, see Table 4.2. In addition, the CFF in the rock mass (excluding fracture zones) and in the fracture zones can be calculated. The predicted CFF and the corresponding spacing of conductive fractures are shown in Table 7.8. By the calculations in KKL12 the uppermost 25 m of the borehole was excluded due to the extreme distances of the predicted sections to the model in this interval.

Although the calculated CFF-values in Table 7.8 are considered to be in the correct order, they are regarded as uncertain, particularly in the boreholes KKL06, KKL12 and KKL14 which values are calculated with the same model. The predicted CFF in these boreholes appear rather low in comparison to the other boreholes. In KKL06 no fracture zone is interpreted.

Fig 7.2.1 Histograms of the predicted number of conductive fractures in 1m-sections in the boreholes KKL01, KKL02, KKL06, KKL09, KKL12 and KKL14 .

Histogram of FE12 N = 405  
Each \* represents 10 obs.

Midpoint	Count
0	267
1	94
2	23
3	6
4	1
5	0
6	1
7	0
8	0
9	1
10	0
11	2
12	0
13	3
14	5
15	2

KKL12

Histogram of FE6 N = 406  
Each \* represents 10 obs.

Midpoint	Count
0	307
1	65
2	19
3	9
4	4
5	2

KKL06

Histogram of FE1 N = 234  
Each \* represents 2 obs.

Midpoint	Count
0	84
1	35
2	27
3	22
4	11
5	19
6	8
7	7
8	3
9	8
10	2
11	3
12	2
13	1
14	1
15	1

KKL01

Histogram of FE14 N = 613  
Each \* represents 10 obs.

Midpoint	Count
0	494
1	98
2	15
3	6

KKL14

Histogram of FE9 N = 407  
Each \* represents 5 obs.

Midpoint	Count
0	246
1	104
2	41
3	12
4	1
5	3

KKL09

Histogram of FE2 N = 157  
Each \* represents 2 obs.

Midpoint	Count
0	76
1	25
2	18
3	14
4	2
5	5
6	4
7	5
8	4
9	1
10	0
11	1
12	1
13	0
14	1

KKL02

Table 7.8 Predicted CFF and number of conductive fractures predicted (n) in boreholes at Klipperås.

Bore-hole	CFF total (1/m)	n	CFF rock mass (1/m)	n	CFF zones (1/m)	n
KKL01	1.14	606	0.97	488	3.93	118
KKL02	0.30	273	0.23	213	5.00	60
KKL06	0.20	156	0.20	156	-	-
KKL09	0.30	241	0.25	176	0.72	65
KKL012	0.22	150	0.17	98	0.41	52
KKL14	0.21	146	0.18	117	0.69	29

The CFF in the rock mass generally vary between 0.17 - 0.25 conductive fractures per meter (except in KKL01). This corresponds to a spacing between conductive fractures of about 4-6 m. The predicted CFF in the fracture zones are significantly higher, particularly in KKL02 (Zone H1) and KKL01 (Zone 10). These zones have also high hydraulic conductivities. It should be noted that Zone 1 and 2 in KKL09 and Zone 5 in KKL14 contain no mapped Fe-coated fractures, see Fig 5.2.1.

## 8. DISCUSSION OF RESULTS

### 8.1 Hydraulic conductivity

The models used for prediction of hydraulic conductivity have demonstrated that about 80-90 % of the variation of the hydraulic conductivity values in the input set can be described by the models. These results are achieved by using 4-5 principal components in the models and by utilizing about 35-45 % of the total information contained in the data variables used in the X-block. Most of the variation of hydraulic conductivity is described by the first principal component of the models, i.e. about 60-70 %. This is considered to be a good result thus leading to a confident prediction of hydraulic conductivity.

Histograms showing the overall distribution of the logarithm of the predicted hydraulic conductivity values in 1 m sections in each borehole are presented in Fig 8.1.1. The class interval is normally one cycle except in KKL14 where half a cycle is used.  $N$  denotes the total number of 1 m-sections predicted in each borehole. The number of sections within each class are shown in the figure. Note that each star represents different numbers in different boreholes.

Most boreholes show a distinct lognormal distribution of the predicted hydraulic conductivity values, e.g. borehole KKL14. These distributions should be compared with the distributions of hydraulic conductivity used as input to the different models shown in Fig 5.1.2. The latter distributions are generally skewed towards low-conductivity values. Table 8.1 shows the number of input sections used ( $n$ ), the total number of sections predicted ( $N$ ), the mean and median values and the standard deviation of the overall hydraulic conductivity distribution predicted in each borehole.

Predicted values in the lower region of the conductivity distributions in Fig 8.1.1 are considered as relatively uncertain. This is mainly due to the uncertainties in assigning

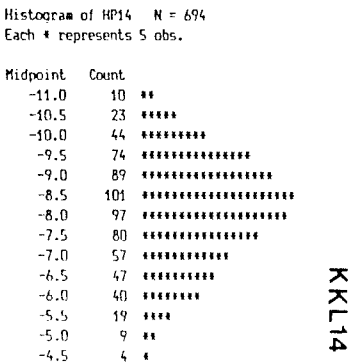
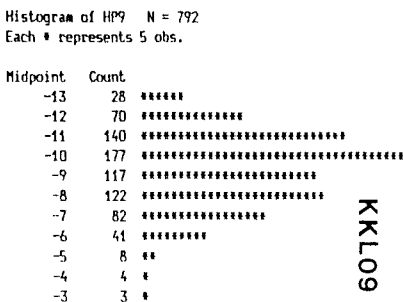
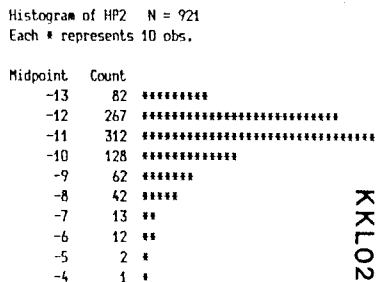
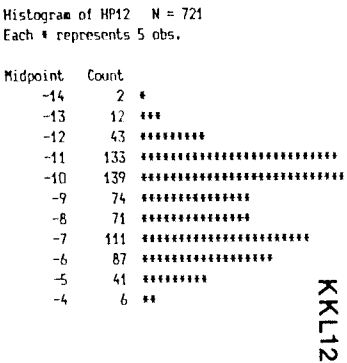
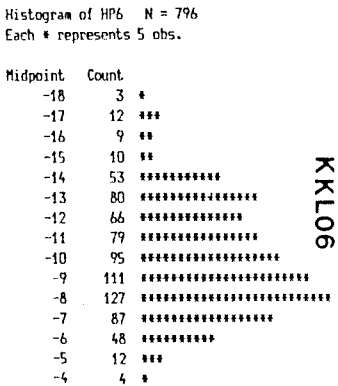
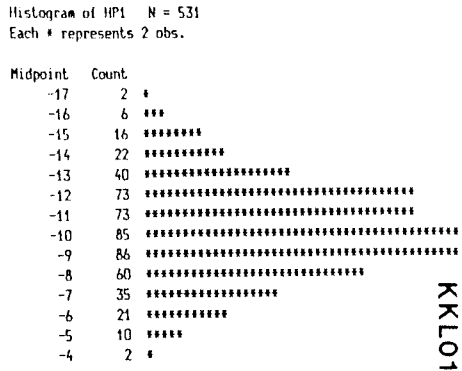


Fig 8.1.1 Histograms of the logarithm of predicted overall hydraulic conductivity (in m/s) in 1 m sections in the boreholes KKL01, KKL02, KKL06, KKL09, KKL12 and KKL14.

Table 8.1 Characterization of the logarithm predicted overall hydraulic conductivity distributions in boreholes at Klipperås.

Borehole	n	N	mean (m/s)	median (m/s)	stdev
KKL01	28	531	-10.19	-10.13	2.39
KKL02	32	921	-10.90	-11.23	1.45
KKL06	0	796	- 9.96	- 9.62	2.71
KKL09	102	792	- 9.38	- 9.62	1.88
KKL12	53	721	- 8.75	- 9.21	2.22
KKL14	18	694	- 8.14	- 8.21	1.34
Total	233	4455			

representative input values to sections with a hydraulic conductivity below the lower measurement limit in the hydraulic tests. No reliable estimates of hydraulic conductivity are available in this region. This means that predicted conductivity values towards the lowest end of the distributions are uncertain. On the other hand, it is very difficult to obtain reliable measurements in such sections. The same is true for sections with a hydraulic conductivity above the upper measurement limit.

Histograms of the residual distances for the X-variables of the 1 m-sections in the boreholes to the actual model are shown in Fig 8.1.2. A compilation of statistical parameters of the distribution of the residual distance in each borehole and the confidence volume of the actual PLS-models (RSD) are given in Table 8.2.

Table 8.2 shows that the median value of the residual distance is within the 67 % confidence volume (1 RSD) of the PLS-models for all boreholes except KKL01 which has a slightly

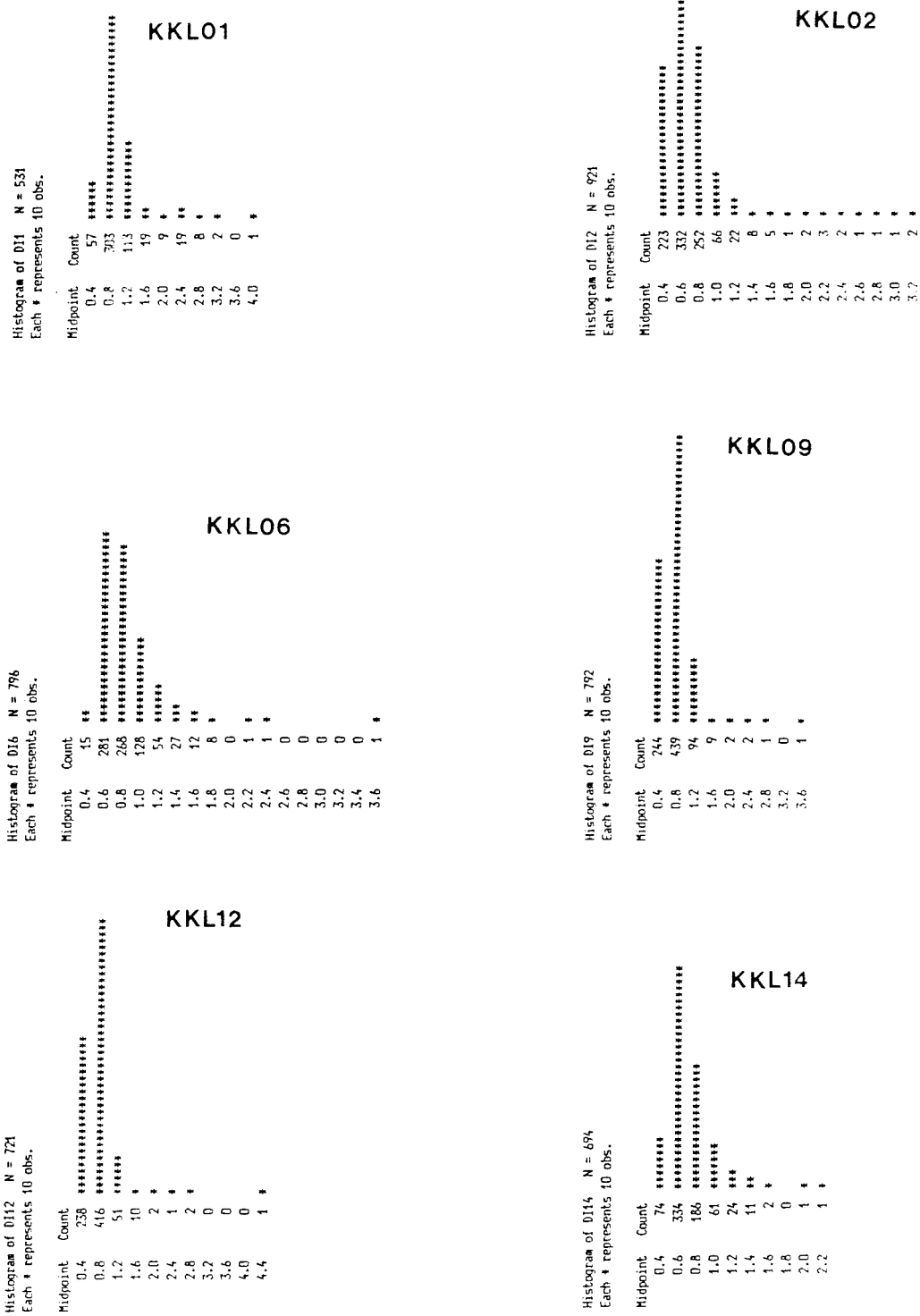


Fig 8.1.2 Histograms of the residual distances of the predicted 1 m sections to the actual models in the boreholes KKL01, KKL02, KKL06, KKL09, KKL12 and KKL14.



Table 8.2 Statistical parameters of the distribution of the residual distance of the 1 m sections to the models in boreholes at Klipperås.

Borehole	N	mean	median	stdev	RSD
KKL01	531	0.985	0.841	0.487	0.798
KKL02	921	0.686	0.635	0.302	0.798
KKL06	796	0.830	0.779	0.280	0.860
KKL09	792	0.754	0.707	0.281	0.810
KKL12	721	0.725	0.657	0.277	0.860
KKL14	694	0.702	0.647	0.215	0.860

higher median value. This is considered to be a good result regarding e.g. the different rock types occurring at the Klipperås site and the large number of sections predicted. As discussed above the largest residual distances normally occur in other rock types than granite (mafic rocks and porphyrys) and in very low-permeability rock. Large residual distances may also be associated with borehole sections with extreme or unusual responses in one or several of the measured variables, e.g. spike-like resistivity and sonic anomalies in highly fractured and altered rock intervals.

The proportion of 1 m-sections with a transmissivity (or hydraulic conductivity) below the measurement limit of the hydraulic test equipment ( $T = 2 \times 10^{-10} \text{ m}^2/\text{s}$ ) used at Klipperås is shown in Table 8.3. The number of sections with predicted K-values (or transmissivities) greater than  $10^{-7} \text{ m/s}$ ,  $10^{-6} \text{ m/s}$  and  $10^{-5} \text{ m/s}$  are also presented in the table. Statistical parameters of the predicted conductivity distribution for values greater than  $2 \times 10^{-10} \text{ m/s}$  are shown in Table 8.4.

Table 8.3 Number of 1 m-sections with predicted transmissivities greater than certain values.

Borehole	N	T>2 E-10 (m <sup>2</sup> /s)	>E-7 (m <sup>2</sup> /s)	>E-6 (m <sup>2</sup> /s)	>E-5 (m <sup>2</sup> /s)	>E-4 (m <sup>2</sup> /s)
KKL01	531	234	44	22	4	0
KKL02	921	157	20	9	2	1
KKL06	796	406	62	26	7	2
KKL09	792	407	91	33	11	5
KKL12	721	405	204	91	24	4
KKL14	694	613	147	48	9	0

Table 8.4 Statistical parameters of the distributions of the logarithm of predicted hydraulic conductivities (or transmissivities) greater than  $2 \times 10^{-10}$  m<sup>2</sup>/s.

Borehole	N	mean	median	stdev
KKL01	234	-8.05	-8.31	1.28
KKL02	157	-8.36	-8.65	1.18
KKL06	406	-7.77	-7.88	1.18
KKL09	407	-7.90	-8.07	1.28
KKL12	405	-7.13	-6.99	1.47
KKL14	613	-7.86	-8.02	1.17

As can be seen from Table 8.3 the number of sections with predicted hydraulic conductivities above certain values reduces considerably for higher conductivities. The number of sections with K-values greater than  $10^{-5}$  m/s is low. As discussed above the distributions of the predicted conductivities below  $2 \times 10^{-10}$  m/s in the boreholes are considered as uncertain.

When studying the conductivity distribution within 20 m-sections, very few 1 m-sections frequently govern the (total) transmissivity of the 20 m-sections. Also the predicted

distributions of hydraulic conductivity within the fracture zones, presented in Section 6.2, exhibit the same pattern. This pattern is also observed from recent detailed hydraulic tests in 2 m and 0.11 m sections within fracture zone 2 at the Finnsjön site (Andersson et al, 1988a). From the hydraulic tests it is concluded that Zone 2, which (geologically) has a thickness of about 100 m, hydraulically consists of 3-4 thin subzones with a thickness of only about 0.5 m each. The measured hydraulic conductivity of the subzones is very high, about  $10^{-3}$  -  $10^{-2}$  m/s.

The investigations at Finnsjön also support one of the main assumptions made in deriving the models used for prediction of hydraulic conductivity in this study, i.e. that high-conductive sections most frequently exhibit a simultaneous low-resistivity (single point resistance) and high sonic travel time anomalies, see Section 5.1.2. At Finnsjön also the red-coloured iron mineral laumontite generally occurs within the high-conductivity subzones. A very uneven flow distribution in crystalline rock is also observed at other research sites, e.g. the Stripa Mine (Neretnieks, 1985 and 1987).

A comparison of the median values of the predicted hydraulic conductivity distributions in Tables 8.1 and 8.4 between the boreholes shows that the subvertical boreholes KKL01 and KKL02 have the lowest median hydraulic conductivity. In the predicted overall conductivity distribution KKL14 has the highest median conductivity but in the predicted distribution for values greater than  $2 \times 10^{-10}$  m/s, KKL12 has the highest median conductivity. The standard deviation is however lower in KKL14 in both cases. The borehole KKL06 has deviating properties from the other boreholes.

In general, the measured and predicted transmissivity values in 20 m-sections show rather good agreement in most boreholes as can be seen from the composite plots in Appendix A and crossplots presented in Section 6.2. The number of 20 m-sections and the correlation coefficients in the crossplots

between measured and predicted transmissivities are shown in Table 8.5.

Table 8.5 Correlation coefficients ( $r$ ) between measured and predicted transmissivity in 20 m-sections in boreholes at Klipperås.

Borehole	N	$r$
KKL01	19	0.836
KKL02	42	0.750
KKL06	38	0.745
KKL09	37	0.808
KKL12	34	0.744
KKL14	33	0.631

N denotes the number of 20 m sections. Table 8.5 shows that the boreholes KKL01 and KKL09 have the highest correlation between the measured and predicted transmissivities and KKL14 the lowest. However, the correlation coefficient does not necessarily reflect the largest deviations between the values.

A compilation of measured and predicted hydraulic conductivities of the fracture zones penetrating the boreholes is shown in Table 8.6. The agreement of the values is rather good although the predicted values generally are higher than the measured. This may be due to overestimations in a few high-conductive 1 m sections within the zones.

The possible explanations for large deviations between measured and predicted transmissivity as discussed in Section 6.2, e.g. presumed packer- or rock leakage etc in the hydraulic tests, are speculative only. They are mainly based on geophysical log responses and information from the core log in the actual intervals and are not supported by other measurements,

Table 8.6 Measured and predicted hydraulic conductivities of the fracture zones in boreholes at Klipperås.

Fracture zone	Borehole	Hydraulic conductivity measured (m/s)	Hydraulic conductivity predicted (m/s)
1	KKL09	3.1 E-10	4.2 E-9
2	KKL09	5.4 E-7	2.0 E-6
2	KKL12	9.6 E-9	2.4 E-7
4	KKL14	3.9 E-7	2.9 E-6
6	KKL12	4.4 E-7	9.0 E-6
7	KKL12	2.5 E-7	3.7 E-7
8	KKL12	3.2 E-7	4.6 E-6
9	KKL12	5.5 E-7	1.1 E-6
10	KKL01	9.3 E-7	7.2 E-6
H1	KKL02	2.0 E-6	3.5 E-5

although such possible explanations also have been discussed in the reports in some cases.

The highest hydraulic conductivity values predicted in 1 m-sections generally correspond to fractured borehole intervals with altered and deformed rock (mainly in granite). The most high-conductive parts within such intervals generally have distinct resistivity- and sonic anomalies. Thus, most of the high-conductivity sections correspond to intervals with increased fracturing, i.e. fracture groups (often with a dominant fracture orientation) and crush zones rather than in single, isolated fractures. This may indicate that the probability of interconnection of fractures away from the borehole increases significantly when several fractures are grouped together. However, it must be remembered that the prediction models used in this study to a large extent are based on geophysical logs and that the predicted values will suffer from any inabilities of these methods to detect conductive features, e.g. single conductors.

Although the predicted hydraulic conductivity distributions presented above look very promising and are generally in good agreement with the measured values in 20 m-sections, the validity of the individual values in 1 m-sections can not be fully assessed without performing detailed hydraulic tests in some of these sections. In preference, borehole intervals where large deviations between the predicted and measured transmissivities occur should be selected for testing, e.g. parts of the interval 400-460 m in KKL12, see Section 6.2.6. If the relatively high hydraulic conductivity measured in this interval can be confirmed by new hydraulic tests, the conductivity must be attributed to single conductors, neither detected by the geophysical logs nor in the core log or by visual inspection of the core.

Some of the discrepancies between the measured and predicted transmissivities may represent the effects of the different radius of investigation of the geophysical logs and the hydraulic tests. While the geophysical logs can be assumed to investigate the properties within a radius of maximum about one meter from the borehole, the hydraulic tests may investigate the conditions at considerably larger distances. As a consequence, the hydraulic tests are dependent not only on fractures that intersect the borehole but also on interconnecting fractures and their continuity away from the borehole. This possible explanation was also discussed by Davison et al (1982) for discrepancies obtained between tubewave measurements and hydraulic tests at the WNRE-site in Canada.

Although several of the geophysical logs have proved to be very useful in predicting hydraulic conductivity, e.g. the single point resistance and the sonic log, there is no individual log that correlate directly to the hydraulic conductivity in the variable plots in this study. If possible, other logs which are more directly related to the hydraulic properties of the rock and also have good resolution (both absolute and vertically) should be tested. In the Stripa Mine the neutron-neutron log

has been used with good results (Fridh, 1988). In the SFR-project at Forsmark both the neutron-neutron and gamma-gamma logs were used. These logs have also been used in the Finnish site characterization program, e.g. in the Lavia borehole.

The potential of tubewave measurements in describing the hydraulic conductivity should be further investigated, possibly by using the EBBA image system in combination with multivariate data analysis as was used in the initial modelling in this study. Other possible methods, e.g. the acoustic-waveform analysis (3D-sonic) discussed by Davison et al (1982) and Mc Ewen (1985) should be investigated. In addition, quick hydraulic test methods which can provide rough estimates of the hydraulic conductivity in short test sections or along a borehole, e.g. flow meter surveys (Hufschmied, 1985), should be developed.

## 8.2 Conductive fracture frequency

The CFF-models also show that fracture groups in general best correlate with the predicted hydraulic conductivity. In the CFF-model for KKL01 and KKL02 the subhorizontal fracture group F7 and single fractures S7 (and S6) in granite dominate on the negative side of PC2, see Fig 7.1.1 and Tables 7.1 and 7.2. Also in the third component (positive side) the correlation of subhorizontal fractures to the predicted hydraulic conductivity is indicated. The positive sides of PC2 and PC4 of the model to predict the hydraulic conductivity (HC model) in KKL01 and KKL02 also confirm the correlation to hydraulic conductivity of subhorizontal fractures in granite (S7 and S6) and fracture groups F7 and F6 in granite, see Fig 6.1.1 and Tables 6.1.1-2.

In the inclined boreholes no such conclusions of dominating directions of conductive fractures can be drawn since the cores are not oriented. The CFF-model for KKL09 indicates however that the fracture groups F4 and F6 best correlate to the

predicted hydraulic conductivity but the correlation is not very strong.

The CFF-models show that both conductive and low-conductive Fe-coated fractures exist. In plots showing low-conductive Fe-fractures often calcite-coated fractures correlate best to the predicted hydraulic conductivity, see e.g. PC4 (negative side) of the CFF-model for KKL01 and KKL02. In the third component (positive side) of the same model both conductive Fe- and calcite-coated fractures occurs. The second component of the CFF-model for KKL12 and KKL14 (positive side) shows both low-conductive Fe- and calcite-coated fractures, see Fig 7.1.3. These examples illustrate the interaction between these two fracture filling minerals as discussed by Tullborg (1986), see Section 2.3. Another example of conductive calcite-coated fractures is in PC3 (positive side) of the HC-model for KKL12 and KKL14, see Fig 6.1.4. Low-conductive fractures are in general coated by epidote.

The predicted CFF along the boreholes is in general, like the hydraulic conductivity, very unevenly distributed. The CFF-predictions suffer from the lack of relevant measured variables to identify this property. As discussed in Section 5.2 the concept of CFF is not very well defined. This study indicates that conductive borehole intervals most frequently are associated with concentrations of fractures, i.e. fracture groups and minor crush zones within the rock mass, rather than isolated single fractures. In such intervals the density of conductive fractures may be considerably increased whereas long intervals of non-conductive fractures may exist in between. Thus the mean CFF along a borehole does not necessarily reflect the actual hydraulic properties of the boreholes.

The degree and type of fracturing is also strongly dependent of the rock type. Thus, statistical calculations of CFF, which generally are based on the assumptions of statistical independence of fractures and (statistically) homogeneous rock should be used with caution at sites like Klipperås. However,



CFF-calculations in different rock types and rock units with such methods may provide valuable information of the hydraulic properties.

An alternative to the CFF approach would be to determine the number of flow zones, i.e. conductive intervals along a borehole. Within the flow zones the fractures are likely to be interconnected. A comparison of the predicted CFF in Table 7.8 with the total fracture frequency mapped, shown in the tables in Section 2.2, reveals that the CFF is only a small portion of the total fracture frequency.

The predicted CFF in Table 7.8 can be compared with CFF-calculations within zone 2 and its adjacent parts at the Finnsjön site, based on statistical methods (Andersson et al, 1988b). These values are generally higher than those in Table 7.8. This could also be expected since the former values represent a fracture zone located in the upper parts of the bedrock.

## 9 SUMMARY AND CONCLUSIONS

### 9.1 Summary of results

This study has shown that the hydraulic conductivity to a large extent can be predicted by combined use of data from geophysical logging and core mapping. The models derived are believed to provide a realistic picture of the actual hydraulic conductivity distributions along the boreholes. With the models about 80-90 % of the variation of the hydraulic conductivity of the input data set could be explained by utilizing about 35-45 % of the total information contained in the data set.

The hydraulic conductivity of totally about 4500 one meter borehole sections has thus been predicted from 233 input values used as best estimates of this parameter. The predicted values generally show good conformance to the actual models.

The distributions of the predicted hydraulic conductivity values are in most cases distinctly lognormal in spite of the input distributions not being typically lognormal. In the overall conductivity distributions predicted, KKL014 has the highest median hydraulic conductivity whereas in the distribution for values greater than  $2 \times 10^{-10}$  m/s, KKL12 has the highest median value. In both distributions KKL01 and KKL02 have the lowest median hydraulic conductivity predicted. The borehole KKL14 has the lowest standard deviation of all boreholes studied.

The study also shows that the predicted hydraulic conductivity is very unevenly distributed along the boreholes, both in the rock mass and in the fracture zones. Generally, very few of the predicted values of the 1 m sections govern the total transmissivity of the measured 20 m sections. The number of sections with a predicted hydraulic conductivity greater than a certain value also decreases rapidly for increasing conductivities.

In general, good agreement between the measured and predicted transmissivities in 20 m sections was obtained. However in a few sections large discrepancies occurred which cannot be fully explained.

The highest hydraulic conductivity values predicted generally correspond to fractured borehole intervals with altered and deformed rock with strong resistivity and sonic log anomalies. High predicted hydraulic conductivity most frequently occur in sections with increased fracture density. This may be a reflection of an increased probability of interconnection of fractures away from the boreholes in such sections. However, the possibility of isolated, single conductors should not be excluded.

This study has also shown that the different rock types generally have highly varying geological and hydrogeological properties, both between boreholes and within the same borehole.

The predicted conductive fracture frequency is also very unevenly distributed along the boreholes. The CFF-model for KKL01 and KKL02 indicates that subhorizontal fractures (mainly in fracture groups) in granite in general best correlate to the predicted hydraulic conductivity although this feature is not extremely well accentuated.

The interaction between fracture fillings of Fe-oxyhydroxide and calcite is demonstrated. Both types of fracture fillings may correspond to both conductive and low-conductive properties of the fractures. Investigations of fracture fillings is considered as very important in predicting the hydraulic conductivity, in particular the Fe-minerals.

The CFF-models suffer from the lack of relevant measured variables to adequately identify this property. The concept of CFF may not either be the most relevant one to describe the conductive properties along the boreholes. An alternative would

be to determine and characterize the number of conductive zones along the boreholes.

The CFF-models derived in this study are much influenced by the frequency of fractures coated with Fe-oxyhydroxide. Since the mapping of this mineral in the cores is non-uniform among boreholes the predicted CFF are not directly comparable between boreholes.

The predicted average CFF in the rock mass generally vary between 0.17 - 0.25 fr/m. This corresponds to an average spacing of about 4-6 m between conductive fractures. In the fracture zones the predicted CFF is significantly higher, particularly in KKL01 and KKL02. These zones have very high hydraulic conductivities.

In summary, the models have confirmed the preliminary results obtained from earlier investigations regarding the correlation between geophysical logs and core logs and hydraulic conductivity on data from the Klipperås site. In addition, the models have provided a computerized analysis technique which makes the data analysis more efficient and objective.

## 9.2 Conclusions

Although good agreements generally have been obtained between measured and predicted transmissivity in 20 m sections the validity of individual values predicted in 1 m sections should be checked by detailed hydraulic tests, particularly in borehole intervals with large discrepancies between measured and predicted values, e.g. the interval 400-460 m in borehole KKL12.

Multivariate data analysis has proved to be a powerful technique to systematically analyse an extensive data material and to study correlation structures within the entire data set. Working with measured hydraulic conductivity values in 20 m

sections only and selecting representative values of 1 m sections is however a rather tedious procedure and requires large computational efforts.

The PLS-modelling is considerably facilitated if data from detailed hydraulic tests are available from parts of one or several boreholes within the area. A model is then readily established which can be tested on all boreholes and the conformance of data from each borehole to this model can be assessed. Although the present models are regarded as rather site-specific (and also borehole specific) they can be tested for conformance (classification) on boreholes at other sites with similar geological conditions.

The results of multivariate analysis may be incorporated and tested in fracture network models (Andersson, 1988) and in regional modelling of sites. Multivariate analysis is particularly well suited for site investigations to establish important geological and hydrogeological features of a large data material. This study has clearly shown that the hydrogeological properties of different rock types must be included in the modelling.

The study has also demonstrated that no individual geophysical log is directly correlated to hydraulic conductivity. The benefits of other logs, e.g. neutron-neutron and gamma-gamma logs, tubewave measurements, flow meter surveys, 3D-sonic logs or alternative logs in relation to the hydraulic conductivity should be further investigated.

The results of the present study does not limit the need of borehole hydraulic testing. The latter methods are, and will be, the most efficient in obtaining reliable values of hydraulic parameters, particularly by a combination of single-hole and cross-hole tests. This depends mainly on the different radius of investigation of e.g. geophysical logs and hydraulic tests. However, predicted hydraulic conductivities in detailed sections from multivariate analysis can provide a

more detailed picture of the conductivity distributions along boreholes than what normally is practically and economically feasible by hydraulic testing.

Thus, a combination of multivariate modelling of available data and hydraulic testing in selected borehole intervals seems to be the most efficient means. Predicted hydraulic conductivity values can also assist in designing the hydrotest program in a borehole once the data from the geophysical logging and core mapping are available. Thus a more flexible hydrotest program can then be performed, e.g. with detailed testing of high-conductive sections and more sparse testing of long low-conductivity rock intervals. Equipments to carry out quick hydrotests in detailed sections should be developed and used in combination with multivariate modelling. In addition, all types of measurements carried out in a borehole should use the same reference level, e.g. top of casing, to facilitate an integrated analysis of the data.

## 10 REFERENCES

- Andersson J-E, Ekman, L and Hansson K. 1988a. Single hole water injection tests in Borehole BFi2 within the Brändan area, Finnsjön study site. The Fracture Zone Project - Phase 3. SGAB IRAP 88208, 26 p.
- Andersson J-E, Ekman L and Winberg A. 1988b. Detailed investigations of fracture zones in the Brändan area, Finnsjön study site. Single hole water injection tests in detailed sections. Analysis of the conductive fracture frequency. SKB Progress Report 88-08.
- Andersson J. 1988. Applications of discrete fracture network models at site characterization and safety analyses. SKB Progress Report 88-35.
- Beydon W B, Cheng C H, Toksöz M N. Detection of subsurface fractures and permeable zones by the analysis of tubewaves. Earth Resources Laboratory. Dep of Earth and Planetary Sci. Massachusetts Inst. of Technology, Cambridge, Ma 02139, USA. Unpublished manuscript.
- Carlsson L, Winberg A and Rosander B. 1984. Investigations of hydraulic properties in crystalline rock. Mat Res Soc Symp Proc Vol 26, 1984. Boston, Elsevier.
- Carlsten S, Olsson O, Sehlstedt S, Stenberg L. 1987. Radar measurements performed at the Klipperås site. SKB Technical Report 87-01, 135 p.
- Davison C C, Keys W S and Paillet F L. 1982. Use of Borehole-Geophysical and Hydrological Tests to Characterize Crystalline Rock for Nuclear-Waste Storage, Whitshell Nuclear Research Establishment, Manitoba, and Chalk River Laboratory, Ontario, Canada. ONWI-418, prepared jointly by Atomic Energy Canada Limited and the U.S. Geological

Survey for Office of Nuclear Waste Isolation, Batelle Memorial Institute, Columbus, OH.

Egerth T. 1986. Compilation of geological and technical borehole data from the Klipperås study site. SKB Progress Report 86-10.

Esbensen K, Lindqvist L, Lundholm I, Nisca D, Wold S. 1987. Multivariate Modelling of Geochemical and Geophysical Exploration Data. Chemometrics and Intelligent Laboratory Systems, Vol 2, 14 p.

Esbensen K, Martens H. 1987. Predicting Oil-Well Permeability and Porosity from Wire-Line Petrophysical Logs - A Feasibility study using Partial Least Square Regression. Chemometrics and Intelligent Laboratory Systems, vol 2, 11 p.

Fridh B. 1988. Geophysical single hole logging. Stripa project. Site characterization and validation. Stage 1. SGAB ID-no 88 201, 63 p.

Gentzschein B. 1986. Hydrogeological investigations at the Klipperås study site. SKB Technical Report 86-08.

Hufschmied P. 1985. Estimation of three-dimensional statistically anisotropic hydraulic conductivity field by means of single well pumping tests combined with flowmeter measurements. Proc. Int. Symp. Stochastic Approach to Subsurface Flow, Int. Assoc. Hydraul. Res., Montvillargenne, pp. 110-116.

Katsube T J, Hume J P. 1987. Permeability determination in crystalline rocks by standard geophysical logs. Geophysics, Vol 52, No 3, 10 p.



- Lindqvist L, Lundholm I. 1985. Effektivare prospektering med hjälp av dataanalys (In swedish). Jernkontorets Annaler nr 4/85.
- Lindqvist L, Lundholm I, Nisca D, Esbensen K, Wold S. 1987. Multivariate Geochemical Modelling and Integration with Petrophysical data. Journal of Geochemical Exploration, vol 29, 15 p.
- Magnusson, K Å, Duran O. 1984. Comparative study of geological, hydrological and geophysical borehole investigations. SKB/KBS Technical Report 84-09. 134 p.
- Mc Ewen T J, Mc Cann D M, Shedlock S. 1985. Fracture analysis from borehole geophysical techniques in crystalline rocks. Q.J. eng. Geol., vol 18, 23 p.
- Neretnieks I. 1985. Transport in fractured rock. Paper presented at the IAH 17th International Congress on the Hydrogeology of Rocks of Low Permeability. Tuscon, Arizona, January 7-11, 1985.
- Neretnieks I. 1987. Channeling effects in flow and transport in fractured rocks - Some recent observations and models. Proceedings from the GEOVAL Symposium in Stockholm, April 1987.
- Olkiewicz A, Stejskal V. 1986. Geological and tectonic description of the Klipperås study site. SKB Technical Report 86-06.
- Persson, K L 1986. Administrativa borrhålsdata från typområdet Klipperås (In Swedish). SKB Progress Report 86-11.
- Poikonen A. 1983. Suitability of certain borehole geophysical methods for structural and hydrogeological studies of Finnish bedrock in connection with disposal of nuclear

- waste. Technical Centre of Finland. Geotechnical Laboratory. Report JT-83-06.
- Sehlstedt S, Stenberg L. 1986. Geophysical investigations at the Klipperås study site. SKB Technical Report 86-07.
- Stenberg L. 1984. Tubewavemätning i borrhål K1 02, Klipperås (In Swedish). SKBF/KBS Progress Report 84-33.
- Stenberg L, Olsson O. 1985. The tube wave method for identifying permeable fracture zones intersecting a borehole. SKB Progress Report 85-14.
- Stenberg L. 1986. Geophysical investigations on core samples from the Klipperås study site. SKB Technical Report 86-09.
- Stenberg L. 1987a. Detailed investigations of fracture zones in the Brändan area, Finnsjön study site, The Fracture Zone Project. Investigations with the tubewave method in boreholes Fi 6 and BFi 1. SKB Progress Report 87-27.
- Stenberg L. 1987b. Geophysical logging performed in borehole BFi 2 within the Brändan area, Finnsjön study site. The Fracture Zone Project. SGAB IRAP 87072, 9 p.
- Tullborg E-L. 1986. Fissure fillings from the Klipperås study site. SKB Technical Report 86-10.
- Tullborg E-L. (1987). Unpublished manuscript.
- Wold S, Carlsson R, Edlund U, Albano C, Hellberg S, Johansson E, Sjöström M. 1983. Optimering och analys av flerdimensionella data (In Swedish). Kemisk tidskrift nr 14.
- Wold S, 1985. En bild säger mer än tusen siffror (In Swedish). Forskning och Framsteg, nr 5.

Wold S, Esbensen K, Geladi P. 1987. Principal Component Analysis. Chemometrics and Intelligent Laboratory Systems, vol 2, 15 p.

Winberg A, Carlsson L. 1987. SFR-calculations of conductive fracture frequency and description of skin effects around tunnels in the rock cavern area, SFR, Forsmark. Report in Swedish prepared for SKB, June 1987.

## 11. APPENDICES

Appendix A Distribution of predicted hydraulic conductivity and conductive fracture frequency in boreholes KKL01, KKL02, KKL06, KKL09, KKL12 and KKL14. (Figures A.1 - A.6).

Appendix B Borehole descriptions (KKL01, KKL02, KKL06, KKL09, KKL12 and KKL14).

Tables B.1 - B.6. Core descriptions.

Figures B.1 - B.6. Schematic lithology and fracture frequency.

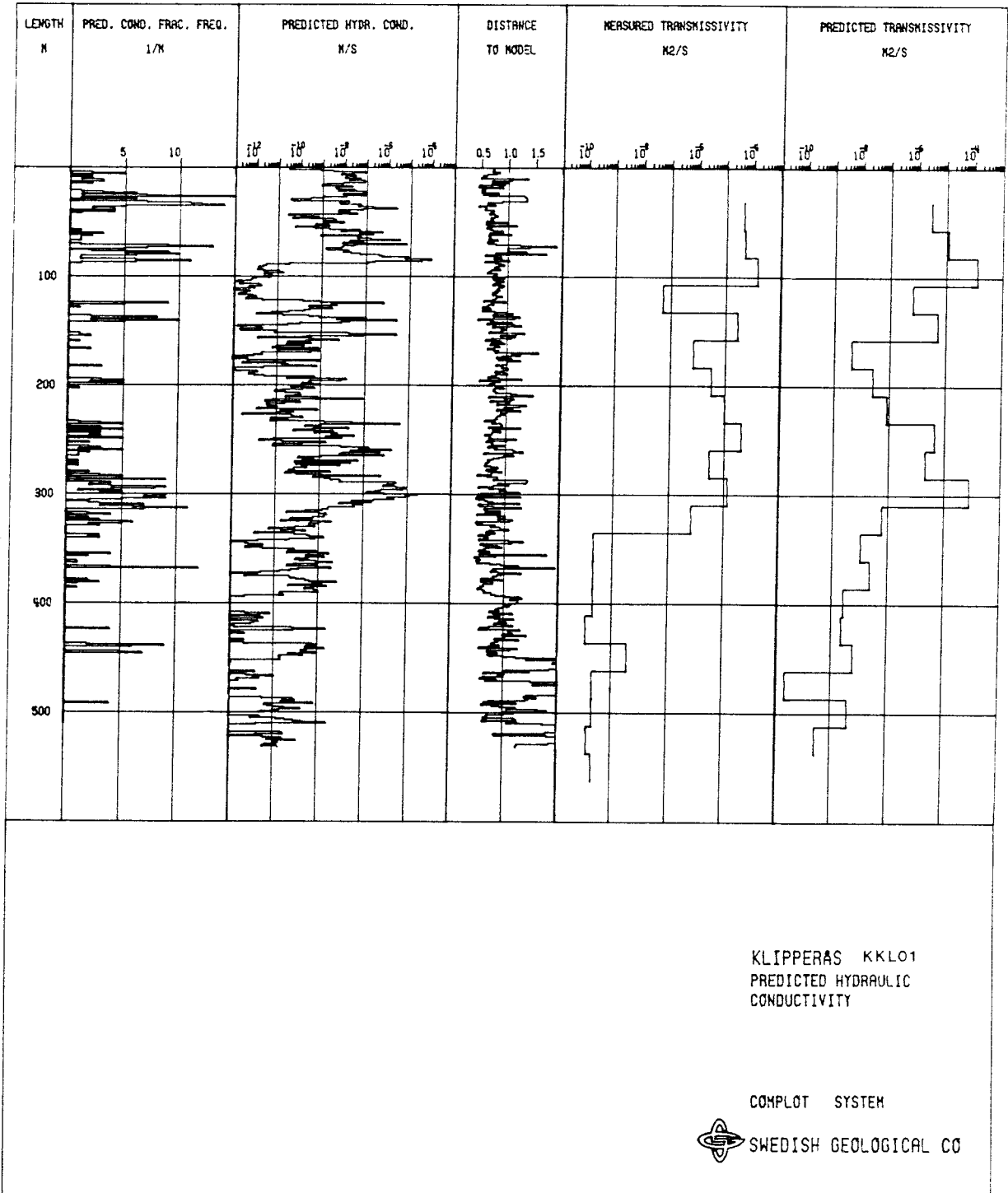


Fig A.1 Composite plot of the predicted distributions in borehole KKL01.

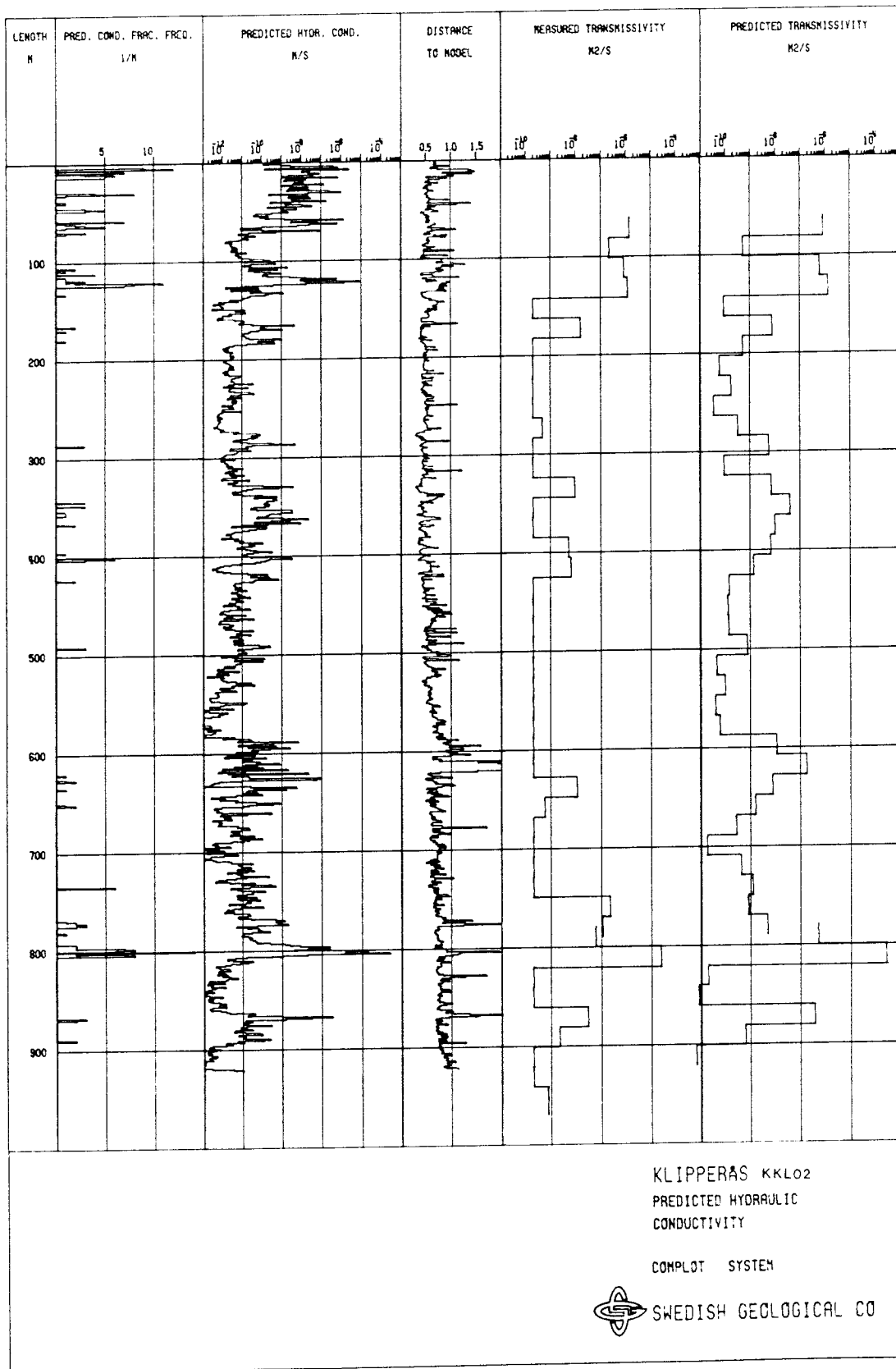


Fig A.2 Composite plot of the predicted distributions in borehole KKL02.

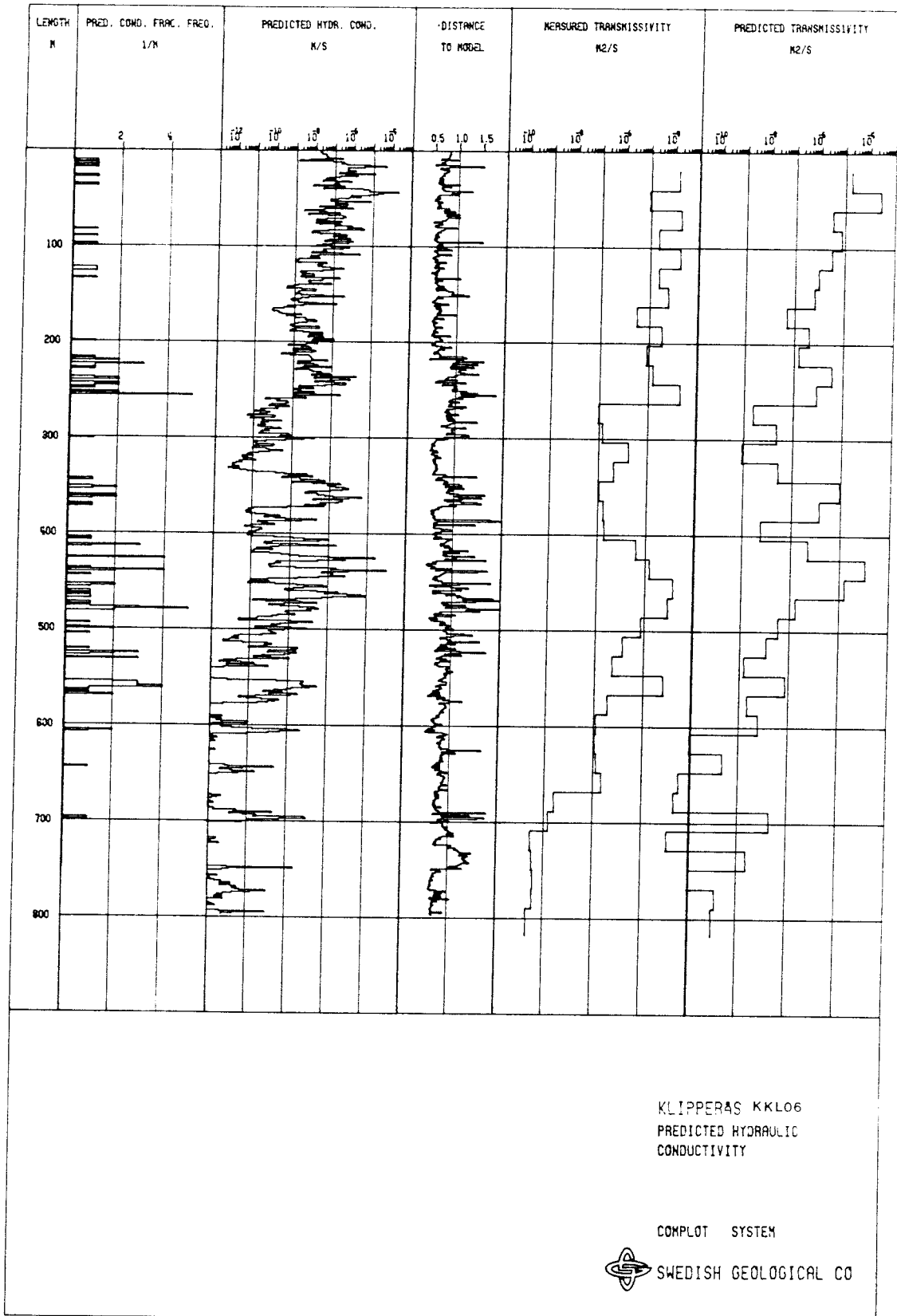


Fig A.3 Composite plot of the predicted distributions in borehole KKL06.

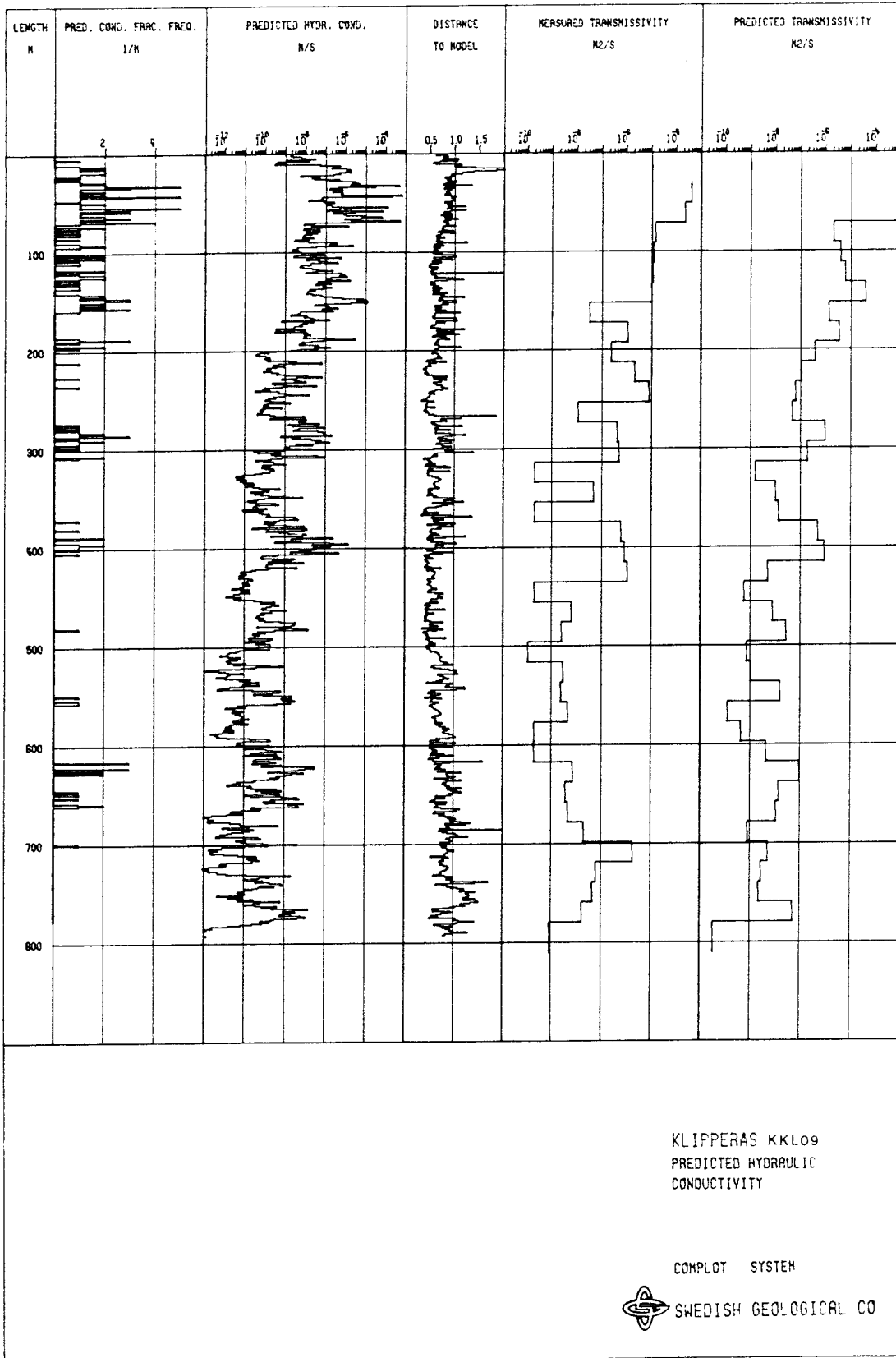


Fig A.4 Composite plot of the predicted distributions in the borehole KKL09.



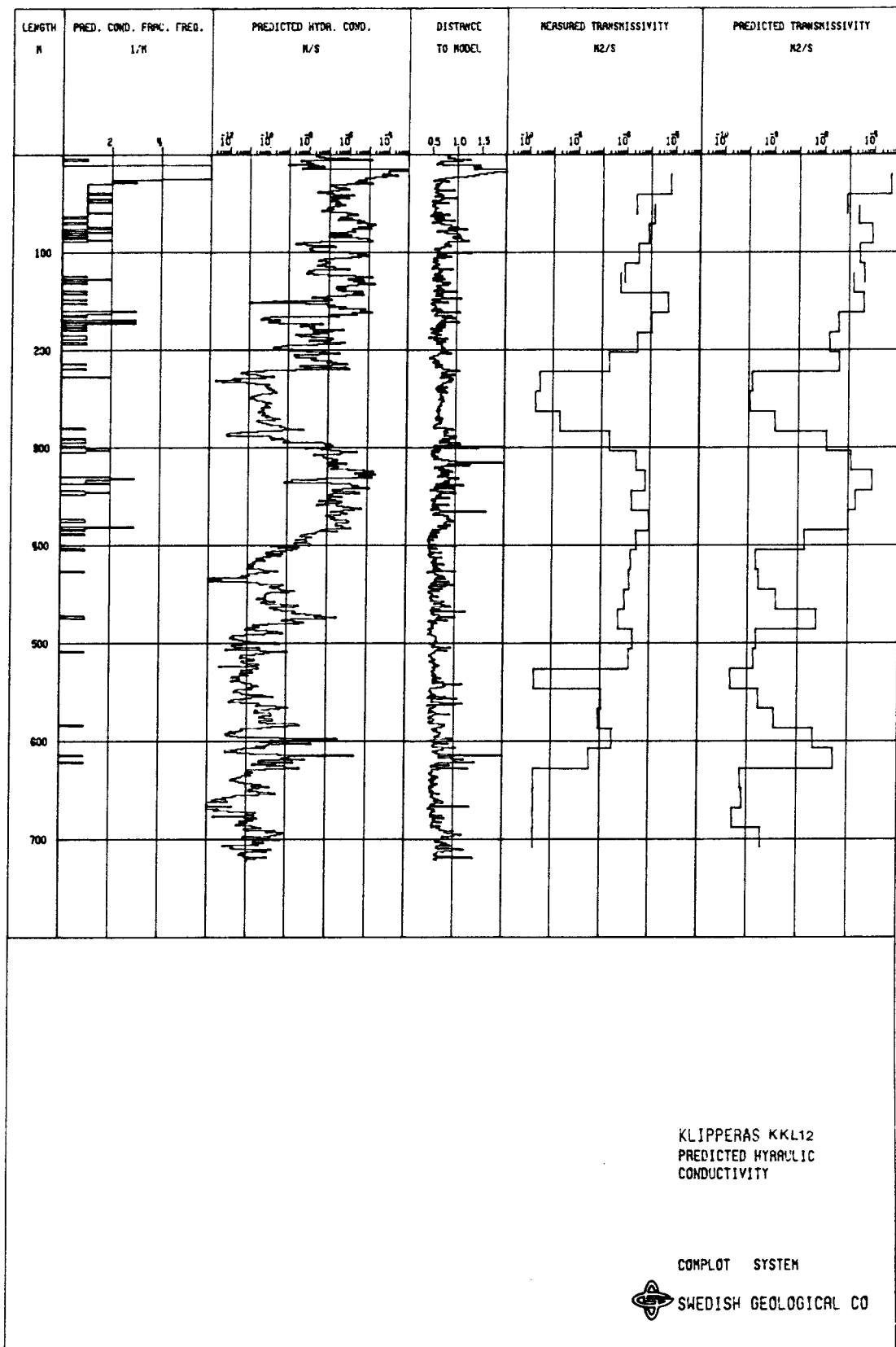


Fig A.5 Composite plot of the predicted distributions in borehole KKL12.

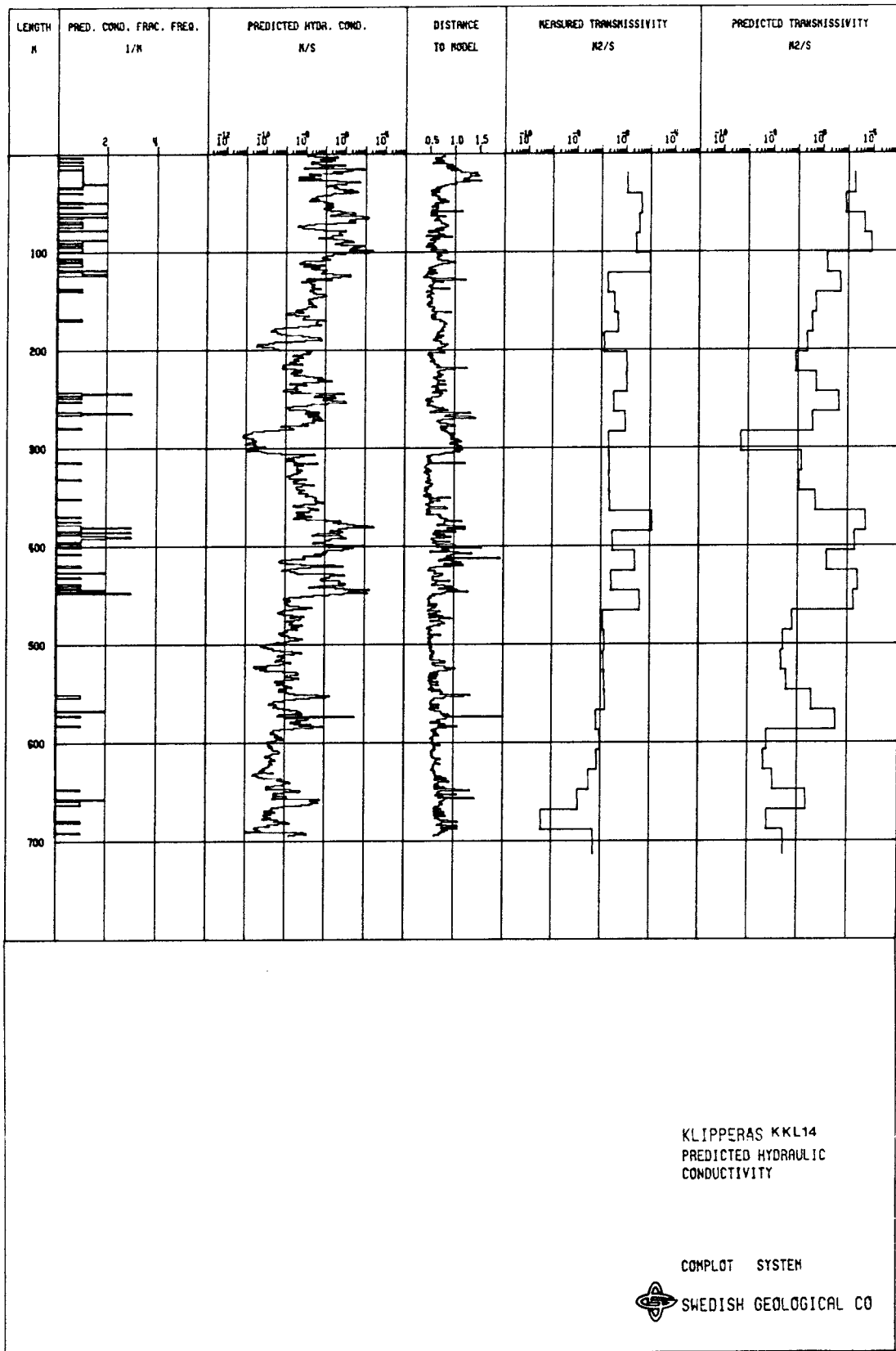


Fig A.6 Composite plot of the predicted distributions in the borehole KKL14.

Borehole KKL01

Local coordinates: 2253 N/ 1674 E  
 Declination: 134°  
 Inclination: 80°  
 Drilling length: 563.95 m

Table B.1 Distribution of rock types in KKL01

Rock type	Total length (m)	%	Longest sequence of a given rock type (m)
Moraine	3.70		
Granite	414.80	73.86	83.8
Greenstone	86.95	15.52	16.8
Porphyry	53.60	9.75	14.0
Aplite	4.90	0.87	2.4
Total	563.95	100.00	

Table B.2 Fracture frequencies related to rock types in KKL01

Rock type	Number of coated fractures	Fracture frequency per 1 m
Granite	2728	6.58
Greenstone	640	7.36
Porphyry	456	8.51
Aplite	17	3.47
Total fractures	3841	6.86

Borehole KKL02

Local coordinates: 1687 N/ 2717 E  
 Declination: 278°  
 Inclination: 78°  
 Drilling length: 958.60 m

Table B.3 Distribution of rock types in KKL02

Rock type	Total length (m)	%	Longest sequence of a given rock type (m)
Moraine	3.85		
Granite	825.45	86.46	152.30
Greenstone	87.15	9.13	31.35
Mafic dyke (Dolerite)	9.15	0.96	9.15
Aplite	0.80	0.1	0.60
Unknown (764.30 - 796.50)	32.20	3.37	
Total	958.60		

Table B.4 Fracture frequencies related to rock types in KKL02

Rock type	Number of coated fractures	Fracture frequency per 1 m
Granite	1907	2.31
Greenstone	583	6.70
Mafic dyke (Dolerite)	80	8.74
Aplite	2	2.50
Total fractures	2572	2.79

Borehole KKL06

Local coordinates: 2000 N/ 3539 E  
 Declination: 276°  
 Inclination: 56°  
 Drilling length: 808.00 m

Table B.5 Distribution of rock types in KKL06

Rock type	Total length (m)	%	Longest sequence of a given rock type (m)
Moraine	7.85		
Granite	568.65	71.07	164.90
Greenstone	118.90	14.86	54.60
Porphyry	92.95	11.62	47.80
Mafic dyke (Basalt)	16.05	2.00	7.70
Aplite	3.60	0.45	3.20
<b>Total</b>	<b>808.00</b>	<b>100.00</b>	

Table B.6 Fracture frequencies related to rock types in KKL06

Rock type	Number of coated fractures	Fracture frequency per 1 m
Granite	2038	8.58
Greenstone	1015	8.54
Porphyry	753	8.10
Mafic dyke (Basalt)	244	15.20
Aplite	58	16.11
<b>Total fractures</b>	<b>4108</b>	<b>5.13</b>

Borehole KKL09

Local coordinates: 1754 N/ 2360 E  
 Declination: 300°  
 Inclination: 56°  
 Drilling length: 801.03 m

Table B.7 Distribution of rock types in KKL09

Rock type	Total length (m)	%	Longest sequence of a given rock type (m)
Moraine	4.70		
Granite	646.75	81.22	141.50
Porphyry	79.65	10.00	48.55
Greenstone	53.20	6.68	7.00
Mafic dyke (Dolerite)	14.75	1.85	12.20
Aplite	2.00	0.25	0.90
Total	801.05	100.00	

Table B.8 Fracture frequencies related to rock types in KKL09

Rock type	Number of coated fractures	Fracture frequency per 1 m
Granite	2598	4.02
Porphyry	420	5.27
Greenstone	457	8.59
Mafic dyke (Dolerite)	92	6.24
Aplite	18	9.00
Total fractures	3585	4.50

Borehole KKL12

Local coordinates: 2370 N/ 2870 E  
 Declination: 346°  
 Inclination: 50°  
 Drilling length: 730.14 m

Table B.9 Distribution of rock types in KKL12

Rock type	Total length (m)	%	Longest sequence of a given rock type (m)
Moraine	3.55		
Granite	618.20	85.08	94.80
Greenstone	55.50	7.64	10.05
Porphyry	47.50	6.54	16.20
Aplite	5.40	0.74	2.25
Total	730.15	100.00	

Table B.10 Fracture frequencies related to rock types in KKL12

Rock type	Number of coated fractures	Fracture frequency per 1 m
Granite	2805	4.53
Greenstone	329	5.93
Porphyry	444	9.45
Aplite	18	9.00
Total fractures	3638	5.00

Borehole KKL14

Local coordinates: 1084 N/ 2400 E  
 Declination: 02°  
 Inclination: 55°  
 Drilling length: 705.22 m

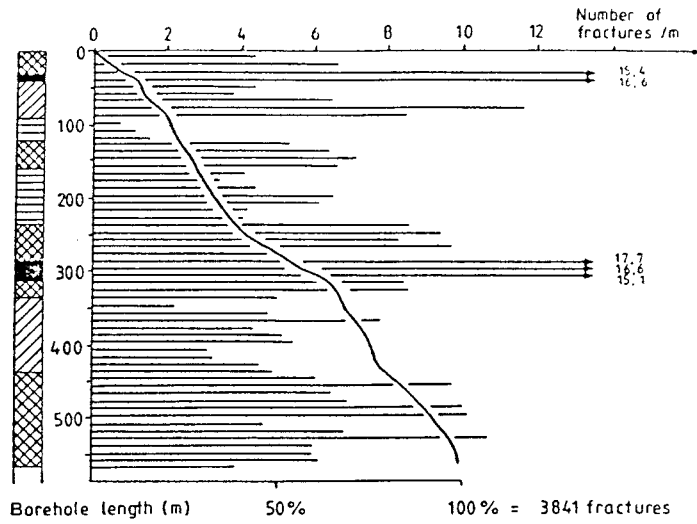
Table B.11 Distribution of rock types in KKL14

Rock type	Total length (m)	%	Longest sequence of a given rock type (m)
Moraine	3.20		
Granite	560.90	79.90	124.30
Porphyry	69.65	9.92	34.25
Mafic dyke (Dolerite)	45.35	6.46	31.45
Greenstone	25.10	3.58	6.95
Aplite	1.00	0.14	0.80
Total	705.20	100.00	

Table B.12 Fracture frequencies related to rock types in KKL14

Rock type	Number of coated fractures	Fracture frequency per 1 m
Granite	2023	3.62
Porphyry	341	4.90
Mafic dyke (Dolerite)	183	4.04
Greenstone	316	12.59
Aplite	5	5.00
Total fractures	2868	4.09

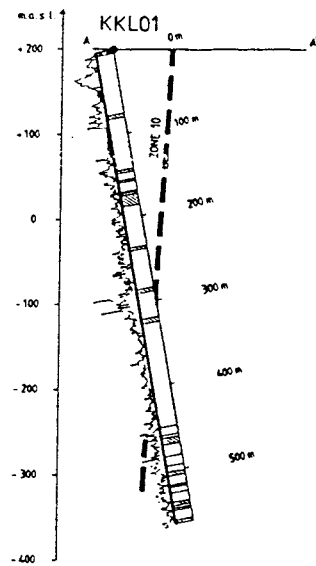




No of fractures /m

- 0 - 0,9
- ▨ 1,0 - 1,9
- ▩ 2,0 - 4,9
- ▧ 5,0 - 9,9
- ≥ 10

Borehole KKL01



LEGEND

Lithology

- ▨ Metarinite
- ▩ Metak dyke
- ▧ Dyke porphyry
- ▧ Aplite
- ▧ Granite
- ▧ Greenstone

∠ Dip

== Roads

fracture frequency

- ▨ Number of fractures/m

KLIPPERÅS, KKL01

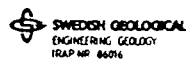
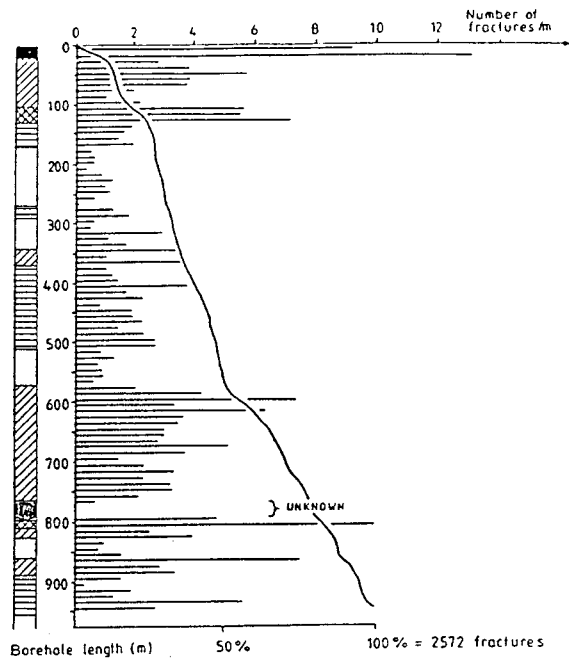


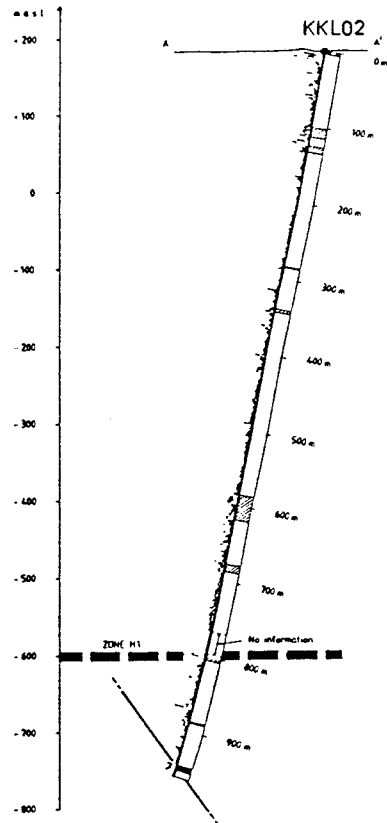
Fig B.1 Schematic lithology and fracture frequency of the borehole KKL01



No of fractures /m

- 0 - 0,9
- ▨ 1,0 - 1,9
- ▩ 2,0 - 4,9
- ▧ 5,0 - 9,9
- ≥ 10

Borehole KKL02



KUPPERÅS, KKL02

- LEGEND
- |                 |              |                    |
|-----------------|--------------|--------------------|
| Lithology       |              | == Road            |
| ▨ Marmor        | ▨ Aplite     | Fracture frequency |
| ▨ mafic dyke    | ▨ Granite    | □ 0-0,9            |
| ▨ Dyke porphyry | ▨ Greenstone | ▨ 1,0-1,9          |
|                 |              | ▩ 2,0-4,9          |
|                 |              | ▧ 5,0-9,9          |
|                 |              | ■ ≥ 10             |

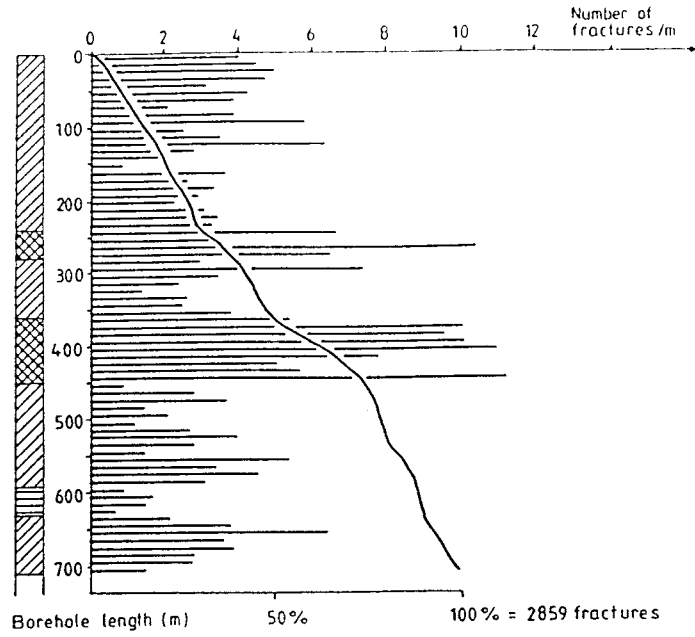
SWEDISH GEOLOGICAL  
ENGINEERING GEOLOGY  
MAP nr. 8606

Fig B.2 Schematic lithology and fracture frequency of the borehole KKL02









No of fractures /m

- 0 - 0,9
- ▨ 1,0 - 1,9
- ▧ 2,0 - 4,9
- ▩ 5,0 - 9,9
- ≥ 10

Borehole KKL14

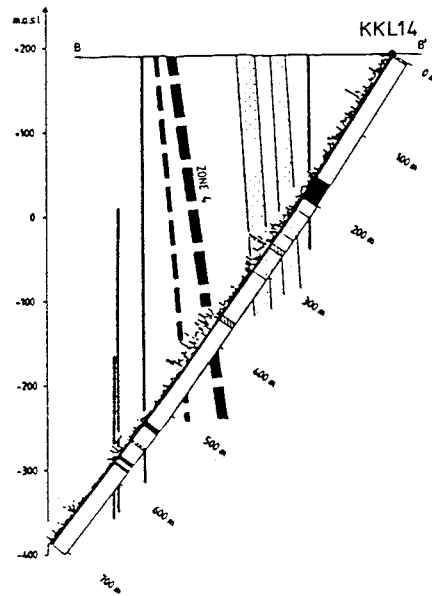


Fig B.6 Schematic lithology and fracture frequency of the borehole KKL14

# List of SKB reports

## Annual Reports

1977-78

TR 121

### **KBS Technical Reports 1 – 120.**

Summaries. Stockholm, May 1979.

1979

TR 79-28

### **The KBS Annual Report 1979.**

KBS Technical Reports 79-01 – 79-27.

Summaries. Stockholm, March 1980.

1980

TR 80-26

### **The KBS Annual Report 1980.**

KBS Technical Reports 80-01 – 80-25.

Summaries. Stockholm, March 1981.

1981

TR 81-17

### **The KBS Annual Report 1981.**

KBS Technical Reports 81-01 – 81-16.

Summaries. Stockholm, April 1982.

1982

TR 82-28

### **The KBS Annual Report 1982.**

KBS Technical Reports 82-01 – 82-27.

Summaries. Stockholm, July 1983.

1983

TR 83-77

### **The KBS Annual Report 1983.**

KBS Technical Reports 83-01 – 83-76

Summaries. Stockholm, June 1984.

1984

TR 85-01

### **Annual Research and Development Report 1984**

Including Summaries of Technical Reports Issued during 1984. (Technical Reports 84-01–84-19)  
Stockholm June 1985.

1985

TR 85-20

### **Annual Research and Development Report 1985**

Including Summaries of Technical Reports Issued during 1985. (Technical Reports 85-01-85-19)  
Stockholm May 1986.

1986

TR 86-31

### **SKB Annual Report 1986**

Including Summaries of Technical Reports Issued during 1986  
Stockholm, May 1987

1987

TR 87-33

### **SKB Annual Report 1987**

Including Summaries of Technical Reports Issued during 1987  
Stockholm, May 1988

1988

TR 88-32

### **SKB Annual Report 1988**

Including Summaries of Technical Reports Issued during 1988  
Stockholm, May 1989

## Technical Reports

1989

TR 89-01

### **Near-distance seismological monitoring of the Lansjärv neotectonic fault region Part II: 1988**

Rutger Wahlström, Sven-Olof Linder,  
Conny Holmqvist, Hans-Edy Mårtensson  
Seismological Department, Uppsala University,  
Uppsala  
January 1989

TR 89-02

### **Description of background data in SKB database GEOTAB**

Ebbe Eriksson, Stefan Sehlstedt  
SGAB, Luleå  
February 1989

TR 89-03

### **Characterization of the morphology, basement rock and tectonics in Sweden**

Kennert Röshoff  
August 1988

TR 89-04

### **SKB WP-Cave Project Radionuclide release from the near-field in a WP-Cave repository**

Maria Lindgren, Kristina Skagius  
Kemakta Consultants Co, Stockholm  
April 1989

TR 89-05

### **SKB WP-Cave Project Transport of escaping radionuclides from the WP-Cave repository to the biosphere**

Luis Moreno, Sue Arve, Ivars Neretnieks  
Royal Institute of Technology, Stockholm  
April 1989

TR 89-06

**SKB WP-Cave Project**  
**Individual radiation doses from nuclides**  
**contained in a WP-Cave repository for**  
**spend fuel**

Sture Nordlinder, Ulla Bergström  
Studsvik Nuclear, Studsvik  
April 1989

TR 89-07

**SKB WP-Cave Project**  
**Some Notes on Technical Issues**

TR 89-08

**SKB WP-Cave Project**  
**Thermally induced convective motion in**  
**groundwater in the near field of the**  
**WP-Cave after filling and closure**

Polydynamics Limited, Zürich  
April 1989

TR 89-09

**An evaluation of tracer tests performed**  
**at Studsvik**

Luis Moreno<sup>1</sup>, Ivars Neretnieks<sup>1</sup>, Ove Landström<sup>2</sup>  
<sup>1</sup> The Royal Institute of Technology, Department of  
Chemical Engineering, Stockholm  
<sup>2</sup> Studsvik Nuclear, Nyköping  
March 1989

TR 89-10

**Copper produced from powder by HIP to**  
**encapsulate nuclear fuel elements**

Lars B Ekbom, Sven Bogegård  
Swedish National Defence Research Establishment  
Materials department, Stockholm  
February 1989